# Detection of space-time perturbations with quantum-enhanced metrology


Diego A. Quiñones Valles

School of Physics & Astronomy

University of Leeds

A thesis submitted for the degree of

*Doctor of Philosophy*

29th September 2017

The candidate confirms that the work submitted is his own, except where work which has formed part of jointly authored publications has been included. The contribution of the candidate and the other authors to this work has been explicitly indicated below. The candidate confirms that appropriate credit has been given within the thesis where reference has been made to the work of others.

The results of Chapter 3 were published in the paper:
**Decoherence in Excited Atoms by Low-Energy Scattering.**
*Diego A. Quiñones; Benjamin Varcoe.*
*Atoms Volume: 4 Issue: 4, 2016.*
The author Diego A. Quiñones performed calculations and writing, while the author Benjamin Varcoe provided supervision.

Part of the results of Chapter 4 were published in the paper:
**Semiclassical approach to atomic decoherence by gravitational waves.**
*Diego A. Quiñones, Benjamin Varcoe.*
*Journal of Physics B: Atomic, Molecular and Optical Physics, Volume 51, Number 2, 2017.*
The author Diego A. Quiñones performed calculations and writing, while the author Benjamin Varcoe provided supervision.

Calculations showed in section 4.3 were published in the paper:
**Quantum principle of sensing gravitational waves: From the zero-point fluctuations to the cosmological stochastic background of spacetime.**
*Diego A. Quinones, Teodora Oniga, Benjamin T. Varcoe, Charles H.-T. Wang.*
*Physical Review D Volume: 96, Issue: 4, Pages: 044018, 2017.*
The author Diego A. Quinones provided calculations of the atomic model along with research on the gravitational spectrum, justification of the atom's response and general references, while supervised by the author Benjamin T. Varcoe. The authors Teodora Oniga and Charles H.-T. Wang wrote the paper and provided calculations on the gravitational interaction and simulations of the change in population.

In addition, the candidate published two articles based on the peer-reviewed papers in the online media outlet "The Conversation":

**Giant atoms could help unveil dark matter and other cosmic secrets**
*Diego A. Quiñones, The Conversation, January 5, 2017*
(https://theconversation.com/giant-atoms-could-help-unveil-dark-matter-and-other-cosmic-secrets-70868)

**How giant atoms may help catch gravitational waves from the Big Bang**
*Diego A. Quiñones, The Conversation, July 17, 2017*
(https://theconversation.com/how-giant-atoms-may-help-catch-gravitational-waves-from-the-big-bang-80430)

*Este trabajo lo dedico a mi familia por su apoyo incondicional*
*y a mi amada Hanna, siempre estas en mi corazon.*

- Diego A.

# Acknowledgements

I would like to thank my supervisor Prof. Benjamin Varcoe for his guidance and for allowing me to work under his supervision. Also to Prof. Jacob Dunningham for the initial opportunity. The various discussions with him and Dr. Paul Knott helped me to clarify several aspects of quantum metrology.

I acknowledge the Mexican National Council for Sciences and Technology (CONACYT) for the financial support given during my PhD studies. I was awarded with the *CONACYT PhD Scholarship for Studies Abroad* grant, which covered my tuition fees and living expenses. It would not have been possible for me to obtain my PhD degree without this grant.

# Abstract

We present a new model of atomic decoherence by space-time perturbations. We propose that decoherence will arise as a result of two possible effects that gravitational fluctuations will have on the atom. One is that the nucleus will be displaced relative to the valence electron, which will be perceived as a sudden change in the electric potential. This will result in the wave function of the atom being partially projected into lower energy levels. The other is that the strain in space will change the local electric field as felt by the electron. This interaction will either induce a change in the angular momentum of the atom or a small shift in the transition of the energy levels, presenting two different experimental approaches for the detection of the effect. We calculate how the decoherence is related to the internal degrees of freedom of the atoms, obtaining that the effect will be more prominent for atoms initially in a highly excited state (Rydberg atoms). By applying the nuclear displacement model for the scattering of neutral particles, we suggest that it could be potentially useful for the detection of weakly-interacting particles, like possible candidates of Dark Matter. The overall effect of gravitational waves for the strained-space model was calculated to be several orders of magnitude higher than for the nuclear displacement model, allowing for detection in different ranges of frequencies. We analyze how different quantum states are affected according to the proposed model, calculating that the information from the measurement of correlated atoms will be significantly higher. The optimal quantum state that minimizes the uncertainty of the measurement is described for an arbitrary number of atoms, giving a relation that follows closely the Heisenberg limit.

# Contents

# List of Figures

# Chapter 1

# Introduction

The discovery of gravitational waves has been one of the most exciting discoveries of the century for Physics (Abbott *et al.*, 2016b; Taylor, 1994; Weisberg *et al.*, 1981). Not only does it confirm one of the key predictions of the theory of general relativity (Hawking, 1979), also opens the possibility of studying the universe throughout a completely new view (Hogan, 1998; Lasky *et al.*, 2016). Similar to how radio wave observation provides a clearer picture of celestial systems, as most of the galactic components are transparent to these kinds of waves (Jauncey, 1977), observation of gravitational waves could provide invaluable information about different parts and eras of the universe, as they pass through all matter mostly unaffected (Copeland *et al.*, 2009; Durrer, 2010; Grishchuk, 2005; Wang *et al.*, 2016). The problem is that this low interaction that makes them so significant also makes them very hard to detect (Lasky *et al.*, 2016; LIGO & Virgo, 2009; Turner, 1997). The direct detection of gravitational waves was recently done by the Laser Interferometer Gravitational-Wave Observatory (LIGO) experiment (Abbott *et al.*, 2016b), later corroborated by the Virgo interferometer (Abbott *et al.*, 2016a, 2017), by measuring tiny changes in the separation length of highly separated mirrors (Aasi *et al.*, 2015). These experiments, though representing a milestone in science and engineering, are still limited in the range of frequencies they are able to detect.

Gravitational waves exist in a wide frequency spectrum, originated from a variety of cosmic events (Andriot & Gomez, 2017; Benacquista, 2002; Bildsten, 1998; Damour & Vilenkin, 2001; Haehnelt, 1994; Poisson, 1993; Ryan, 1995, 1997),

composing a gravitational background similar to the Cosmic Microwave Background (Fixsen, 2009; Nelemans, 2009). Some of the high-frequency end of the gravitational background is believed to have originated during the early stages of the universe by phase transitions and oscillations of cosmic strings (Durrer, 2010; Grishchuk, 2005), potentially containing invaluable information about the origin of the universe and its nature.

Another possible contributor to the gravitational background are gravitational fluctuations of the vacuum, which arise according to quantum gravity theories and other unification models (Hogan, 2000; Wang *et al.*, 2016). The detection of such fluctuations, and even the lack of, could help to verify or disprove many theories that have been proposed beyond the Standard Model. All of these are big motivations for new experimental schemes that aim to detect gravitational waves with different ranges of frequency (Aguiar *et al.*, 2002; Amaro-Seoane *et al.*, 2012; de Waard *et al.*, 2003; Desvignes *et al.*, 2016; Hobbs *et al.*, 2010; Sesana, 2016; Uchiyama *et al.*, 2004; Yamamoto *et al.*, 2008).

A potentially powerful probe for gravitational detection are atoms (Graham *et al.*, 2013; Hogan *et al.*, 2011; Oniga & Wang, 2016; Pinto, 1995; Zhao *et al.*, 2007). Atomic based technologies are currently used in gravimeters (Abend *et al.*, 2016; Altin *et al.*, 2013; Andia *et al.*, 2013) and for measuring relativistic effects (Hafele & Keating, 1972; Pound & Snider, 1964; Vessot *et al.*, 1980), also providing some of the most accurate measurements of the gravitational constant (Fixler *et al.*, 2007; Schlamminger, 2014). This was made possible because of modern experimental techniques that allow the manipulation of atomic systems to previously unthinkable degrees, paving the way to the observation of very small effects (Dickerson *et al.*, 2013; Fan *et al.*, 2015; Hoth *et al.*, 2016; Lan *et al.*, 2012). Gravitational radiation is supposed to carry energy (Bondi, 1957; Einstein, 1918; Merritt *et al.*, 2004; Weisberg *et al.*, 1981), which transfers to some small degree into matter it encounters in its path. This exchange of energy will alter the state of the particles that compose the matter, potentially inducing some level of decoherence to the system (Blencowe, 2013; Fischer, 1994; Oniga & Wang, 2016; Parker & Pimentel, 1982; Pinto, 1995; Zhao *et al.*, 2007). Therefore, by measuring the change in energy in atoms or the induced decoherence, it should

be possible to detect a gravitational fluctuation and also to obtain information about its properties.

The outcome of the interaction of atoms with gravitational waves is expected to be very small (Fischer, 1994; Parker & Pimentel, 1982; Zhao *et al.*, 2007), and therefore very difficult to be observed experimentally. Because of this, it may be necessary to use atoms in a special quantum state in order to enhance the sensitivity of the detection scheme (Johnsson *et al.*, 2016; Kimble *et al.*, 2001; Ma *et al.*, 2017). Applying these quantum states for measurement improvement, known as quantum metrology (Giovannetti *et al.*, 2006; Guo-Yong & Guang-Can, 2013), has been proven to increase significantly the resolution of the estimation of very small effects (Facon *et al.*, 2016; Guo *et al.*, 2015; Martin Ciurana *et al.*, 2017), even for interactions that occur within very small periods of time (Juffmann *et al.*, 2016), which will be the case for incoming gravitational waves from a particular source (Abbott *et al.*, 2016a,b, 2017). Furthermore, using spatially separated probes like atoms with two spatial modes or remotely entangled atoms could additionally increase the visibility of the effect and give information about the spatial properties of the gravitational radiation (Cadoret *et al.*, 2009; Dimopoulos *et al.*, 2009; Dupont-Nivet *et al.*, 2016; Himemoto & Taruya, 2017; Kolkowitz *et al.*, 2016; Sidhu & Kok, 2017).

In this thesis we present a study of the interaction of atoms and gravitational waves. We propose a new model of decoherence induced in atomic systems by low energy interactions, which is applied to the scattering of particles and then extended for the interaction of semiclassical gravitational waves. The model allows us to calculate the expected decoherence in the atomic state as a a function of the properties of both the atom and the interacting agent. We calculate how the initial state of the atom evolves as a result of the interaction in order to determine the ideal system that should be used to maximize the decoherence, and therefore the probability of detection. Finally, we analyze the response to gravitational interactions of different states commonly used in quantum metrology in order to determine which of them can further enhance the detection and to what degree.

## 1.1 Outline

In Chapter 2 we introduce the core ideas of our model and propose a classical approach to the problem. This representation gives an intuitive picture of the effect of low energy interactions with the atom, while providing a simple estimation of the order of the perturbation. In the model, an atom interacts with a particle in the form of scattering by the atomic nucleus. An exchange of energy between the nucleus and the particle will occur, resulting in a displacement of the nucleus with respect to its original position. Using the Bohr atomic model, we calculate the change in the potential of the atom after its nucleus is suddenly displaced with respect to the electron. Through this calculation, we find that the resulting potential can be represented as a sum of different functions, similar to a state superposition, effectively changing the energy of the system. The overall change in the potential energy is calculated proportional to the initial potential, suggesting that the effect will be more prominent for atoms with a high energy.

In Chapter 3, using similar assumptions for the nature of the interaction, we calculate the resulting wave function of the atom after a sudden change in the potential as felt by the electron. The results suggest that the atom will end in a superposition of the initial state and lower energy levels. This will introduce an additional phase between two consecutive eigenstates, generating a small amount of decoherence in the atomic state. We calculate the order of decoherence as a function of the initial state of the atom, obtaining that it increases with the principal quantum number, therefore making the effect more prominent for highly excited states (Rydberg states). The rise of decoherence in the system is then proven by calculating a reduction of the non-diagonal elements of the density matrix, which should manifest itself as a loss of visibility in the fringes of an interference pattern. We estimate the temporal evolution of the state of an atom scattering either massless or massive particles as a function of the properties of said particles. With the obtained equations, we analyze the change in the atomic state for different cases of interacting particles we considered interesting. From this we obtain that the expected decoherence should be higher for a particular type of Dark Matter than for cosmic rays, making the model potentially useful for the detection of said Dark Matter particle.

In Chapter 4 we analyze how the interaction of gravitational waves alters the state of the atom. The scattering model was applied, obtaining a change too small to be experimentally significant. We propose a new model of interaction, inspired by our previous one, in which the local potential of the atom is altered by the strain in space from the gravitational wave. In this model, the gravitational wave will change the potential of the nucleus as perceived by the valence electron, effectively altering its wave function. Our calculations show that this interaction will result in the atom also evolving into a state superposition, but this time of eigenstates with azimuthal quantum numbers that differ by multiples of 2. The atom will experience a shift in its transition energies, so we calculate the deviation of a Rabi cycle as a result of this shift. It was once more obtained that the effect will be more prominent for transitions involving high values of the principal quantum number. In the last part of the chapter, we analyze the collective behaviour of an ensemble of mutually interacting atoms. We discuss the emergence of superradiance as the result of correlated atoms subjected to a common gravitational fluctuation.

In Chapter 5 we analyze the transformation of different initial states using the obtained equations. We calculate the quantum Fisher information of the resulting states, which is the amount of information that will be obtained from the system after it is measured. We are able to show that a change in the measurement basis of a single atom will not improve the estimation of the properties of the gravitational interaction. We extend the analysis for the case of multiple probes, obtaining that correlated atoms will provide higher amounts of information than the same number of statistically independent atoms. We examine the information of different quantum states commonly used in quantum metrology schemes, observing no major improvement by using entanglement of distinguishable macroscopic states. We then describe the optimal quantum state for an arbitrary number of atoms that minimize the measuring error, which follows very closely the Heisenberg limit.

In Chapter 6 we present our conclusions and a discussion on the results of the study. We also provide an outlook for future works, highlighting potential experimental approaches and their limitations.

# Chapter 2

# Classical model of interaction

The simplest model for the interaction between a gravitational wave and an atom is scattering (Taylor, 2005). The energy exchange between the atom and the gravitational radiation from the scattering of the latter should alter the state of the atom so, by observing a particular change in the atom, it would be possible to determine that an event had occurred.

It should be expected that most of the scattering from the atom is done by the nucleus given that its mass is several orders of magnitude larger than the mass of the electrons (Gross & Jackiw, 1968; Sorge, 2015; Takahashi *et al.*, 2005). We propose that a single scattering event by the nucleus will change its position relative to its original reference frame. If this shift is fast enough, the electron will not be able to follow the nucleus smoothly, perceiving it at a different distance. The overall change in the relative position of the components of the atom will alter the energy of the system.

To calculate the energy change we try first to use Bohr's atomic model (Bohr, 1913). This modelling, along with classical mechanics and electromagnetism, will give us an indication if any change in the energy of the system will occur as a result of the proposed interaction and could help to estimate the order of the perturbation in the atom. A significant result will also justify extending our assumptions to a more realistic model. The classical approximation also works better for atoms in a highly excited state (Rydberg atoms) (Gallagher, 2007), which are systems we are interested in because studies have suggested that they may be more sensitive to gravitational fluctuations (Fischer, 1994; Pinto, 1995).

Results in the following chapters will further highlight the relevance of these kinds of states.

In the Bohr atomic model, the electron circles around the nucleus in stable orbits where the Coulomb attractive force is in balance with the centrifugal force experienced by the transiting electron. The radius of the orbit is given by the equation

$$r_n = \left(\frac{m_e + m_N}{m_N}\right)^3 \frac{n^2\hbar^2}{m_e Z k_C e^2} \ , \tag{2.1}$$

where $m_e$ is the mass of the electron, $m_N$ is the mass of the nucleus, $k_C$ is the Coulomb constant, $e$ is the fundamental electric charge and $\hbar$ is the reduced Planck constant. More precisely, both the electron and the nucleus move around the centre of mass of the system. We take this into account in our calculations, but for convenience we will choose in our equations for the coordinate system to be centered in the nucleus rather than the centre of mass. The factor $n$ is an integer number, with $n > 0$, that arises from the discretization of the orbits, which is related to the principal quantum number in the quantum model of the atom. The symbol $Z$ generally represents the atomic number, but in more accurate calculations the product $Ze$ is equal to the effective charge felt by the electron from a shielded nucleus, so $Z$ does not need be an integer number. Due to most of the experiments with trapped atoms using alkali metals *i.e.* atoms with one electron in the last occupied orbital (Cooper & Freegarde, 2013; Pedrozo-Penafiel *et al.*, 2012; Stancari *et al.*, 2007), we will focus our calculations in these kinds of systems by assuming $Z = 1$; this approximation is also more precise for Rydberg atoms (Gallagher, 2007). With this in mind, we have that the binding energy of the electron in the last orbital will be

$$E_n = -\frac{k_C e^2}{r_n} \ . \tag{2.2}$$

As described before, in our model an incoming particle will interact locally with the nucleus, shifting the relative position between the nucleus and the orbiting electron, represented in figure 2.1. The exact nature of the nucleus-particle interaction will depend on the properties of the particle, but we will first only analyze the resulting change in the energy from the displacement of the nucleus.

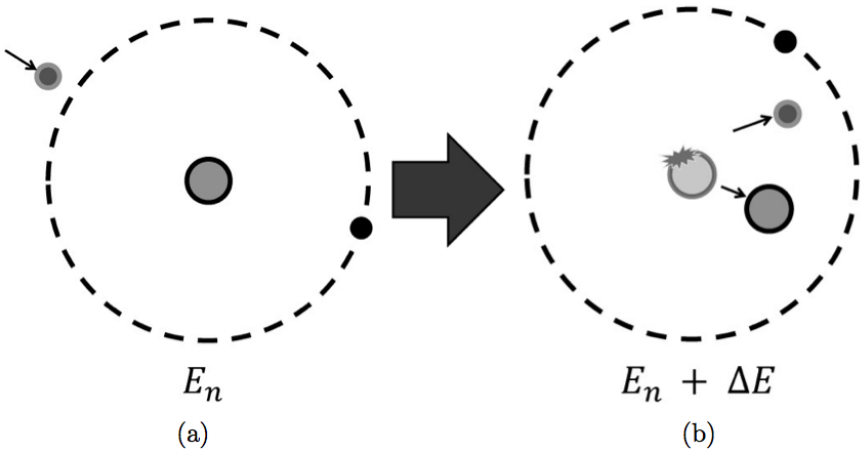


Figure 2.1: (a) An incoming particle approaches an atom with initial energy $E_n$. (b) The particle collides with the atomic nucleus, displacing it. This will change the energy of the atom by an amount $\Delta E$.

## 2.1 Nuclear displacement by scattering

As represented in figure 2.2, the nucleus that was initially at a distance $r_n$ from the electron will move along the vector $\vec{r}_d$ after a scattering event, resulting in a final distance $\vec{r}$ between electron and nucleus. The distance between the electron and the nucleus after the displacement will be given by

$$|\vec{r}|^2 = |\vec{r}_n + \vec{r}_d|^2 = {r_n}^2 + {r_d}^2 - 2r_n r_d \cos\theta \ . \tag{2.3}$$

where $\theta$ is the angle between the vectors $\vec{r}_n$ and $\vec{r}_d$. This results in the potential felt by the electron after the displacement of the nucleus

$$E = -\frac{k_C e^2}{r} = \frac{-k_C e^2}{({r_n}^2 + {r_d}^2 - 2r_n r_d \cos\theta)^{1/2}} \ . \tag{2.4}$$

If the interaction is very weak, it should be expected that the displacement of the nucleus will be very small compared to the size of the orbit ($r_d \ll r_{n=1}$). Otherwise, if the displacement of the nucleus were of the order of the Bohr radius, then the energy of the interaction will be big enough to ionize the atom, which is a case that we will exclude. Because of our assumption that $r_d/r_n < 1$, we can

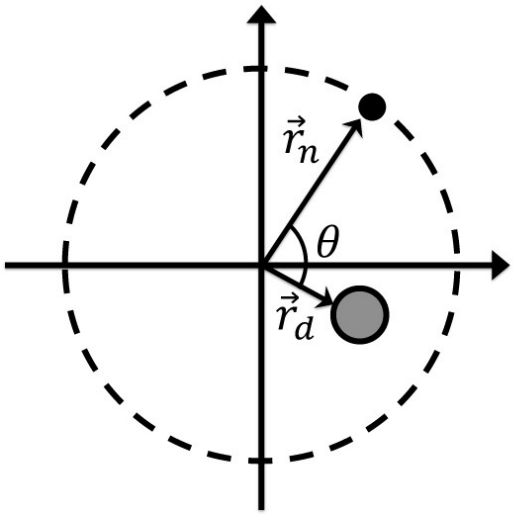


Figure 2.2: An atom with electron travelling around an orbital of radius $r_n$. The nucleus originally at the centre is displaced along the vector $\vec{r}_d$ after interacting with an incoming particle.

use the the mathematical identity

$$\left(1 + \frac{{r_d}^2}{{r_n}^2} - 2\frac{r_d}{r_n}\cos(\theta)\right)^{-1/2} = \sum_{m=0}^{\infty} P_m\left(\cos\theta\right)\left(\frac{r_d}{r_n}\right)^m , \tag{2.5}$$

where $P_m$ are the Legendre polynomials. We can substitute the identity in equation 2.5 into equation 2.4, so the resulting binding energy can be calculated with

$$E = -\frac{k_C e^2}{r_n}\sum_{m=0}^{\infty} P_m\left(\cos\theta\right)\left(\frac{r_d}{r_n}\right)^m . \tag{2.6}$$

The magnitude of $r_d$ and the properties of the polynomials $P_m$ ensure that the summation in the right side of equation 2.6 is convergent.

### 2.1.1 Spectral decomposition

If we define the magnitude of the displacement $r_d$ as

$$r_d = \left(\frac{m_e + m_N}{m_N}\right)^3 \frac{d^2\hbar^2}{m_e k_C e^2} \ , \tag{2.7}$$

where $d < 1$, we get that

$$\frac{k_C e^2}{r_n}\left(\frac{r_d}{r_n}\right)^m = k_C e^2 d^{2m}\left[\left(\frac{m_e + m_N}{m_N}\right)^3 \frac{n^{2(m+1)}\hbar^2}{m_e k_C e^2}\right]^{-1} \ . \tag{2.8}$$

Because both $n$ and $m$ are integers, the number $n_m \equiv n^{m+1}$ will also be an integer, so by defining

$$r_{n,m} \equiv \left(\frac{m_e + m_N}{m_N}\right)^3 \frac{n_m^2\hbar^2}{m_e k_C e^2} \ , \tag{2.9}$$

we can establish a new energy

$$E_{n,m} \equiv -\frac{k_C e^2}{r_{n,m}} \ , \tag{2.10}$$

which we use to arrive at the expression

$$\frac{k_C e^2}{r_n}\left(\frac{r_d}{r_n}\right)^m = d^{2m} E_{n,m} \ . \tag{2.11}$$

By substituting this into equation 2.6, we get that the potential energy after the displacement of the nucleus can be expressed as

$$E = \sum_{m=0}^{\infty} P_m\left(\cos\theta\right) d^{2m} E_{n,m} \ . \tag{2.12}$$

This equation tells us that the binding energy of the atom after the interaction can be expressed as a sum of potentials with discrete values, similar to a superposition in quantum mechanics. In figure 2.3 we plot the different potentials from equation 2.12. By adding the potentials corresponding to the first two terms of the sum in equation 2.12, we are able reproduce with significant accuracy the potential of a charge displaced to the right, as shown in figure 2.4. This illustrates that the biggest contribution to the potential is made by the first two terms in the summation ($m = 0, 1$). A similar result of the spectral decomposition and the relative magnitude of the terms will be observed in our calculations for the quantum model of the atom in Chapter 3.

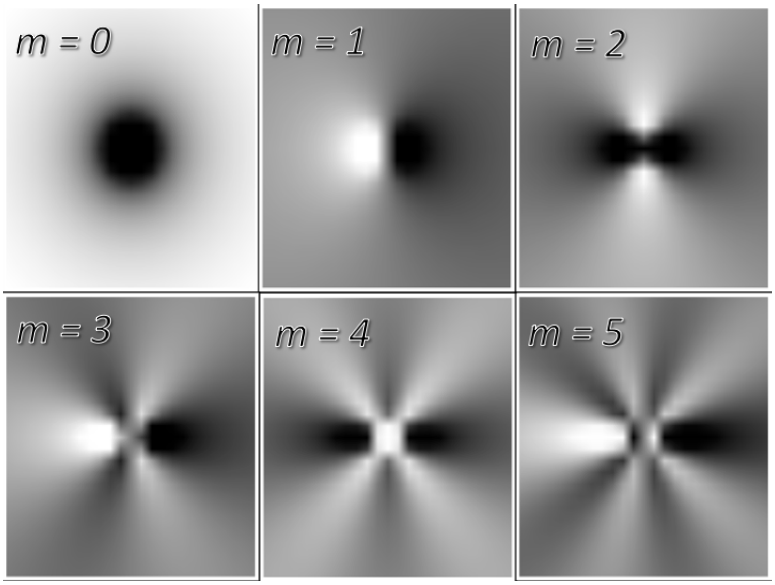


Figure 2.3: Normalized potential corresponding to the terms of the sum in equation 2.12 for different values of $m$. Darker areas correspond to higher potential.

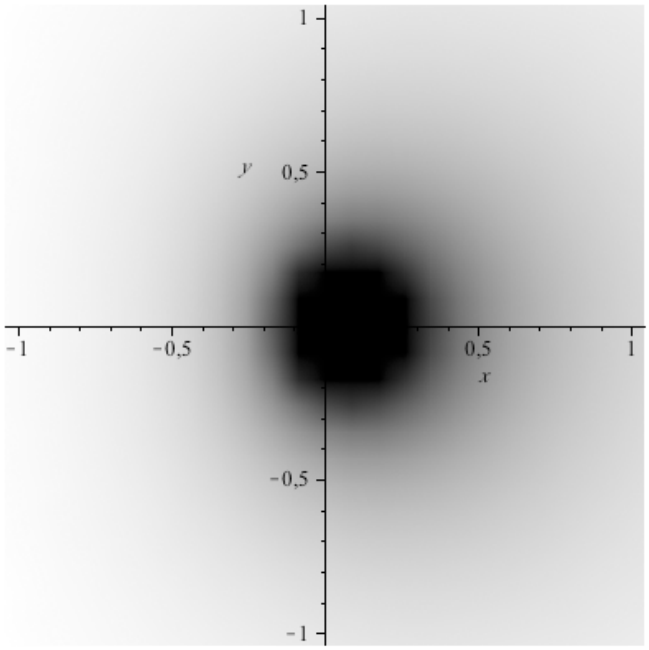


Figure 2.4: Potential calculated by adding the first two terms of the summation in equation 2.12 ($m = 0, 1$).

## 2.2 Energy shift

After the interaction, the nucleus will be closer to or further from the electron depending on the angle $\theta$ at which the electron is located, so the potential will be dependent on the angular component. Using equations 2.2 and 2.12 we have that the change in energy will be

$$\begin{aligned}\Delta E = E - E_n &= -\frac{k_C e^2}{r_n}\sum_{m=0}^{\infty} P_m\left(\cos\theta\right)\left(\frac{r_d}{r_n}\right)^m + \frac{k_C e^2}{r_n} \\ &= -\frac{k_C e^2}{r_n}\sum_{m=1}^{\infty} P_m\left(\cos\theta\right)\left(\frac{r_d}{r_n}\right)^m \ .\end{aligned} \tag{2.13}$$

To obtain the average change in energy, we integrate over all possible angles,

$$\overline{\Delta E} = -\frac{k_C e^2}{r_n}\sum_{m=1}^{\infty}\left(\frac{r_d}{r_n}\right)^m \frac{1}{2\pi}\int_0^{2\pi} P_m\left(\cos\theta\right)\mathrm{d}\theta \ . \tag{2.14}$$

Because of the properties of the polynomials, the integral will be equal to zero when $m$ is an odd number. After calculating the integral of the even polynomials, we get that the average change in energy will be

$$\begin{aligned}\overline{\Delta E} &= -\frac{k_C e^2}{r_n}\left[\frac{1^2}{2^2}\left(\frac{r_d}{r_n}\right)^2 + \frac{3^2}{8^2}\left(\frac{r_d}{r_n}\right)^4 + \frac{5^2}{16^2}\left(\frac{r_d}{r_n}\right)^6 + \frac{35^2}{128^2}\left(\frac{r_d}{r_n}\right)^8 \ldots\right] \\ &= -\frac{k_C e^2}{r_n}\sum_{k=1}^{\infty} C_k^2\left(\frac{r_d}{r_n}\right)^{2k} \ .\end{aligned} \tag{2.15}$$

The coefficients $C_k$ can be calculated with

$$C_k = \binom{2k}{k}\frac{1}{4^k} = \frac{(2k)!}{4^k(k!)^2} \sim \frac{1}{\sqrt{\pi k}} \ . \tag{2.16}$$

As previously stated, it is expected that the nucleus is displaced a very small amount, so $r_d/r_n \ll 1$. Because of this, we can disregard most of the terms of the sum in equation 2.15, obtaining that

$$\overline{\Delta E} \approx -\frac{k_C e^2}{4r_n}\left(\frac{r_d}{r_n}\right)^2 = \frac{E_n}{4}\left(\frac{r_d}{r_n}\right)^2 \ . \tag{2.17}$$

This equation tells us that the average change in energy of the system is proportional to the order of the displacement, which is a very intuitive result. It

also indicates that the change is smaller for a bigger radius, which can be explained by the fact that the further the electron is from the nucleus, the less it will perceive any perturbation (similar to trying to observe displacements in very distant objects). For a hydrogen atom in its ground state ($n = 1$), we have that a displacement of a thousandth of the Bohr radius ($r_d = 10^{-3} a_0$) will result in a change of energy of $\overline{\Delta E} \approx -3.4\ \mu\text{eV}$, which is of the order of the energy difference between hyperfine levels in the atom. In this case, the proposed interaction may induce a flip in the spin projection of the electron, which should be observable in the laboratory (Heinrich *et al.*, 2004). Although this magnitude in the displacement may not be likely for the scattering of gravitational waves or gravitons, it may be achievable by the scattering of heavy particles, like neutrons, which can be done as an experimental test for the model.

To calculate the change in energy for a given interaction it is necessary to first estimate the displacement distance $r_d$. For the current classical model it would be hard to justify any displacement for the nucleus without an almost immediate reaction by the electron, as classically the information about the slightest change in position will be transmitted instantly; this will result in an arbitrarily small displacement distance $r_d$, so no actual change in energy will occur.

Using the model of a retarded potential after the nucleus starts moving (Griffiths, 2007), we have that the displacement distance will be equal to

$$r_d = v \cdot t \ , \tag{2.18}$$

where $v$ is the velocity the nucleus gains as a result of the scattering and $t$ is the time it takes for information to travel from the nucleus to the electron. Because this information is supposed to travel at the speed of light, the travel time will be

$$t = \frac{r_n}{c} \ , \tag{2.19}$$

with $c$ the speed of light. The velocity $v$ the nucleus will have in relation to its original rest frame will be

$$v = \sqrt{\frac{2E_k}{m_N}} \ , \tag{2.20}$$

with $E_k$ the kinetic energy the electron gains from the scattering. Using equations 2.18 to 2.20 we calculate the coefficient

$$\frac{r_d}{r_n} = \sqrt{\frac{2E_k}{m_N c^2}} \ . \tag{2.21}$$

The term $m_N c^2$ can be easily identify as the invariant energy of the nucleus $E_N$ from Einstein's famous mass-energy equivalence formula (Einstein, 1905). Using this in equation 2.17 will give the relation

$$\overline{\Delta E} \approx \frac{E_n}{2}\left(\frac{E_k}{E_N}\right) \ . \tag{2.22}$$

This equation tells us that the change in energy increases with the transferred energy in the interaction and decreases with the mass of the atom, which is easy to understand. Also, we see that this change will increase with the initial energy of the atoms, which is an outcome that will persist in following chapters.

With equation 2.22 we have a notion of the order of the energy change, which will be extremely small as the invariant energy of the nucleus is expected to be much bigger than its kinetic energy. If we keep the energy exchange $E_k$ below the binding energy of the atom, the maximum energy change $\overline{\Delta E}$ will be lower than 0.1 $\mu$eV for a hydrogen atom. This is a very small number (just a fraction of the hydrogen line's energy (Griffiths, 1982)) and would be very hard to detect because radiation with this energy is in the radio wave range (Dupays *et al.*, 2003), so there will be a lot of noise to overcome. Rather than trying to detect any change in the energy of the system, a better approach will be to measure decoherence in the system that will arise as a result of the interaction of a space-time fluctuation, as other studies have suggested (Bonifacio *et al.*, 2009; Wang *et al.*, 2006). For this we require a quantum modelling of the interaction from which we can obtain the evolution of the system.

# Chapter 3

# Quantum model of decoherence by scattering

Although the classical modelling of the interaction is useful to estimate the magnitude of the energy change in the atom and provides a picture of the effect that is easy to visualize, it is necessary to use a more realistic model of the atom in order to accurately calculate the evolution of the system. Furthermore, the classical model just gives the average change in the potential energy, which may not necessarily manifest as a change in the energy levels of the atom, so it can't be applied to estimate detuning in its transitions or decoherence in the state.

We study the evolution of the interacting system using the atomic model provided by quantum mechanics under the following assumptions:

1. The interaction will manifest as a sudden displacement of the nucleus relative to its original rest frame;

2. The shift in position will be very fast, so that the process will be non-adiabatic;

3. The energy of the interaction will be below the ionization energy of the atom.

The first assumption is the same as for our model in Chapter 2, so similarities in the results can be expected. The second assumption guarantees that the system will not evolve into an equivalent state and therefore a change in its energy should

emerge. The last assumption is necessary for the validity of some of the employed mathematical identities, but also has an experimental basis as ionized atoms will not contribute to the atomic spectrum.

## 3.1 Wave-function transformation

To properly estimate any change in the system, it is necessary to calculate the wave function of the atom from which we can obtain the eigenstates and corresponding energy levels. In the quantum model of the atom, the wave-function $\psi$ usually describes the state of the outer-most electron (Griffiths, 1995), which relates to the energy $E$ of the system through the formula

$$H\psi = E\psi \ , \tag{3.1}$$

where $H$ is the Hamiltonian. The interaction will have the initial wave function of the system $\psi_0$ evolving into the state $\psi'$. Because the nucleus will be displaced along the vector $\vec{r}_d$, the resulting wave function will depend on the initial state and the displacement vector,

$$\psi_0(\vec{r}) \rightarrow \psi'(\vec{r}, \vec{r}_d) \ . \tag{3.2}$$

If the displacement is done fast enough, the electron will perceive a sudden change in the electric potential as examined in section 2.2. It may seem reasonable to think that the transformed equation should correspond to the solution of equation 3.1 using the new perceived potential in the Hamiltonian, but this solution will just be the same as the original with a displaced origin.

Another approach lies in applying perturbation theory to find the resulting wave function. It can be argued that the new potential can be described as the original potential plus a perturbation, as was calculated in the previous chapter (the addition of the first two potentials in figure 2.3 will result in the displaced potential in figure 2.4). The problem will be that any calculated change in the wave function will be due to the omission of all the remaining terms in the decomposition, rather than from the effect of the interaction. There is no way in which a displaced charge can be represented as the charge in its original position

plus a small perturbation, even for very small displacements, as the change in the electric field extends equally over all the space.

Our proposal is that the sudden shift in the potential will project the original wave function of the electron into the eigenstates of the new position of the atom, according to the adiabatic theorem (Griffiths, 1995). The resulting wave function can then be expressed as

$$\psi' = \sum_n C_n \psi_n \ , \tag{3.3}$$

where $\psi_n$ are the eigenfunctions of the unperturbed potential. The coefficients $C_n$ can be calculated by integrating over the fraction of solid angle $d\Omega$,

$$C_n = \int \psi_n^* \psi' dr d\Omega \ . \tag{3.4}$$

Solving equation 3.4 numerically requires a lot of computational power, even for the simplest atomic system. Instead of solving this equation for every particular case, we use some approximations that allow us to find an analytical solution. First, we focus our calculations on hydrogen-like atoms, which are atoms with only one electron in the last orbital and the remaining particles in an effective point charge. These kinds of atoms can easily be described mathematically and most atomic systems can be approximated to this description if they are in a Rydberg state (Gallagher, 2007), the relevance of which was previously stated. For hydrogen-like atoms, the potential is given by

$$V(r) = -\frac{k_c Z e^2}{r} \ . \tag{3.5}$$

By solving the Schrödinger equation with this potential, it is obtained that the wave-function can be separated in a radial part $R(r)$ and an angular part $Y(\theta, \phi)$ such that

$$\psi = R(r) Y(\theta, \phi) \ , \tag{3.6}$$

where the radial part is equal to

$$R_{n,l}(r) = -\sqrt{\frac{(n-l-1)!}{2n[(n+l)!]^3}} \left(\frac{2Z}{na_0}\right)^{l+\frac{3}{2}} r^l e^{-\frac{Zr}{na_0}} L_{n-1-1}^{2l+1}\left(\frac{2Zr}{na_0}\right) \ , \tag{3.7}$$

with $a_0$ the Bohr radius and $L_i^j$ the generalized Laguerre polynomials. The factors $n$ and $l$ are integer numbers with $n > 0$ and $l \leq n-1$ called quantum numbers.

More specifically, $n$ is known as the principal quantum number and $l$ as the azimuthal quantum number. For future calculations, we will consider $Z = 1$, which implies a small correction to the quantum number $n$ (Kostelecky & Nieto, 1985). In the case of Rydberg atoms, this correction will be mostly negligible (Gallagher, 2007). The angular part of the function is expressed in term of spherical harmonics that depend on the quantum numbers $l$ and $m$,

$$Y_l^m(\theta,\phi) = (-1)^m \sqrt{\frac{(2l+1)(l-m)!}{4\pi(l+m)!}} P_l^m\Big(\cos(\theta)\Big) e^{i\phi} \ , \tag{3.8}$$

where $P_l^m$ are the associated Legendre polynomials. We initially analyze the special case of an atom with no angular momentum ($l = m = 0$); the general case is described later in this chapter, obtaining similar results. For an atom in an initial state with principal quantum number $n_0$ and no angular momentum, the wave function is

$$\psi_0(r) = \sqrt{\frac{(n_0-1)!}{2n_0(n_0!)^3}} \left(\frac{2}{n_0 a_0}\right)^{3/2} e^{-\frac{r}{n_0 a_0}} L^1_{n_0-1}\left(\frac{2r}{n_0 a_0}\right) \ . \tag{3.9}$$

We argue that the displacement will be in an uncertain direction, so rather than considering it to move along a specific vector, we will describe the nucleus as being delocalized within a radius $r_d$ from its original position,

$$r \to r + r_d \ . \tag{3.10}$$

By using this change in equation 3.9 we arrive at

$$\psi_0 \to \psi' = \frac{1}{\sqrt{2}n_0 \cdot n_0!} \left(\frac{2}{n_0 a_0}\right)^{3/2} e^{-\frac{r+r_d}{n_0 a_0}} L^1_{n_0-1}\left(2\frac{r+r_d}{n_0 a_0}\right) \ . \tag{3.11}$$

Equation 3.11 implies that we are centering our coordinate system in the inertial reference frame of the nucleus. Also, because of the lack of angular dependence, it assumes that no angular momentum exchange occurs between the particle and the nucleus. Two arguments can be made for this assumption: first, the particle interacts only with the nucleus so the wave-function of the electron is not expected to gain an angular dependence as a result of momentum exchange; second, this equation accounts only for the minimum expected change in energy, so it would

represent the limit of the observable effect. The gain of an angular component will be analyzed in the general case.

Using the mathematical identity (Abramowitz & Stegun, 1983)

$$L^1_{n_0-1}(k_0 r + k_0 r_d) = \sum_{i=1}^{n_0} L^1_{i-1}(k_0 r) L^{-1}_{n_0-i}(k_0 r_d) \ , \tag{3.12}$$

where

$$k_0 = \frac{2}{a_0 n_0} \ , \tag{3.13}$$

with equation 3.11, we arrive at the identity

$$\psi' = e^{-\frac{k_0}{2} r_d} \sum_{n_0-i}^{n_0} \frac{i \cdot i!}{n_0 \cdot n_0!} L^{-1}_{n_0-i}(k_0 r_d) R_i(r) \ , \tag{3.14}$$

where $R_i$ is a radial component as described in equation 3.7 for $n = i$ and $l = 0$. Using this representation in equation 3.4 we get that

$$C_n = e^{-\frac{k_0}{2} r_d} \sum_{i=1}^{n_0} \frac{i \cdot i!}{n_0 \cdot n_0!} L^{-1}_{n_0-i}(k_0 r_d) \int_0^\infty R_i(r) R_n(r) dr \ . \tag{3.15}$$

The functions $R_j$ are orthonormal, so the result of the integral in equation 3.15 will be non-zero only when $i = n$, so we have that

$$\begin{aligned} C_n &= e^{-\frac{k_0}{2} r_d} \sum_{i=1}^{n_0} \frac{i \cdot i!}{n_0 \cdot n_0!} L^{-1}_{n_0-i}(k_0 r_d) \delta_{n,i} \\ &= e^{-\frac{k_0}{2} r_d} \frac{n \cdot n!}{n_0 \cdot n_0!} L^{-1}_{n_0-n}(k_0 r_d) \quad \text{for } n \leq n_0 \ . \end{aligned} \tag{3.16}$$

With this, we finally arrive at the identity

$$\psi' = \sum_{n=1}^{n_0} e^{-\frac{k_0}{2} r_d} \frac{n \cdot n!}{n_0 \cdot n_0!} L^{-1}_{n_0-n}(k_0 r_d) \psi_n \ . \tag{3.17}$$

This equation tells us that after the interaction, the atom is left in a superposition of all the eigenstates with principal quantum number equal to and lower than the number of the initial state. An explanation for this can be that the interaction transfers potential energy in the atom into kinetic energy, similar to the model in Chapter 2.

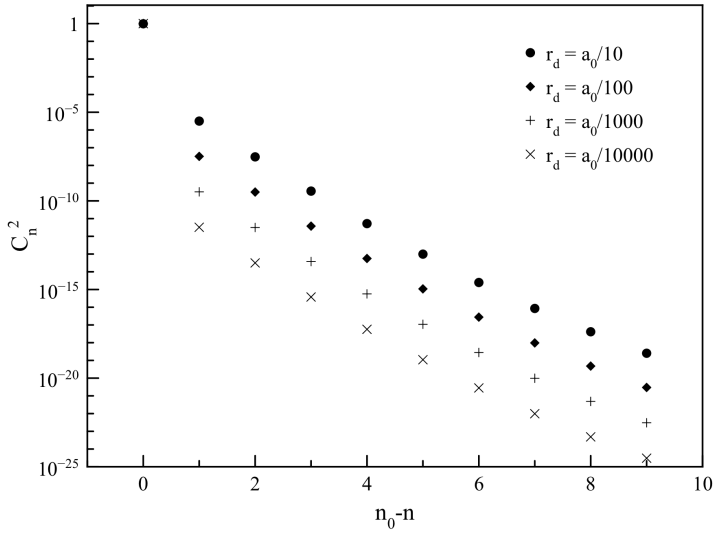


Figure 3.1: Coefficients of the eigenstate decomposition of the atomic state after the scattering of a particle by the nucleus obtained by using equation 3.16 with different values of nuclear displacement $r_d$. The initial state of the atom has no angular momentum and principal quantum number $n_0 = 10$.

In figure 3.1 we plot the value of the coefficients for different displacement distances. Two things can be appreciated from this graph: first, that projection over states different from the initial state ($n < n_0$) increase with the displacement radius. This means that the magnitude of the effect increases with the perturbation of the atom, which is an intuitive result. Secondly, coefficients of the decomposition decay rapidly as the principal quantum number of the state differs from the initial number $n_0$.

Because the coefficients of the initial state (with $n = n_0$) and the closest-energy state (with $n = n_0 - 1$) are significantly bigger than the other coefficients (with $n < n_0 - 1$), we can use the approximation

$$\psi' \approx C_{n_0}\psi_{n_0} + C_{n_0-1}\psi_{n_0-1} \ , \tag{3.18}$$

where the coefficients $C_{n_0}$ and $C_{n_0-1}$ are equal to

$$C_{n_0} = e^{-\frac{k_0}{2}r_d} \ , \ C_{n_0-1} = -k_0 r_d \frac{n_0 - 1}{n_0^2} e^{-\frac{k_0}{2}r_d} \ , \tag{3.19}$$

according to equation 3.16.

### 3.1.1 Angular momentum transfer

The obtained results are limited to interactions with no angular momentum exchange between the atom and the scattered particle ($\Delta l = 0$). For the general case the scattering moves the nucleus along the angle $\theta$ by a distance $r_d$, giving the transformation

$$r \to r + r_d \cos\theta, \tag{3.20}$$

which results in the wave function after the interaction changing as

$$\psi_0 \to \psi' = \frac{-1}{\sqrt{2}n_0 \cdot n_0!}\left(\frac{2}{n_0 a_0}\right)^{3/2} e^{-\frac{r+r_d\cos\theta}{n_0 a_0}} L^1_{n_0-1}\left(2\frac{r + r_d\cos\theta}{n_0 a_0}\right) . \tag{3.21}$$

With this new transformation, we calculate the eigenstate decomposition of the state after the interaction as described in equations 3.3 and 3.4. Using a mathematical identity similar to equation 3.12, we can separate the radial and angular part of the wave function,

$$\psi' = \frac{k_0^{3/2}}{\sqrt{2}n_0 \cdot n_0!}\sum_{m=1}^{n_0} e^{-\frac{k_0}{2}r_d\cos\theta} L^{-1}_{n_0-n}(k_0 r_d\cos\theta) e^{-\frac{k_0}{2}r} L^1_{m-1}(k_0 r) . \tag{3.22}$$

From here we obtain that the integral of the radial part is the same as in the previous section (equations 3.15 and 3.16), but in this case the integral of the radial part has no analytical solution.

Because we expect the coefficients of the levels closer to the initial state ($n = n_0, n_0 - 1$ and $l = 0, 1$) to have a significantly higher value, as in the case of no angular momentum transfer (equation 3.16), we calculate numerically the value just for these coefficients. Their values were found to be approximately

$$C_{n_0,l=0} \approx 1 - \frac{1}{4}\left(\frac{r_d}{n_0 a_0}\right)^2 , \tag{3.23}$$

$$C_{n_0-1,l=0} \approx \frac{n_0 - 1}{n_0^2}\left(\frac{r_d}{n_0 a_0}\right)^2 e^{-\frac{r_d}{n_0 a_0}} , \tag{3.24}$$

$$C_{n_0,l=1} \approx -\frac{1}{\sqrt{3}}\left(\frac{r_d}{n_0 a_0}\right) e^{-\frac{r_d}{n_0 a_0}} . \tag{3.25}$$

These terms are similar to the ones in equation 3.16, but increase faster as a function of the displacement distance $r_d$, which is an intuitive result because, by

having more accessible states for the atom to decay, the probability increases according to Fermi's golden rule (Dirac, 1927). The fact that interactions without angular momentum exchange show smaller coefficients for states other than the initial means that these kinds of interactions will be the lower bound of the possible observable effect for our model. In other words, the decomposition calculated in the previous section (equation 3.18) will be the minimum change that a state will undergo as a result of a single interaction. Because it would be the limit for experimentally testing our theory, following analyses will use the coefficients as calculated in equation 3.16.

### 3.1.2 Optimal angle

The described interaction will generate a relative amplitude between consecutive energy levels with $n = n_0$ and $n = n_0 - 1$. This phase depends on the principal quantum number of the states, so it may be possible to find an initial superposition state that maximizes said phase, enhancing the probability of detection.
An atom initially in the eigenstate with $n = n_0$, in the bra-ket notation,

$$|\psi_0\rangle = |n_0\rangle \ , \tag{3.26}$$

will be the transformed by the interaction, as described in equation 3.18, into the state

$$|\psi\rangle = C_{n_0} |n_0\rangle + C_{n_0-1} |n_0 - 1\rangle \ . \tag{3.27}$$

Here we have that the change in the relative amplitude between the states $|n_0\rangle$ and $|n_0 - 1\rangle$ will be

$$\Delta p = \frac{C_{n_0-1}}{C_{n_0}} \ . \tag{3.28}$$

Using the coefficients given in equation 3.19, we obtain that the change will be

$$\Delta p = -\frac{2(n_0 - 1)}{n_0^2} \left( \frac{r_d}{n_0 a_0} \right) \ . \tag{3.29}$$

If we rather have an atom initially in the superposition of states

$$|\psi_0\rangle = \frac{1}{\sqrt{2}} \left( |n_0\rangle + |n_0 - 1\rangle \right) \ , \tag{3.30}$$

then after the interaction we will obtain the transformation

$$|\psi_0\rangle \to |\psi\rangle = \frac{1}{\sqrt{2}}\left(C_{n_0}|n_0\rangle + C_{n_0-1}|n_0-1\rangle + C^*_{n_0}|n_0-1\rangle + C^*_{n_0-1}|n_0-2\rangle\right) \ , \tag{3.31}$$

where the coefficients $C^*_i$ are the same as in equation 3.19, but replacing $n_0$ with $n_0 - 1$. We have that the the change in the relative amplitude will be

$$\begin{aligned}
\Delta p &= \frac{C_{n_0-1} + C^*_{n_0}}{C_{n_0}} - 1 \\
&= \left[-\frac{2(n_0-1)}{n_0^2}\left(\frac{r_d}{n_0 a_0}\right)e^{-\frac{r_d}{n_0 a_0}} + e^{-\frac{r_d}{(n_0-1)a_0}}\right]/e^{-\frac{r_d}{n_0 a_0}} - 1 \\
&= -\frac{2(n_0-1)}{n_0^2}\left(\frac{r_d}{n_0 a_0}\right) + e^{-\frac{1}{n_0-1}\left(\frac{r_d}{n_0 a_0}\right)} - 1 \\
&\approx -\frac{2(n_0-1)}{n_0^2}\left(\frac{r_d}{n_0 a_0}\right) - \frac{1}{n_0-1}\left(\frac{r_d}{n_0 a_0}\right) \ .
\end{aligned} \tag{3.32}$$

We obtain that the change in the relative population increases by an additional term $r_d/(n_0-1)n_0 a_0$ compared to the case of the initial state without superposition in equation 3.29. This can be attributed to the phase of the factor $C_{n_0-1}$ being opposite to the initial phase of the state, which further decreases the population in the state $|n_0-1\rangle$. This result is a first indication that the effect can be amplified by using non-classical states, which will be explored in Chapter 5.

In order to maximize the change in phase, we consider the general superposition state of the form

$$|\Theta\rangle = \cos\theta\,|n_0\rangle + \sin\theta\,|n_0-1\rangle \ , \tag{3.33}$$

and its perpendicular state

$$|\Theta_\perp\rangle = \sin\theta\,|n_0\rangle - \cos\theta\,|n_0-1\rangle \ , \tag{3.34}$$

such that $\langle\Theta|\Theta_\perp\rangle = 0$. These states are orthonormal ($\langle\Theta|\Theta\rangle = \langle\Theta_\perp|\Theta_\perp\rangle = 1$) and form a complete basis in the same space as the vectors $|n_0\rangle$ and $|n_0-1\rangle$,

$$|\psi\rangle = A\,|\Theta\rangle + B\,|\Theta_\perp\rangle \ . \tag{3.35}$$

After the interaction, an initial state $|\Theta\rangle$ will evolve as

$$\begin{aligned}
|\Theta'\rangle &= \cos\theta[C_{n_0}|n_0\rangle + C_{n_0-1}|n_0-1\rangle + \sin\theta[C^*_{n_0}|n_0-1\rangle + C^*_{n_0-1}|n_0-2\rangle] \\
&= C_{n_0}\cos\theta\,|n_0\rangle + (C_{n_0-1}\cos\theta + C^*_{n_0}\sin\theta)\,|n_0-1\rangle + C^*_{n_0.1}\sin\theta\,|n_0-2\rangle \ .
\end{aligned} \tag{3.36}$$

The relative amplitude of the states will be given by

$$\frac{\langle\Theta_\perp|\Theta'\rangle}{\langle\Theta|\Theta'\rangle} = \frac{R\left[\frac{2(n_0-1)}{n_0^2}\cos\theta + \frac{1}{n_0-1}\sin\theta\right]\cos\theta}{1 - R\left[\frac{2(n_0-1)}{n_0^2}\cos\theta + \frac{1}{n_0-1}\sin\theta\right]\sin\theta} \ , \tag{3.37}$$

where

$$R \equiv \left(\frac{r_d}{n_0 a_0}\right) \ . \tag{3.38}$$

To maximize this function we need to find the solution to the equation

$$\frac{d}{d\theta}\frac{\langle\Theta_\perp|\Theta'\rangle}{\langle\Theta|\Theta'\rangle} = 0 \ , \tag{3.39}$$

which gives us the equation

$$\begin{aligned}&\left[\frac{4}{n_0-1}\left(\frac{n_0-1}{n_0}\right)^4 + \frac{1}{n_0-1}\right]R - 4\left(\frac{n_0-1}{n_0}\right)^2\left[1 + \frac{R}{n_0-1}\right]\sin(2\theta_{max}) \\ &+ \left[\frac{4}{n_0-1}\left(\frac{n_0-1}{n_0}\right)^4 - \frac{R}{n_0-1} - 2\right]\cos(2\theta_{max}) = 0 \ ,\end{aligned} \tag{3.40}$$

with $\theta_{max}$ is the angle that maximizes the change in the relative amplitude. Previous calculations suggest that $R \ll 1$, so we can make the approximation

$$2\left(\frac{n_0-1}{n_0}\right)^2\left[\frac{1}{n_0-1}\left(\frac{n_0-1}{n_0}\right)^2\cos(2\theta_{max}) - \sin(2\theta_{max})\right] \approx \cos(2\theta_{max}) \ , \tag{3.41}$$

from which we can get the result

$$\theta_{max} \approx \frac{1}{2}\tan^{-1}\left(\frac{2(n_0-1)^2 - n_0^4}{2n_0^2(n_0-1)^2}\right) \ . \tag{3.42}$$

The value of the angle $\theta_{max}$ for different initial energy levels is shown in figure 3.2. As the value of $n_0$ increases, the optimal angle will tend to $\theta_{max} \sim -0.23182$. Using equation 3.42 we obtain the limits for the angle that maximize the relative change

$$-0.53 < \theta_{max} < -0.23. \tag{3.43}$$

We will take this information into consideration for future calculations for maximizing the probability of detection.

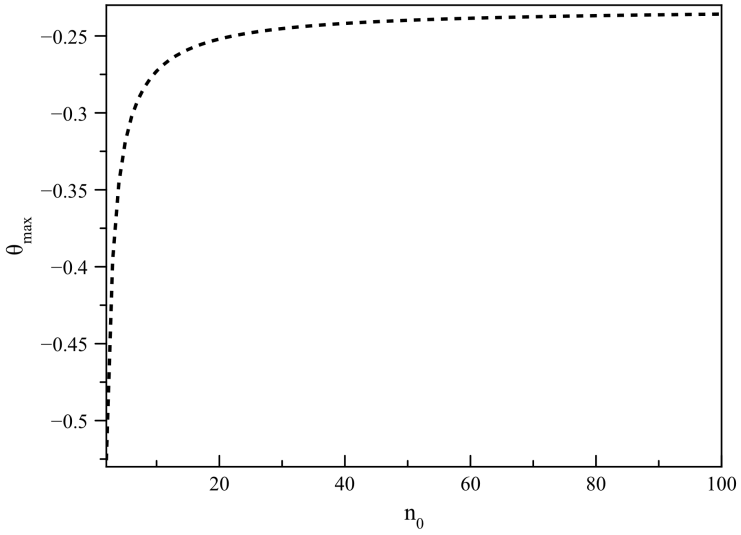


Figure 3.2: Angle that maximizes the change in the relative amplitude after a single scattering as a function of $n_0$ for an initial state described in equation 3.33

### 3.1.3 Function of the perturbation

In order to calculate the magnitude of the coefficients $C_i$ we need to estimate the value of the displacement $r_d$. This parameter depends on how much the nucleus is displaced before the electron perceives its movement. We calculate this distance from the product of the velocity $v_d$ that the nucleus gains as a result of the transferred energy with a time-interval $\tau$, which is small enough to consider the interaction a non-adiabatic process,

$$r_d = v_d \cdot \tau \ . \tag{3.44}$$

The first component can be obtained by calculating the change in the kinetic energy $\Delta E$,

$$v_d = \sqrt{\frac{2\Delta E}{m_N}} \ , \tag{3.45}$$

where $m_N$ is the mass of the nucleus. The exact value for the exchange of energy between the particle and the nucleus will depend on the nature of the interaction.

For simplicity, we approximate the interaction as an inelastic collision, for which the change in energy can be calculated to be

$$\Delta E = \frac{m_p^2 v_p^2}{m_N + m_p} \ , \tag{3.46}$$

where $m_p$ and $v_p$ ar the mass and velocity of the scattered particle, respectively.

For the time $\tau$ we considered different approaches: first, we considered the time it takes for an electron to go around the nucleus in the Bohr model but abandoned the idea because there is no solid justification for using this time as the adiabatic limit. A second consideration for the time was the Planck time, which is the smallest time at which any interaction can occur. We found this time to be unnecessarily restrictive and even physically too small as, according to certain models of a quantized space, no actual displacement could happen within this period (Caldirola, 1980; Yang, 1947).

The time we ultimately chose is the period of production of force-carrying photons (Peskin & Schroeder, 1995). This is the time lapsed between the production of two consecutive photons that carry the electro-magnetic force between the nucleus and the electron, and is given by the formula

$$\tau = \frac{\hbar^3}{4\mu^3} \left( \frac{n_0 m_e}{k_C e^2} \right)^2 \ , \tag{3.47}$$

where $\mu$ is the reduced mass of the atom. Any displacement occurring within this time will be perceived by the electron as occurring instantly because information about the position of the nucleus cannot be generated any faster. For this time, using equations 3.44 and 3.46, we have then that the displacement radius will be

$$r_d = \frac{\hbar^3}{4\mu^3} \left( \frac{n_0 m_e}{k_C e^2} \right)^2 \sqrt{\frac{2 m_p^2 v_p^2}{m_N (m_N + m_p)}} \ . \tag{3.48}$$

If the particle is part of an ensemble that follows a thermal distribution, which is a possibility for stochastic gravitational waves (Kolb & Turner, 1990), we can use kinetic theory to express the velocity in terms of the temperature $T$ of the ensemble (Liboff, 2003),

$$v_p^2 = \frac{3 k_B T}{m_p} \ , \tag{3.49}$$

where $k_B$ is the Boltzmann constant. By substituting equation 3.49 into equation 3.48 we find the relation between the properties of the system and the expected displacement distance. With this relation, we calculate the coefficient of the initial state after the interaction as

$$C_{n_0} = \exp\left[-\frac{n_0\hbar}{2k_C e^2}\left(\frac{m_e + m_N}{m_N}\right)^3 \sqrt{\frac{6m_p k_B T}{m_N(m_N + m_p)}}\right] . \tag{3.50}$$

This form of equation 3.50 may not be immediately useful as it depends on the mass of the scattered particle $m_p$, which gravitational waves lack. Nevertheless, it should hold for the scattering of any particles interacting solely with the nucleus, which are required to have a neutral electrical charge. This would make the scheme useful for the detection of neutral particles, which we will discuss further in section 3.3.2.

To provide a concise estimation of the change in the atomic state, we calculate the effect that a neutron will have after colliding with the nucleus. Figure 3.3 shows this calculation for different initial states of the atom; the considered temperatures correspond to the energy of common neutron sources (Carron, 2007). The figure shows that higher speed of the scattered particle leads to a lower coefficient of the initial energy level, as should be expected. The effect is also observed to be more prominent for high values of $n_0$, being consistent with our previous results and also other studies suggesting that Rydberg states are more susceptible to decoherence by collision of particles (Diaz-Torres, 2010; Miller & Olkiewicz, 2011).

Using the same relation for the displacement distance in equation 3.49, we calculate the coefficient of the closest energy level ($n = n_0 - 1$); the atom will have the highest probability to be found in this state (second only to the initial state) after the interaction. We plotted the coefficient $C_{n_0-1}$ for different initial states, which is shown in figure 3.4. It can be seen that for the highest velocity, the magnitude of $C_{n_0-1}$ stops growing around $n_0 = 25$ and starts to become smaller. This occurs whenever the magnitude of the displacement radius becomes of the order of the size of the atom ($r_d/a_0 \sim 1$), which requires a relatively high energy transference ($\Delta E \sim 10$ eV). Here the ionization of the atom must be taken into account, which is a case that our model excludes by construction.

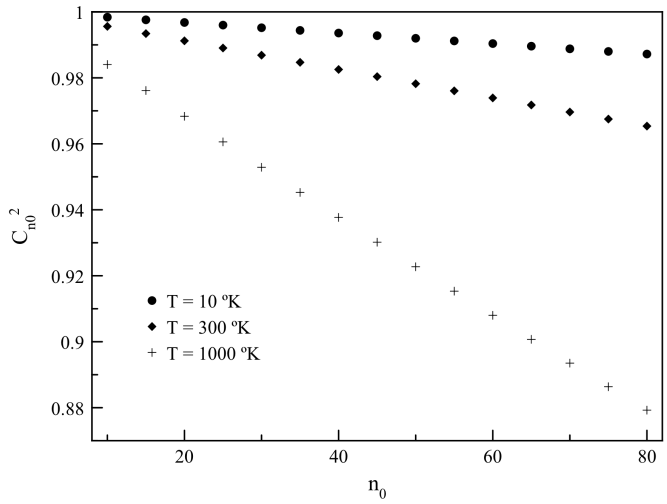


Figure 3.3: Coefficient of the initial eigenstate of an atom after neutron scattering by the nucleus as a function of the initial principal quantum number for different neutron temperatures. The mass of the nucleus is $m_N = 1.66 \times 10^{-27}$ kg and for the neutron $m_p = 1.67 \times 10^{-27}$ kg.

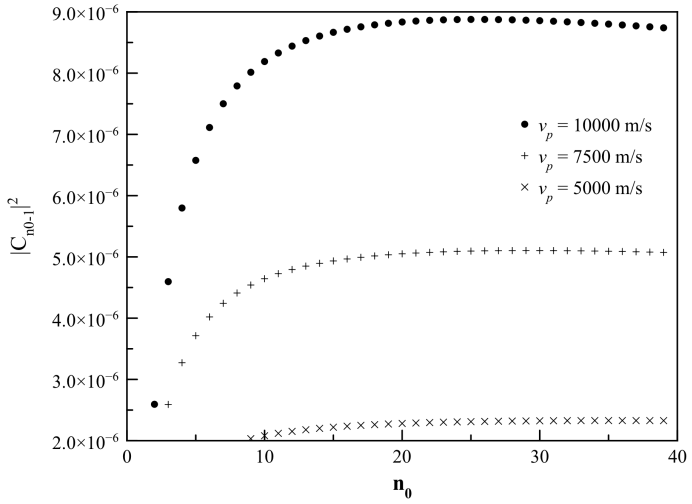


Figure 3.4: Projection after a scattering over the eigenstate one energy level lower than the initial state as a function of the principal quantum number for different velocities. The mass of the nucleus is $m_N = 1.66 \times 10^{-27}$ kg and the the scattered particle $m_p = 1.67 \times 10^{-27}$ kg.

## 3.2 Stochastic interactions

It may be not fully clear that the results obtained in previous sections imply that decoherence in the atomic state arises from the interaction, because they can be interpreted simply as a loss in population for a given energy level that happens at a predictable rate. The argument can be made that the stochastic nature of the interaction (as the momentum of the scattered particle and the scattering angle can't be exactly predicted) will produce an uncertain displacement of the nucleus. This will generate a phase distribution between the energy levels of an ensemble of atoms, which will diminish the coherence of any dynamics that operate within these states.

A more formal demonstration can be made by analyzing the change in the density matrix of the system (Zurek, 2003). In quantum mechanics, the density matrix $\rho$ is a mathematical construct that describes a quantum system with one or more subsystems. If the state of the system can be represented by a vector state $|\psi\rangle$ such that

$$\rho = |\psi\rangle \langle\psi| \ , \tag{3.51}$$

the system is said to be in a *pure state*. If the representation in equation 3.51 can not be found for a particular state, the state is called a *mixed state*. For a mixed state the non-diagonal elements are equal to zero and it presents statistical features of a classic system. Therefore, the smaller the non-diagonal elements are, the closer the system will obey classic probabilities, effectively losing its *quantumness* (Zurek, 2003).

The state of the atom after the interaction can be described as an operator $\Phi$ acting on the initial state

$$|\psi\rangle = \Phi |\psi_0\rangle \ . \tag{3.52}$$

For our model, if we truncate the decomposition of the final state, only taking into account the states $|n_0\rangle$ and $|n_0 - 1\rangle$, we have that the operator $\Phi$ will be equal to

$$\Phi = \begin{pmatrix} C_{n_0} & 0 \\ C_{n_0-1} & C^*_{n_0} \end{pmatrix} \ , \tag{3.53}$$

where the coefficients $C_i$ are calculated in section 3.1 as a function of the momentum of the scattered particle (the coefficient $C^*_{n_0}$ for an initial state $|n_0 - 1\rangle$).

Because the scattered particle belongs to a group with a momentum distribution, we have that the density matrix of the system $\rho$ after the interaction can be calculated as

$$\rho = \int_0^\infty \Phi(p) \left|\psi_0\right\rangle \left\langle\psi_0\right| \Phi^\dagger(p) P(p) dp \ , \tag{3.54}$$

where $P(p)$ is the probability distribution for the momentum $p$ of the group of particles. By restricting the Hilbert space to the states $|n_0\rangle$ and $|n_0 - 1\rangle$ then the post-interaction density matrix will be

$$\rho = \begin{pmatrix} \rho_{11} & \rho_{12} \\ \rho_{21} & \rho_{22} \end{pmatrix} \ , \tag{3.55}$$

where $\rho_{ij}$ (with $i \neq j$) are the off-diagonal elements. For a general initial state,

$$\left|\psi_0\right\rangle = a \left|n_0\right\rangle + b \left|n_0 - 1\right\rangle \ , \tag{3.56}$$

the density matrix $\rho_0$ of the initial state will be

$$\rho_0 = \begin{pmatrix} |a|^2 & ab^* \\ a^* b & |b|^2 \end{pmatrix} \ , \tag{3.57}$$

where $a^*$ and $b^*$ are the complex conjugate of $a$ and $b$, respectively. Given the transformation matrix in equation 3.53 and using equation 3.54, we have that the off-diagonal elements can be calculated as

$$\rho_{ij} = \int_0^\infty (C_{n_0} C_{n_0 - 1} |a|^2 + C_{n_0} C_{n_0}^* a b^*) P(p) dp \ . \tag{3.58}$$

The displacement coefficient $r_d$ can be expressed as a function of the momentum of the particle as

$$r_d = \frac{\hbar^3}{m_N} \left(\frac{m_e^3}{8\mu^5}\right)^{1/2} \left(\frac{n_0}{k_C e^2}\right)^2 p \ . \tag{3.59}$$

Given that the particles follow a thermal distribution of energy, we have the probability distribution

$$P(p) = \frac{4}{\sqrt{\pi}} \left(\frac{m_p}{2k_B T}\right)^{3/2} \frac{p^2}{m_p^2} e^{-\frac{p^2}{2m_p k_B T}} \ . \tag{3.60}$$

We substitute equations 3.59 and 3.60 into equation 3.58, obtaining the solution

$$\rho_{ij} = e^{\left(\frac{2n_0 - 1}{2n_0 - 2}\right)^2 k_p} a b^* - 12 \frac{n_0 - 1}{n_0^2} k_p e^{k_p} |a|^2 \ , \tag{3.61}$$

with

$$k_p = k_B m_p T \left(\frac{m_e^3}{\mu^5}\right) \left(\frac{\hbar^3 n_0}{m_N a_0}\right)^2 \left(\frac{1}{k_C e^2}\right)^4 . \tag{3.62}$$

We have that the constant $k_p$ can be calculated to be $k_p \ll 1$ even for very large values of $m_p$ and $n_0$. With this consideration, we obtain that the value of the off-diagonal elements of the density matrix after the interaction will be

$$\rho_{ij} \approx ab^* - 12\frac{n_0 - 1}{n_0^2} k_p |a|^2 . \tag{3.63}$$

By comparing this with the elements of the initial density matrix in equation 3.57, we obtain that there will be a change in the off-diagonal elements of

$$\Delta\rho_{ij} \approx -12\frac{n_0 - 1}{n_0^2} k_p |a|^2 . \tag{3.64}$$

This quantity is less than 0, proving that there is a reduction of the off-diagonal elements and therefore a loss of coherence in the state after the interaction. Given that the factor $k_p$ is proportional to the square of $n_0$, according to equation 3.62, the relation expressed in equation 3.64 also shows that the induced decoherence increases with the principal quantum number of the initial state, which is our previous claim. Because $\rho_0$ was calculated for a pure state (equation 3.56), the described calculations will not apply directly for mixed states, although a similar decoherence is expected to be observed.

### 3.2.1 Loss of visibility in interference pattern

An interference fringe pattern contains information about the phase of the system and decoherence in the atomic state will produce a loss of visibility of the pattern (Sanz & Borondo, 2007). Because the proposed effect will result in a reduced coherence of the state, as shown in section 3.2, it could be possible to obtain information about the interaction by measuring any loss of visibility in the interference pattern generated by atoms. The loss in visibility can be calculated using the formula

$$\delta v = \left|\frac{\delta\rho}{\rho_0}\right| , \tag{3.65}$$

where $\rho_0$ is the density matrix of the initial state and

$$\delta\rho = \rho - \rho_0 . \tag{3.66}$$

If we have $N$ atoms and prepare half of them into the state $|n_0\rangle$, and the other half in the state $|n_0 - 1\rangle$ we will have the matrix density

$$\rho_0 = \frac{N}{2}\begin{pmatrix} 1 & 0 \\ 0 & 1 \end{pmatrix} . \tag{3.67}$$

The system described here is in a mixed state, so calculations about the resulting decoherence may differ from the ones in section 3.2. Using the operator $\Phi$ given in equation 3.53, we get that the density matrix will evolve as the result of the interaction as

$$\rho = \frac{N}{2}\begin{pmatrix} C_{n_0}^2 & C_{n_0}C_{n_0-1} \\ C_{n_0}C_{n_0-1} & C_{n_0}^{*\,2} + C_{n_0-1}^2 \end{pmatrix} . \tag{3.68}$$

Using this matrix, along with equation 3.66 and 3.67, we obtain that

$$\frac{\delta\rho}{\rho_0} = \begin{pmatrix} C_{n_0}^2 - 1 & C_{n_0}C_{n_0-1} \\ C_{n_0}C_{n_0-1} & C_{n_0}^{*\,2} + C_{n_0-1}^2 - 1 \end{pmatrix} . \tag{3.69}$$

By using this in equation 3.65, we calculate the loss of visibility to be

$$\delta v = 1 + C_{n_0}^2 C_{n_0}^{*\,2} - C_{n_0}^2 - C_{n_0}^{*\,2} - C_{n_0-1}^2 . \tag{3.70}$$

Using the value of the coefficients $C_i$ as calculated in section 3.1, we get that

$$\begin{aligned} \delta v &= 1 + e^{-\frac{2r_d}{n_0 a_0}\left(\frac{2n_0-1}{n_0-1}\right)} - e^{-\frac{2r_d}{n_0 a_0}} - e^{-\frac{2r_d}{n_0 a_0}\left(\frac{n_0}{n_0-1}\right)} - \left(\frac{2r_d}{n_0 a_0}.\frac{n_0-1}{n_0^2}\right)^2 e^{-\frac{2r_d}{n_0 a_0}} \\ &\approx \left(\frac{2r_d}{n_0 a_0}\right)^2 \left[\frac{3n_0-2}{2n_0-2} - \left(\frac{n_0-1}{n_0^2}\right)^2\right] , \end{aligned} \tag{3.71}$$

obtaining that the loss of visibility will increase for the spectrum of Rydberg atoms, this being consistent with our previous results.

For large values of $n_0$, the magnitude of $\delta v$ will approximate to the probability of transition as a result of the interaction ($\sim |C_{n0-1}|^2$). In this case, measuring the loss of visibility in the interference pattern and measuring the change in population of the atomic state will give the same results. A quick calculation gives us that precision interferometry of caesium atoms measuring a loss of visibility of $\delta v = 0.03$ (Peters *et al.*, 1997) puts a limit to the energy of the interaction of $\Delta E < 15.275$ keV, which is a relatively high bound. A better estimation will require us to calculate the decoherence in time for the interacting system.

## 3.3 Temporal evolution

Under certain conditions, it is expected that the nucleus will perform multiple scatterings if it is allowed enough time for interactions to occur. By calculating how this will change coefficients in the decomposition, we will be able to describe the evolution in time of the atomic state.

After one interaction, an atom with an initial state $\psi^{(0)}(r)$ will evolve to the state $\psi^{(1)}(r) = \psi^{(0)}(r + r_d)$ as described earlier in this chapter. When another interaction occurs, the atom will change into the state $\psi^{(2)}(r) = \psi^{(1)}(r+r_d)$ whose eigenstate decomposition is calculated in the same way as for the state after the first collision (equations 3.3 to 3.16), resulting in

$$\psi^{(2)}(r) = e^{-2\frac{k_0}{2}r_d} \sum_{n'=1}^{n_0} L^{-1}_{n_0-n'}\left(k_0 r_d\right) \sum_{n''=1}^{n'} \frac{n'' \cdot n''!}{n_0 \cdot n_0!} L^{-1}_{n'-n''}\left(k_0 r_d\right) \psi(r)_{n''} \ . \tag{3.72}$$

Here we have that the coefficients of the decomposition are given by

$$C^{(2)}_n = e^{-2\frac{k_0}{2}r_d} \frac{n \cdot n!}{n_0 \cdot n_0!} \sum_{n'=n}^{n_0} L^{-1}_{n_0-n'}\left(k_0 r_d\right) L^{-1}_{n'-n}\left(k_0 r_d\right). \tag{3.73}$$

Using the same logic as for the state $\psi^{(2)}(r)$, We calculate the coefficients for the state after a third collision $\psi^{(3)}(r) = \psi^{(2)}(r + r_d)$ and so on until we calculate the coefficients for an arbitrary number of collisions. We obtain that after $q$ collisions, the atom will be left in the state

$$\psi^{(q)} = \sum_{n^{(q)}=1}^{n_0} C_{n^{(q)}} \psi_{n^{(q)}} \ , \tag{3.74}$$

where the coefficients $C_{n^{(q)}}$ are calculated to be

$$\begin{aligned} C_{n^{(q)}} =& e^{-q\frac{k_0}{2}r_d} \frac{n^{(q)} \times n^{(q)}!}{n_0 \times n_0!} \sum_{n^{(q-1)}=n^{(q)}}^{n_0} \sum_{n^{(q-2)}=n^{(q-1)}}^{n_0} \cdots \\ & \sum_{n^{(0)}=n^{(1)}}^{n_0} L^{-1}_{n_0-n^{(0)}}(k_0 r_d) L^{-1}_{n^{(0)}-n^{(1)}}(k_0 r_d) \ldots L^{-1}_{n^{(q-1)}-n^{(q)}}(k_0 r_d) \ . \end{aligned} \tag{3.75}$$

Again we have that the coefficients of the initial state and the closest energy level are several order of magnitude higher than for lower energy levels. Even for a very

high number of interactions, which may not be very probable, we can disregard the rest of the coefficients as their contribution will not be significant. With this consideration, we have that an atom in an initial state with principal quantum number $n_0$ after $q$ scatterings by the nucleus will evolve into the state

$$\psi_{n_0} \xrightarrow{q} \psi(q) \approx C_{n_0}(q)\psi_{n_0} + C_{n_0-1}(q)\psi_{n_0-1} \tag{3.76}$$

where the coefficients $C_i$, according to equation 3.75, will be

$$C_{n_0}(q) = e^{-q\frac{k_0}{2}r_d} \ , \tag{3.77}$$

$$C_{n_0-1}(q) = -q(k_0 r d)\frac{n_0 - 1}{{n_0}^2}e^{-q\frac{k_0}{2}r_d} \ . \tag{3.78}$$

It is important to call attention to the coefficient $C_{n_0-1}$, which is not exponentially dependent upon the number of collisions $q$ (which is time-dependent, as shown next). An exponential dependence is typical for the effect of other sources of decoherence, like energy relaxation of the electron or the interaction of the atom with background radiation (Loudon, 2000). This difference in behavior allows the proposed effect to be distinguishable over other mechanisms of decoherence, hence making the measuring of coefficient $C_{n_0-1}$ particularly important. Also, because it is a function of $n_0$, the change in the atom can be modulated by using different initial states, helping to distinguish the event over other noise sources.

If the probability of interaction is very low, it will be unlikely that the nucleus will undergo more than one scattering event. Under this assumption, if multiple atoms are prepared in the same initial state, the square of the coefficients $C_i$ will represent the population of the corresponding eigenstate. This is relevant, as potential experiments should use the highest possible number of atoms to increase the probability of observing an event and the resolution of the measurements, which will be further discussed in Chapter 5.

To obtain the time dependence of the coefficients $C_i$, we have that the average number of interactions within a certain interval $t$ is given by

$$q(t) = \sigma F_p t \ , \tag{3.79}$$

where $\sigma$ is the effective cross section and $F_p$ is the flux of particles. By substituting this expression into equation 3.77 we obtain the time evolution of the coefficient

$$C_{n_0}(t) = e^{-\frac{k0}{2} r_d \sigma F_p t} \ , \tag{3.80}$$

recalling that the displacement radius was calculated in section 3.1.3 as

$$r_d = \sqrt{\frac{2\Delta E}{m_N}} \frac{\hbar^3}{4\mu^3} \left( \frac{n_0 m_e}{k_C e^2} \right)^2 \ . \tag{3.81}$$

With these relations we proceed to estimate the evolution in time of the atomic state, first for the scattering of photons and then for the scattering of particles with non-zero mass.

### 3.3.1 Photon scattering

An alternative form of equation 3.79 that is useful to calculate the number of scattered photons is

$$q(t) = \sigma \frac{\eta_E c}{h\nu} t \ , \tag{3.82}$$

where $\eta_E$ is the energy density of the electromagnetic radiation, $c$ is the speed of light and $\nu$ is the radiation's frequency. For low energy photons we can consider Thomson scattering by the atomic nucleus (Johnson *et al.*, 2012), which gives the cross section

$$\sigma_T = \frac{8\pi}{3} \left( \frac{k_c e^2}{m_N c^2} \right)^2 \ . \tag{3.83}$$

The average change in the energy of the photon by the scattering, given in the inertial frame of the nucleus, is

$$\Delta E = \frac{h^2 \nu^2}{m_N c^2} \ , \tag{3.84}$$

Using equations 3.80 to 3.84 in conjunction with relations from section 3.1.3, we finally arrive at the function

$$C_{n_0}(t) = \exp \left[ -\frac{\sqrt{8}\pi n_0 \eta_E {m_e}^2 \hbar^3}{3 a_0 \mu^3 {m_N}^3 c^4} t \right] \ . \tag{3.85}$$

With this formula, we calculate how the state of an atom differs from its original state as a function of time for different energy densities of radiation surrounding

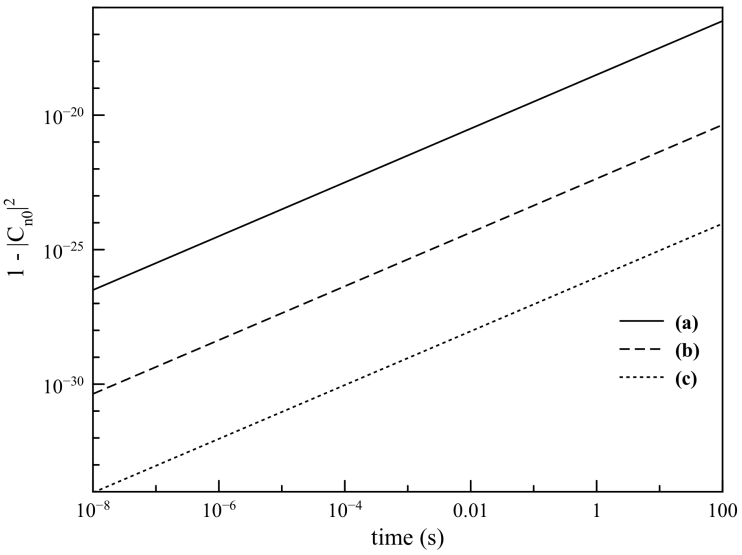


Figure 3.5: Difference in the projection of the initial state of an atom with $n_0 = 60$ and $m_N = 1.66 \times 10^{-27}$ kg as a function of time corresponding to the scattering of **(a)** solar radiation ($\eta_E = 8.49$ MeV/cm$^3$), **(b)** laboratory ambient lights ($\eta_E = 1.17$ keV/cm$^3$) and **(c)** the cosmic microwave background ($\eta_E = 0.25$ eV/cm$^3$).

the atom, which is shown in figure 3.5. The analyzed energy densities correspond to **(a)** the solar radiation on the earth's surface considering a constant insolation of 52.2 PW ($\eta_E = 8.49$ MeV/cm$^3$) (Bird *et al.*, 1983), **(b)** the environment of an atomic physics laboratory with the ambient lights turned on, given a measurement of 4$\mu$W with a detector of 9.5 mm of diameter ($\eta_E = 1.17$ keV/cm$^3$) and **(c)** the cosmic microwave background ($\eta_E = 0.25$ eV/cm$^3$)(Blair, 1974). These cases represent common circumstances for atoms to be exposed to and cover a fair range of energy densities. The effect of the photon scattering is shown to be very small even for very long times and the most energetic radiation. The results may still be relevant for ultra-precise metrology experiments because of the difficulty of shielding the atoms from different kinds of radiation, for which the effect may present a fundamental precision limit. Other studies have analyzed the decoherence induced by the scattering of non-resonant photons, but they are based on the localization of the atom by the scattered light (Ozeri *et al.*, 2007; Uys *et al.*, 2010).

### 3.3.2 Massive particle scattering

We also analyze the effect of scattering of massive particles by the nucleus. This is done having in mind the interaction of the graviton, the force-carrying particle of gravity. Although the graviton is expected to be massless (due to the apparent infinite range of the gravitational force), our model can be applied to set an upper limit to its mass and interaction cross-section (Abbott *et al.*, 2017).

The energy transferred to the nucleus for a scattering event of a massive particle at the most probable angle is given by

$$\Delta E = \frac{\mu}{m_N m_e} \left(m_p v_p\right)^2 \ , \tag{3.86}$$

where $m_p$ and $v_p$ are the mass and the velocity of the scattered particle, respectively. We then have that the coefficient of the initial state evolves as

$$C_{n_0}(t) = \exp\left[-\frac{n_0 \sigma F_p m_p v_p}{\sqrt{8} a_0 m_N} \left(\frac{\mu}{m_e}\right)^{1/2} \left(\frac{m_e}{k_c e^2}\right)^2 \left(\frac{\hbar}{\mu}\right)^3 t\right] \ . \tag{3.87}$$

We use this equation to calculate the evolution of an atom continuously scattering massive particles, as presented in figure 3.6. We analyze two cases that we consider the most significant in terms of limiting the stability of states:

**(1)** Scattering of neutrons.

**(2)** Scattering of dark matter.

In **(1)** we consider neutrons from secondary cosmic rays, having a flux of $F = 2 \times 10^4$ neutrons/$s \cdot m^2$, a cross-section of $\sigma = 3$ barn and a kinetic energy of 0.07 GeV (Hillas, 1927). In **(2)** we analyze the local distribution of dark matter with a reported density of $5.41 \times 10^{-22}$ kg/m$^3$ (Bovy & Tremaine, 2012). We assume that dark matter is thermalized by the background radiation ($T = 2.726$ °K) and that it is composed of axions, with a mass of $m_p = 1$ eV/c$^2$ and a cross-section of $\sigma = 0.01$ barn (Bateman *et al.*, 2015; Dzuba *et al.*, 2010). For experimental observation, all axion-electron interactions can be excluded, as they will result in excitation or even ionization of the atom (Aprile *et al.*, 2014; Dzuba *et al.*, 2010). We choose the axion as the particular candidate of dark matter because of its low mass compared to others, namely the Weakly-Interacting Massive Particle (WIMP), whose interaction is expected to ionize the atom (Savage *et al.*, 2009).

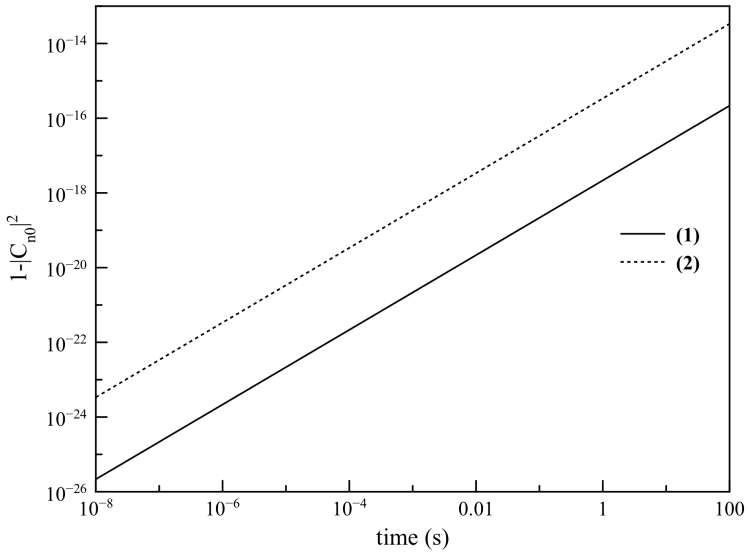


Figure 3.6: Difference in the projection of the initial state of an atom with $n_0 = 60$ and $m_N = 1.66 \times 10^{-27}$ kg as a function of time corresponding to the interaction with **(1)** neutrons from secondary cosmic rays and **(2)** local dark matter composed of axions .

We can see in figure 3.6 that, within the same period, the effect of massive particle scattering seems to be more prominent than for the case of photon scattering in figure 3.5. This is understandable as the effect depends on the amount of momentum transferred to the nucleus, which should be significantly higher for massive particles. These results imply that the scattering of cosmic rays could impose the ultimate limit to the stability of excited atomic systems and to the resolution of Earth-based atomic technology.

It is remarkable that the particular case we analyzed of local dark matter will perturb the atoms to a higher degree than the cosmic rays. This presents the possibility of applying our theory to the detection of such particles, or at least to impose a limit to their mass, by analyzing the coherence in highly stable atomic systems, like the hydrogen maser (Droz *et al.*, 2009; Howe & Walls, 1983). The interaction of exotic matter has already been modelled as a s-wave scattering, with the proposed method of detection based on a model very similar to ours (Bateman *et al.*, 2015). A search for exotic interactions using the decoherence of a Ramsey

interferometer has been suggested previously (Everitt *et al.*, 2011, 2013), but the mechanism for linking the decoherence of internal degrees of freedom of the atom with momentum transfer was left open, which is solved by our model.

After determining that our model is potentially useful for the detection of weakly-interacting particles, we now proceed to calculate the evolution in the atomic state for gravitational interactions.

# Chapter 4

# Decoherence by space-time perturbations

## 4.1 Scattering model

We now apply the model developed in Chapter 3 first for the case of scattering of gravitational waves. For a flat space (linear gravity), there is a duality between the electromagnetic field and the space-time gauge leading to the Gravito-Compton effect (Rothman & Boughn, 2006) in which particles with gravitational charge (mass) scatter gravitational radiation; this is an analogue to the Compton effect, where photons are scattered by electrically charged particles, hence its name. According to the theory, the cross section $\sigma_G$ of the interaction will be given by

$$\sigma_G = \frac{8\pi}{3}\left(\frac{Gm}{c^2}\right)^2 , \tag{4.1}$$

where $G$ is the gravitational constant, $c$ is the speed of light and $m$ is the mass of the scattering object. Because in our model the scattering is done by the nucleus, the mass $m$ will correspond to the nuclear mass $m_N$ from previous expressions. To simplify, we can write equation 4.1 in terms of the Schwarzschild radius $r_{Sh}$ of the mass of the nucleus as

$$\sigma_G = \frac{2\pi}{3} r_{Sh}^2 , \tag{4.2}$$

with $r_{Sh} = 2Gm_N/c^2$. This is the radius of a sphere such that, if all the mass $m_N$ were to be contained within its volume, the escape velocity from the surface

of the sphere would equal the speed of light (Schwarzschild, 1916). For an atom, this radius will be $r_{Sh} \sim 10^{-54}$ m, which is extremely small.

According to section 3.3, we can calculate the evolution of the atomic state with the product of the displacement radius $r_d$, related to the energy exchange, and the number of interactions per second $q$, related to the cross section of the interaction. Based on the Gravito-Compton analogy, the interaction of the gravitational wave will produce a change in energy of

$$\Delta E = \frac{E_G^2}{m_N c^2 + E_G} \ , \tag{4.3}$$

where $E_G$ is the energy carried by the gravitational wave. Using equations 4.1 to 4.3, along with the relations calculated in Chapter 3, we have that the components $r_d$ and $q$ are equal to

$$r_d = \frac{\hbar^3}{\sqrt{8 m_N} \mu^3} \left( \frac{n_0 m_e}{k_C e^2} \right)^2 \frac{E_G}{(m_N c^2 + E_G)^{1/2}} \ , \tag{4.4}$$

$$q = F_G \frac{8\pi}{3} \left( \frac{G m_N}{c^2} \right)^2 t \ , \tag{4.5}$$

where $F_G$ is the flux of gravitational waves. By using the numerical value of all the constants in equations 4.4 and 4.5, we have that the product of the components will be of the order

$$q \ r_d \sim 10^{-100} P_G t \ . \tag{4.6}$$

The value of this product can increase by using a large number of atoms. In this case the probability of interaction will grow not only because of the higher number of targets, but also because of an increment in the Schwarzschild radius, as the gravitational wave will interact with the mass of the ensemble as a whole. As an example, for an ensemble of $10^{10}$ rubidium atoms prepared at $n_0 = 60$ the exponent of coefficient $C_0$ will be $r_d q k_0 / 2t \approx 7.36 \times 10^{-63}$, for the interaction with the gravitational radiation of two merging black holes with estimated $F_G \approx 4.77 \times 10^{28}$ m$^{-2}$s$^{-1}$ and $E_G \approx 0.62$ peV (Abbott *et al.*, 2016b). Experimental observations of this change in the state of the atoms will be quite challenging given the small magnitude of the effect.

Even for the case of a large number of highly excited atoms, and a very energetic gravitational source, the calculated effect is too small to have experimental implications. Still for the scattering of gravitons, whose cross section is estimated several order of magnitude higher than for gravitational waves in equation 4.2 (Rothman & Boughn, 2006), the proposed interaction will not result in any observable change. Rather than trying to apply quantum states to increase the sensitivity of the atoms for the scattering of gravitational waves for the current model, we instead propose a new model of interaction. Before this, we examine another possible use of the current model.

### 4.1.1 Space quantization

Another application for the model of nucleus delocalization is the testing of space quantization. An atom travelling through a quantized space will generate an uncertainty in the position of the nucleus relative to that of the electron in the form

$$r_d = \lambda_c L_P \ , \tag{4.7}$$

where $L_P = 1.6162 \times 10^{-35}$ m is the Planck length and $\lambda_c$ is a dimensionless cut-off parameter (Wang *et al.*, 2006). This will be the size of the space quanta and the minimum change in the relative position between the nucleus and the electron. Because the electron obtains information about the position of the nucleus every period $\tau$, which is the force-carrying photon production time mentioned in section 3.1.3, the position uncertainty will be generated at a rate

$$\frac{1}{\tau} = \frac{4\mu^3}{\hbar^3}\left(\frac{k_c e^2}{n_0 m_e}\right)^2 = \frac{q}{t} \ . \tag{4.8}$$

The product of the components $r_d$ and $q$ will be then

$$q\ r_d \sim 10^{-18}\lambda_c t \ , \tag{4.9}$$

which is a more reasonable quantity in comparison to the scattering of gravitational waves in equation 4.6. In figure 4.1 we plot the change in population of an atomic state for an atom in a quantized space.

Given the values observed in this figure, the model can potentially be used to measure the parameter $\lambda_c$ or at least to impose a bound to its value, which could

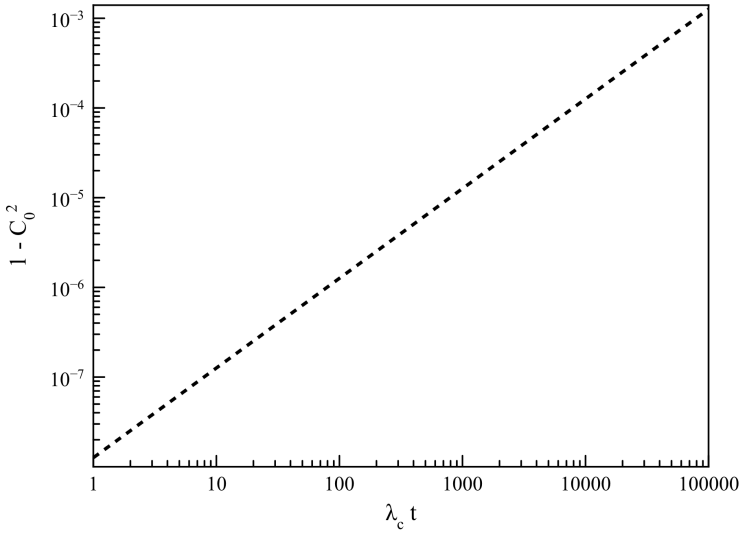


Figure 4.1: Change in the population of the initial state as a function of the cut-off parameter $\lambda_c$ and time for an atom in a quantized space with $n_0 = 2$.

help testing some theories of space-time quantization. For this particular case, it will be preferable to use states with low $n_0$ in order to maximize the rate of photon exchange, which will increase the loss of coherence. Experiments will also require maximization of the travelling time of the atoms to ensure that enough decoherence will be generated. In order to obtain an accurate estimation, further considerations should be taken into account, like a possible non-homogeneous space and the uncertainty in the period $\tau$, although this is beyond the scope of this study.

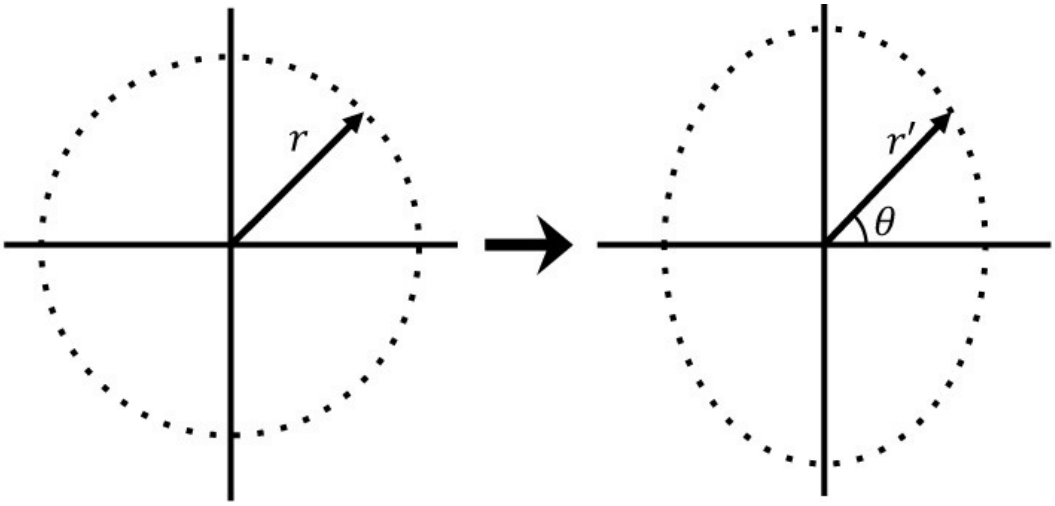


Figure 4.2: The space in the transversal plane of a gravitational wave will be compressed in a certain direction and expanded in the perpendicular axis.

## 4.2 Wave function transformation

It may not be possible to observe the effect of the displacement of the nucleus by the scattering of gravitational waves as calculated in equation 4.6 within realistic settings, so we propose that gravitational waves may have other effects in the atom, presenting a new model of interaction inspired by our previous one. Similar to how the change in the potential by the displacement of the nucleus will change the state of the atom, we suggest that gravitational waves will distort the local potential as perceived by the electron, prompting a similar state change.

A gravitational wave will compress the space along one of the axes of the transversal plane and will expanded it along the perpendicular direction within the same plane (see figure 4.2). We model the distortion of the space in this plane, as seen by an external observer, as

$$r \to r' = r \frac{1 - S_p}{\sqrt{\cos^2\theta + \left(\frac{1-S_p}{1+S_p}\right)^2 \sin^2\theta}} \equiv r A_\theta \ , \tag{4.10}$$

where $S_p$ is the space strain of the gravitational wave in the transversal plane. It is worth clarifying that this distortion does not represent a change in the orbital of the electron, but rather a change in the relative distance for an electron at the

position $\vec{r}$. This is because: 1) in the quantum model the electron is not orbiting the nucleus, like in the Bohr model, and 2) the electron is bound to the nucleus, so the electromagnetic force will compensate for the distance expansion/contraction, correcting the orbital. A way to understand the change in the potential perceived by the electron is to envision the gravitational wave shifting the wavelength of the force-carrying photons from the nucleus, so the effective force will be different at a given angle. Modern interferometry-based gravitational detectors have already detected very small changes in the wavelength of perpendicular light beams caused by gravitational waves (Abbott *et al.*, 2016a, 2017), providing some validity to our proposal.

To calculate the change in the atomic state, we first consider a hydrogen-like atom in an excited state with principal quantum number $n_0$, and no angular momentum (azimuthal quantum number $l = 0$), like in previous chapters and under same arguments. For this system the initial wave function will be

$$\psi_{n_0,0} = \sqrt{\left(\frac{2}{n_0 a_0}\right)^3 \frac{(n_0-1)!}{8\pi n_0 (n_0!)^3}} e^{\frac{r}{n_0 a_0}} L^1_{n_0-1}\left(\frac{2r}{n_0 a_0}\right) . \tag{4.11}$$

If the wavelength of the gravitational wave is significantly bigger than the size of the atom, we can consider the strain $S_p$ constant trough the transversal planes along the atom, so we can use the transformation 4.10 directly in equation 4.11. By doing this we obtain that the wave function will change as

$$\psi_{n_0,0} \to \psi'_{n_0,0} = \sqrt{\left(\frac{2}{n_0 a_0}\right)^3 \frac{(n_0-1)!}{8\pi n_0 (n_0!)^3}} e^{\frac{rA_\theta}{n_0 a_0}} L^1_{n_0-1}\left(\frac{2rA_\theta}{n_0 a_0}\right) . \tag{4.12}$$

We now proceed to find the decomposition of this new wave function in terms of the eigenstates $\psi_{n,l,m}$, which correspond to an atomic system in an unperturbed space,

$$\psi'_{n_0,0} = \sum_{n,l,m} C_{n,l,m}\psi_{n,l,m}(r,\theta,\phi) . \tag{4.13}$$

The coefficients in the decomposition are calculated with

$$C_{n,l,m} = \int_0^\infty r^2 dr \int_0^\pi sin\theta \; d\theta \int_0^{2\pi} d\phi \; \psi^*_{n,l,m}\psi'_{n_0,0} . \tag{4.14}$$

Solving equation 4.14 numerically is once again very time consuming, so we use other approximations that allow us to find an analytical solution. First, we have the mathematical identity (Abramowitz & Stegun, 1983)

$$L^1_{n_0-1}\left(\frac{2rA_\theta}{n_0a_0}\right) = e^{-\frac{2r}{n_0a_0}(1-A_\theta)}\sum_{k=0}\frac{(1-A_\theta)^k}{k!}\left(\frac{2r}{n_0a_0}\right)^k L^{1+k}_{n_0-1}\left(\frac{2r}{n_0a_0}\right) \ . \quad (4.15)$$

Then, for very small values of the strain constant ($S_p \ll 1$), we can use the approximations

$$e^{-\frac{r}{n_0a_0}(3-2A_\theta)} \approx e^{-\frac{r}{n_0a_0}} \ , \quad (4.16)$$

$$(1-A_\theta)^k \approx [S_p cos(2\theta)]^k \ . \quad (4.17)$$

By substituting equations 4.15 to 4.17 into equation 4.12 we are able to separate the wave function into a radial part and an angular part

$$\psi'_{n_0,0} = \sum_{k=0}\frac{{S_p}^k}{k!}{R'}_{n_0,k}(r)\ {Y'}_k(\theta) \ , \quad (4.18)$$

with

$$\begin{aligned} {R'}_{n_0,k}(r) &= \sqrt{\left(\frac{2}{n_0a_0}\right)^3\frac{(n_0-1)!}{2n_0(n_0!)^3}}e^{-\frac{r}{n_0a_0}}\left(\frac{2r}{n_0a_0}\right)^k L^{1+k}_{n_0-1}\left(\frac{2r}{n_0a_0}\right) \ , \\ {Y'}_k(\theta) &= \frac{1}{\sqrt{4\pi}}cos^k(2\theta)L^{1+k}_{n_0-1}\left(\frac{2r}{n_0a_0}\right) \ , \end{aligned} \quad (4.19)$$

similar to the calculations in Chapter 3. With this, we have that the integral of the radial component in equation 4.14 is equal to

$$\int_0^\infty {R'}_{n_0,k}(r)\ R_{n,l}(r)\ dr = \sqrt{\frac{(n_0-1)!(n_0-l-1)!}{[n_0!(n_0+l)!]^3}}\frac{[(n_0+k)!]^3}{(n_0-l-1)!}\delta_{n_0n} \ , \quad (4.20)$$

where $\delta$ is the Kronecker delta. Equation 4.20 tells us that the projection of the wave function is only on the eigenstate with same principal quantum number as the initial state. This is different from the results obtained in Chapter 3, where the interaction will partially project the wave function into lower principal quantum number states. The result can be explained by the fact that in the current model

Table 4.1: Value of the component $\Theta_{k,l}$ by solving equation 4.21 for different values of $k$ and $l$.

| | $l$=0 | $l$=2 | $l$=4 | $l$=6 |
|---|---|---|---|---|
| $k$=0 | 1 | 0 | 0 | 0 |
| $k$=1 | -1/3 | 4/15 | 0 | 0 |
| $k$=2 | 7/15 | -8/105 | 32/315 | 0 |
| $k$=3 | -9/15 | 4/21 | -32/1155 | 128/3003 |

the atom does not perform any scattering or acquire any additional momentum, so no transference from potential to kinetic energy should occur.

By solving the integral for the angular component in equation 4.14 we obtain

$$\int_0^{\pi}\int_0^{2\pi} sin\theta\ {Y'}_k(\theta)\ Y_l^m(\theta,\phi)\ d\phi\ d\theta = \begin{cases} \sqrt{2l+1}\ \Theta_{k,l}\delta_{m,0} & \text{for } l = 0,2,4,... \\ 0 & \text{for } l = 1,3,5,... \end{cases} . \tag{4.21}$$

Equation 4.21 indicates that after the gravitational interaction, the atom will be perceived as having a small projection into states with even azimuthal number. This is a significant result, as the graviton is theorized to have intrinsic angular momentum $l = 2$, so a transition in the atom mediated by this particle should be expected to have $\Delta l = \pm 2$. The coefficients from equation 4.21 can then be interpreted as the atom absorbing $l/2$ number of gravitons. The non-trivial values of the term $\Theta_{k,l}$ are shown in table 4.1, where it can be seen that $\Theta_{k,l} = 0$ for $k < l/2$. With the product of the results in equation 4.20 and 4.21 we obtain the value of the coefficients $C_{n,l,m}$.

From equation equation 4.18 we get that the coefficients are proportional to ${S_p}^k$. Because $S_p$ is expected to be extremely small ($\sim 10^{-20}$) (Abbott *et al.*, 2017), we disregard all terms in the summation for $k \geq 2$, so we get that the state of the atom evolves into

$${\psi'}_{n_0,0,0} \approx C_0(n_0)\psi_{n_0,0,0} + C_2(n_0)\psi_{n_0,2,0}\ , \tag{4.22}$$

with

$$\begin{aligned} C_0(n_0) &= 1 - \frac{S_p}{3}(n_0+1)^3 \ , \\ C_2(n_0) &= S_p \frac{4(n_0+1)}{3(n_0+2)^2}\sqrt{({n_0}^2-1)({n_0}^2-4)/5} \ . \end{aligned} \tag{4.23}$$

We find therefore that an atom with no initial angular momentum will be perceived as having part of its wave function projected into a state with the same principal quantum number but azimuthal number equal to two after it interacts with a gravitational wave. The projection is proportional to the strain in space caused by the gravitational wave and increases for atoms in a higher energy level, which is consistent which previous results.

### 4.2.1 General model

For an atomic state corresponding to a principal quantum number $n_0 \geq 2$ and azimuthal quantum number $l_0 \geq 1$, the wave function is altered by the gravitational wave as

$$\psi_{n_0,l_0,} \rightarrow \psi' = \sum_{n,l} C_{n,l}\psi_{n,l} \ , \tag{4.24}$$

with a change similar to the one described in equation 4.10. Following the same steps as for an initial state with no angular momentum (equations 4.14 to 4.17), and after solving the proper integrals, we find that the state of the atom is perceived as partially projected into states with azimuthal number equal to the initial state plus or minus multiples of two ($l = l_0 \pm 2, 4, 6, ...$),

$$\begin{aligned} \psi' =& C_{n_0,l_0}\psi_{n_0,l_0} + C_{n_0,l_0+2}\psi_{n_0,l_0+2} + C_{n_0,l_0+4}\psi_{n_0,l_0+4} + C_{n_0,l_0+6}\psi_{n_0,l_0+6} + ... \\ &+ C_{n_0,l_0-2}\psi_{n_0,l_0-2} + C_{n_0,l_0-4}\psi_{n_0,l_0-4} + C_{n_0,l_0-6}\psi_{n_0,l_0-6} + ... \quad . \end{aligned} \tag{4.25}$$

Similar to the case of no initial angular momentum, the projection is mostly over the initial state and states with azimuthal numbers that differ by two ($l = l_0 \pm 2$). With this consideration we have that the wave function evolves into

$$\psi' \approx C_0\psi_{n_0,l_0} + C_{+2}\psi_{n_0,l_0+2} + C_{-2}\psi_{n_0,l_0-2} \ , \tag{4.26}$$

where the coefficients $C_i$ are calculated to be

$$\begin{aligned}
C_0 &= 1 - S_p \frac{(n_0 + l_0 + 1)^3}{(2l_0 - 1)(2l_0 + 3)} \\
C_{+2} &= 2S_p \frac{(l_0 + 1)(l_0 + 2)}{2l_0 + 3} \sqrt{\left(\frac{n_0 + l_0 + 1}{n_0 + l_0 + 2}\right)^3 \frac{(n_0 - l_0 - 1)(n_0 - l_0 - 2)}{(2l_0 + 1)(2l_0 + 5)}} \\
C_{-2} &= 2S_p \frac{l_0(l_0 - 1)(n_0 + l_0 + 1)^3}{2l_0 - 1} \sqrt{\frac{(n_0 + l_0)^3 (n_0 + l_0 - 1)^3}{(n_0 - l_0)(n_0 - l_0 + 1)(2l_0 + 1)(2l_0 - 3)}} \, .
\end{aligned} \tag{4.27}$$

We now have that the change in the initial state will increase as a function of both $n_0$ and $l_0$. As an example, by preparing atoms with very high quantum numbers $n_0 + l_0 \sim 100$ (Dutta *et al.*, 2001), we can increase the effect of the interaction by around $\Delta C_0 \sim 10^6$.

We considered two possible interpretations to results from equation 4.26, according to the nature of the interaction: first, the gravitational wave exchanges energy with the atom, altering the angular momentum of the electron. Second, the gravitational wave only shifts the relative energy between the energy levels of the atom, as perceived by an external observer.

### 4.2.2 Atomic transition

In our first interpretation, the gravitational wave induces a transition in the atom by an exchange of angular momentum through the graviton. It can be argued that, because no energy transference occurs, the transition is only possible due to the degeneracy of the energy levels. If so, the transition could not take place in non-hydrogen atoms due to the quantum defect and the Lamb shift (Griffiths, 1995) separating the levels, which should be specially relevant for more complex atoms, like rubidium. Nevertheless, both the quantum defect and the Lamb shift decrease rapidly with the principal quantum number, so their effect will be negligible for Rydberg atoms (Afrousheh *et al.*, 2006; Low *et al.*, 2012).

A single interaction with gravitons will change the wave function from the initial state $\psi^{(0)}$ to the state $\psi^{(1)}$,

$$\psi^{(0)}(l_0) \to \psi^{(1)} = C_0(l_0)\psi(l_0) + C_{+2}(l_0)\psi(l_0 + 2) + C_{-2}(l_0)\psi(l_0 - 2) \, , \tag{4.28}$$

as previously calculated. A second interaction will then produce a change in the wave function $\psi^{(1)}$,

$$\begin{aligned}\psi^{(1)} \to \psi^{(2)} = C_0(l_0)\,[C_0(l_0)\psi(l_0) + C_{+2}(l_0)\psi(l_0+2) + C_{-2}(l_0-2)\psi(l_0-2)] \\ + C_{+2}(l_0)\,[C_0(l_0+2)\psi(l_0+2) + C_{+2}(l_0+2)\psi(l_0+4) + C_{-2}(l_0)\psi(l_0-2)] \\ + C_{-2}(l_0)\,[C_0(l_0-2)\psi(l_0-2) + C_{+2}(l_0-2)\psi(l_0) + C_{-2}(l_0-2)\psi(l_0-4)]\ .\end{aligned} \tag{4.29}$$

In equation 4.27 we can see that the coefficients $C_i$ depend linearly on the strain factor $S_p$. Because of the assumed magnitude of this term, we can make the approximations

$$C_0 C_0 \approx 1 - 2S_p \frac{(n_0+l_0+1)^3}{(2l_0-1)(2l_0+3)} \equiv 1 - 2c_0\ , \tag{4.30}$$

$$C_0 C_{+2} \approx C_{+2}\ ,\ C_0 C_{-2} \approx C_{-2}\ , \tag{4.31}$$

$$C_{+2} C_{+2} \approx 0\ ,\ C_{-2} C_{-2} \approx 0\ ,\ C_{+2} C_{-2} \approx 0\ . \tag{4.32}$$

with

$$c_0 = S_p \frac{(n_0+l_0+1)^3}{(2l_0-1)(2l_0+3)}\ . \tag{4.33}$$

Using these approximations in equation 4.29, we have that the wave function after the second interaction will be

$$\psi^{(2)} \approx [1 - 2c_0(l_0)]\,\psi(l_0) + 2C_{+2}(l_0)\psi(l_0+2) + 2C_{-2}(l_0)\psi(l_0-2)\ . \tag{4.34}$$

Following the same logic (similar to the method used in section 3.3), we calculate the wave function after a third and fourth interaction, and so on. We get that after $q$ interactions, an atom in an initial state $\psi_{n_0,l_0}$ will evolve as

$$\psi_{n_0,l_0} \xrightarrow{q} \psi^{(q)} \approx (1 - q\ c_0)\,\psi_{n_0,l_0} + qC_{+2}\psi_{n_0,l_0+2} + qC_{-2}\psi_{n_0,l_0-2}\ , \tag{4.35}$$

By finding the rate of interaction, equation 4.35 tells us how the state of the atom is expected to change in time while being subject to gravitational fluctuations. The number of events $q$ will be given by

$$q = \sigma_G F_G t\ , \tag{4.36}$$

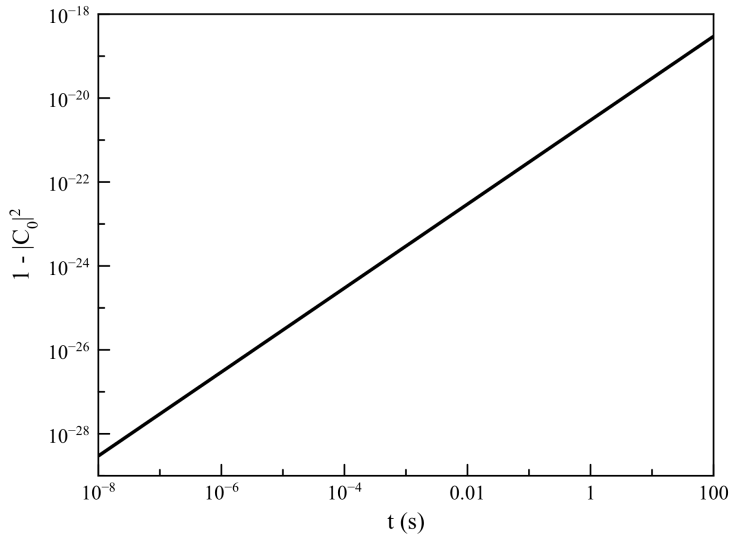


Figure 4.3: Change in population of the initial state for an ensemble of $10^{10}$ rubidium atoms prepared with $n_0 = 50$ and $l_0 = 0$ interacting with a stream of gravitational waves with $F_G = 4.77 \times 10^{28} m^{-2} s^{-1}$ and $E_G = 0.62 peV$.

where $\sigma_G$ and $F_G$ are the cross-section and flux of gravitons, respectively. The cross-section of the graviton for interactions with matter is theorized to be about (Rothman & Boughn, 2006)

$$\sigma_G \sim G\hbar \ . \tag{4.37}$$

Using the same parameters as in the example described in section 4.1, we calculate the evolution in time of the atomic ensemble for the new model, which is plotted in figure 4.3. It can be seen that there is a greater change in the population of the initial state compared to that calculated for scattering in equation 4.6.

An experimental test of this model can be performed by preparing a large number of atoms in an excited state and measuring the decline in the population of the state after the atoms interact with the gravitational wave. The measured change is then adjusted to the evolution of the system predicted with equation 4.35, which will give us the value of the parameter $S_p$. The decay rate can be modulated by changing the initial state of the atoms, which can be used to refine the measurements. For a coherence time of 0.02 s (Deleglise *et al.* (2008)), the

expected change in the population will be a fraction of $\sim 10^{-23}$, which is several orders of magnitude smaller than the current achievable resolution.

### 4.2.3 Transition detuning

Our second interpretation describes a shift in the relative energy of the states as a result of the change in the perceived potential. The atom interacting with a gravitational wave will experience a change in the energy of its eigenstates

$$E_{n,l} \to E'_{n,l} \ , \tag{4.38}$$

which is a function of the coefficients $C_0$, $C_{+2}$ and $C_{-2}$ as

$$E'_{n,l} = {C_0}^2 E_{n,l} + {C_{+2}}^2 E_{n,l+2} + {C_{-2}}^2 E_{n,l-2} \ . \tag{4.39}$$

The coefficients $C_i$ depend non-linearly on the principal quantum number (equation 4.23), so the difference in energy between two distinct energy levels,

$$\Delta E = E_2 - E_1 \ , \tag{4.40}$$

will be different after the interaction by $\Delta$,

$$\Delta E' = E'_2 - E'_1 = \Delta E + \Delta \ . \tag{4.41}$$

Light originally used to drive a transition between states with energy $E_1$ and $E_2$ will be then detuned by

$$\Delta = \Delta E' - \Delta E = (E'_2 - E_2) - (E'_1 - E_1) \ , \tag{4.42}$$

while the atom interacts with the gravitational wave. With the change in energy described in equation 4.39, we have that

$$E'_i - E_i = -E_i \left( 1 - {C_0}^2 - {C_{+2}}^2 \frac{E_{i+2}}{E_i} - {C_{-2}}^2 \frac{E_{i-2}}{E_i} \right) \ . \tag{4.43}$$

For the values of $C_j$ indicated in equation 4.27, we have that this difference will be

$$E'_i - E_i = -E_i \left[ 2S_p \frac{(n_i + l_i + 1)^3}{(2l_i - 1)(2l_i + 3)} + \kappa({S_p}^2) \right] \ , \tag{4.44}$$

where $\kappa({S_p}^2)$ is a factor that is proportional to ${S_p}^2$. Because this term is very small, we can make the approximation

$$E_i' - E_i \approx -2S_p \frac{E_i(n_i + l_i + 1)^3}{(2l_i - 1)(2l_i + 3)} \ . \tag{4.45}$$

With this we finally arrive at the relation

$$\Delta = -2S_p \left[ \frac{E_2(n_2 + l_2 + 1)^3}{(2l_2 - 1)(2l_2 + 3)} - \frac{E_1(n_1 + l_1 + 1)^3}{(2l_1 - 1)(2l_1 + 3)} \right] \ . \tag{4.46}$$

Light with energy $\Delta E$ will be detuned for the transition by $\Delta \sim S_p \Delta E$, around a fraction of $10^{-20}$ of the original energy difference. For comparison, the most precise measurement of transition detuning is performed on strontium atomic clocks, in which the frequency is measured with an uncertainty of $\sim 10^{-15}$ (Akamatsu *et al.*, 2014).

For atoms prepared with $n_0 \sim 50$ (Kubler *et al.*, 2010; Singer *et al.*, 2004), the detuning will be augmented by $\sim 10^5$ compared to the lowest energy levels, even for transitions of states with close quantum numbers. As a more concise example, the H110$\alpha$ emission of the Carina nebula at 4.8 GHz (Brooks *et al.*, 2001) would experience a change in its wavelength of $\Delta\lambda \approx 5.6 \times 10^{-16}$m if a gravitational wave passed through. A change of this magnitude could be measured using extremely accurate interferometry, like the one currently applied in gravitation wave detection (Abbott *et al.*, 2016b, 2017), making the proposed effect potentially observable with current technology.

It should be noted that only for times much shorter than the period of the gravitational wave ($t \ll \tau_{gw}$) can the strain in the transversal plane $S_p$ be considered constant. For longer times, the strain in space by gravitational waves will fluctuate, so the detuning of the light should be calculated as a function of time for long-duration experiments,

$$\Delta(t) = -2 \left[ \frac{E_2(n_2 + l_2 + 1)^3}{(2l_2 - 1)(2l_2 + 3)} - \frac{E_1(n_1 + l_1 + 1)^3}{(2l_1 - 1)(2l_1 + 3)} \right] S(t) \ . \tag{4.47}$$

Another possible way to test this model is by analyzing the Rabi oscillations of an ensemble of atoms (Johnson *et al.*, 2008). If a deviation in the population of the energy levels is observed after a period of time and it can be adjusted to

correspond to the detuning in the electromagnetic field as described by equation 4.47, we can infer that the atoms were interacting with gravitational waves. To calculate the deviation, we have that for a two-level system the probability of finding an atom in the excited state will be

$$P_e(\Delta\omega, t) = \frac{\omega^2}{\Delta\omega^2 + \omega^2} \sin^2\left(\frac{\sqrt{\Delta\omega^2 + \omega^2}}{2} t\right) , \tag{4.48}$$

where $\omega$ is the Rabi frequency and $\Delta\omega$ is the frequency detuning, which is related to the energy shift in equation 4.47 simply by $\Delta\omega = \Delta/\hbar$. In this case, light that was previously resonant to the transition will be detuned because of the shift in the energy of the transition. The Rabi cycle will deviate from its resonant dynamics $P_e(\Delta\omega = 0, t)$ by

$$\begin{aligned} \delta P &= P_e(0, t) - P_e(\Delta\omega, t) \\ &= \sin^2\left(\frac{\omega}{2} t\right) - \frac{\omega^2}{\Delta\omega^2 + \omega^2} \sin^2\left(\frac{\sqrt{\Delta\omega^2 + \omega^2}}{2} t\right) . \end{aligned} \tag{4.49}$$

When the detuning is much smaller than the Rabi frequency ($\Delta \ll \omega$), we can use the approximation

$$\sqrt{\Delta\omega^2 + \omega^2} \approx \omega + \Delta\omega^2/2\omega , \tag{4.50}$$

which can be substituted in equation (4.49) to obtain

$$\delta P \approx \sin^2\left(\frac{\omega}{2} t\right) \left[1 - \frac{\omega^2}{\Delta\omega^2 + \omega^2} \cos^2\left(\frac{\Delta\omega^2}{4\omega} t\right)\right] . \tag{4.51}$$

Using equation 4.51 for short times (compared to the period of the gravitational wave), we get that the deviation can be approximated as

$$\delta P \approx \left(\frac{\Delta\omega^2}{4\omega} t\right)^2 . \tag{4.52}$$

This equation indicates that the deviation increases with the detuning and decreases with the Rabi frequency, making again the effect more prominent in transitions of states with high quantum numbers (Dutta *et al.*, 2001). For comparison, the deviation in the Rabi cycle $\delta P$ for the transition 50S – 51P of a rubidium

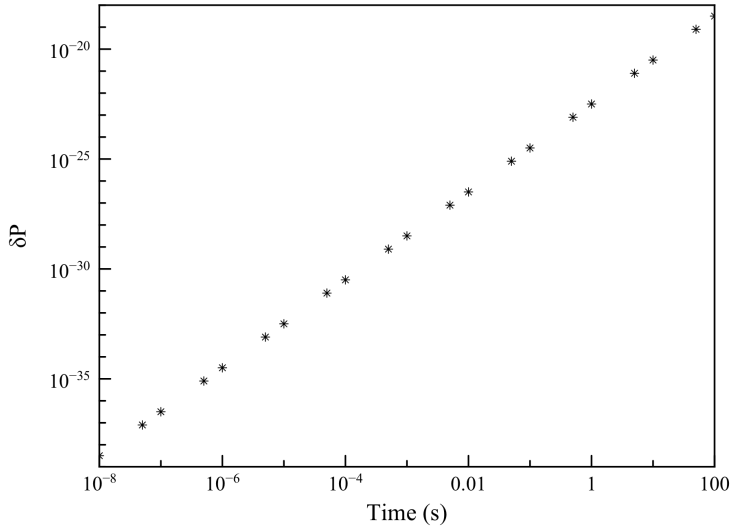


Figure 4.4: Deviation in the Rabi cycle for a 50S – 51P transition with a Rabi frequency of 47 kHz, which arises from the interaction with a gravitational wave with peak strain of $Sp = 10^{-20}$.

atom (Brune *et al.*, 1996) exposed to gravitational waves will be $10^4$ times higher than the deviation for the transition 1S – 2P for the same atom.

For longer times ($t > \pi\omega/\Delta\omega^2$), the deviation will be mostly due to the increased frequency of the cycle. In this case, the ideal transition will be obtained by maximizing the energy difference between the levels (Dudin *et al.*, 2012). If a system undergoing Rabi oscillations is measured at times corresponding to N completed cycles ($t = 2N\pi/\omega$), the expected deviation will be

$$\delta P(t = 2N\pi/\omega) \approx \left(\frac{N\pi\Delta\omega^2}{2\omega^2}\right)^2 . \tag{4.53}$$

In figure 4.4 we show the expected measured deviation for completed cycles using the mentioned 50S – 51P transition. In this figure it can be seen that the effect becomes significant for very long times, which may require for experiments to implement a high-Q cavity in order to extend the coherence time of the atoms by suppressing most of the undesired transitions (Varcoe *et al.*, 2000; Walther *et al.*, 2006). For the aformentined coherence time (0.02 s) the deviation in the cycle will be $\sim 10^{-27}$, still below current experimental sensitivity.

Although a large ensemble of Rydberg atoms can be prepared (Dudin *et al.*, 2012) to improve the probability of detection, collective effects should be taken into consideration (Quinones *et al.*, 2017) especially for such highly excited atoms, as they exhibit long-range correlations (Browaeys & Lahaye, 2013; Lee *et al.*, 2012; Lukin *et al.*, 2001).

## 4.3 Collective interaction of Rydberg atoms

One of the main features of Rydberg atoms is their high polarizability, which increases as $\sim n^7$ (Gallagher, 2007). This results in the atoms having long-range dipolar interaction between them. The interaction will produce a displacement of the energy levels, shifting the transition energy. If the shift is big enough, it will suppress the transition by means of photon absorption or stimulated emission, because the light will be out of resonance. When two atoms are close enough (at a distance called the blockade radius), the excitation of one of the atoms will produce a shift in the transition energy of other one equal to the linewidth of the transition, completely blocking it (Browaeys & Lahaye, 2013; Singer *et al.*, 2004); this effect is known as Rydberg blockade. It is not expected for the interaction of the gravitational wave to be blocked. A gravitational fluctuation will rather provide an additional shift to the transition energy as calculated before. Nevertheless, the quadrupole transition by the gravitational wave will change if a collective interaction of the atoms with a common field (in this case the oscillating gravitation field) arises.

To analyze the interaction with the field, we start from the quantum field equation

$$\ddot{\phi} = \nabla^2\phi - (1+2\nu)\mu^2\phi \ , \tag{4.54}$$

where $\nu$ is the external potential and $\mu = m/\hbar$ is the inverse of the reduced Compton wavelength. This equation gives the solution

$$\phi_n = \sqrt{\frac{\hbar}{2w_n}}(a_n e^{-\imath w_n t} + a_n^\dagger e^{\imath w_n t})\psi_n \ , \tag{4.55}$$

with $w_n = \mu + E_n/\hbar$ and with $a_n$ and $a_n^\dagger$ the annihilation and creation operators, respectively. If $|n\rangle$ represents the state for a given energy level, the ladder operator

$a_n$ will be such that $a_n^\dagger |0\rangle = |n\rangle$. Using this solution in conjunction with the general master equation for matter interacting with gravitational waves (Oniga & Wang, 2016)

$$\dot{\rho} = -\frac{i}{\hbar}[H_{int}, \rho] + D_\rho \ , \tag{4.56}$$

where $H_{int}$ describes the interaction with fields other than the gravitational one and $D_\rho$ is the non-Markovian quantum dissipator,

$$D_\rho = \Gamma_0\{s(1-s)[N\rho + N_{GW}(\omega_0)\rho']\}' \ , \tag{4.57}$$

will lead to a gravitational spontaneous emission rate

$$\Gamma = \frac{2Gm^2\omega^5 q_{1,2}^2}{45\hbar} \ , \tag{4.58}$$

where $G$ is the gravitational constant and $q_{1,2}^2$ is the square modulus of quadrupole moment of the transition between the states $|n_1, l_1\rangle$ and $|n_2, l_2\rangle$. The full mathematical derivation of this result can be seen in the reference (Quinones *et al.*, 2017). It is noticeable that the rate increases with the energy of the transition, which is consistent with our previous results.

If the wavelength of the gravitational wave is bigger than the size of the ensemble (which should be true for most gravitational waves), the transition rate will have a dependence on the number of atoms of the form

$$\Gamma_{GW} = \frac{N^2}{4}\Gamma N_{GW}(\omega) \ , \tag{4.59}$$

where $N$ is the number of atoms in the ensemble and $N_{GW}(\omega)$ is the distribution function of the gravitational waves (Gross & Haroche, 1982). A quadratic dependence on the number of emitters, in this case the atoms, is known as *superradiance* (Bekenstein & Schiffer, 1998). Equation 4.59 can be applied to calculate the transition rate of the interaction with vacuum fluctuation if its distribution function $N_{VF}(\omega)$ is used instead of $N_{GW}$ (Quinones *et al.*, 2017).

We apply the same amplification effect to our transition model in section 4.2.2, obtaining the change in time of the initial state population for the same system as shown in figure 4.5. A significant change can be seen compared to the non-interacting case in figure 4.3. For the same period of 0.02s, the expected change in population will be $\sim 10^{-13}$, which starts to become experimentally significant.

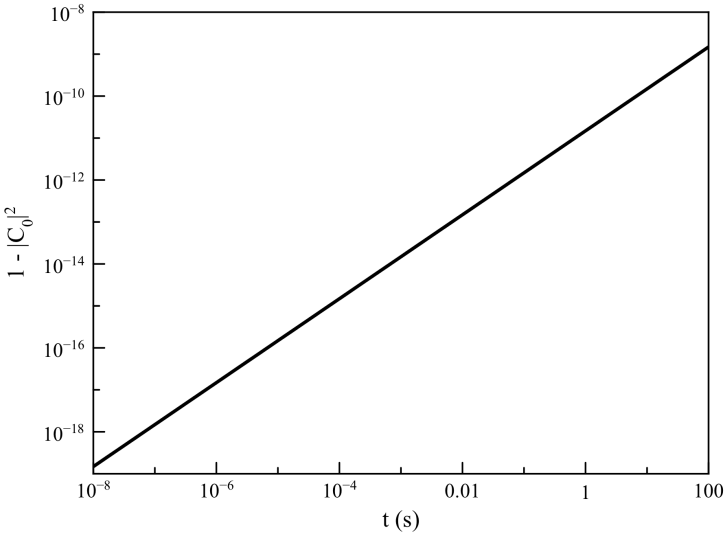


Figure 4.5: Change in population of the initial state for an ensemble of $10^{10}$ mutually interacting rubidium atoms with $n_0 = 50$ and $l_0 = 0$ exposed to a common gravitational field with $F_G = 4.77 \times 10^{28} m^{-2} s^{-1}$ and $E_G = 0.62 peV$.

From these results it can be concluded that correlated atoms, in this case by long-range dipolar interactions, will be more sensitive to gravitational perturbation, compared to uncorrelated atoms. With this in mind, we analyze how atoms with other kind of correlations (entanglement) will change as a result of their interaction with gravitational waves.

# Chapter 5

# Metrology of quantum states

In previous chapters it was calculated that a relative phase will arise between two eigenstates of the atom after its interaction with a gravitational wave. Depending on the model, these eigenstates will differ in their principal or azimuthal quantum numbers. The change can be amplified by using atoms prepared in a highly excited state, but even for the optimal case (as described in Chapter 4) it will be very challenging to detect the effect with current technology. In section 4.3 it was described how correlated atoms (through mutual dipolar interactions) change their state in a higher degree after interacting with gravitational fluctuations. It could be expected that atoms prepared in different quantum states that present correlations will evolve in a way that will make the effect easier to be detected.

Several studies have analyzed how the correlation of the experiment's probes enhance their sensitivity to a change of phase, which gives a better estimation of the interaction for lower experimental resources (Johnsson *et al.*, 2016; Ma *et al.*, 2017). These resources can be the number of probes, in our case the number of atoms in the ensemble (Facon *et al.*, 2016), or the interaction time, which for the case of gravitational waves is expected to be very small (Juffmann *et al.*, 2016). In order to calculate any possible improvement to the measurements, we analyze the evolution of the atom after the interaction for different initial quantum states. We start our calculations for an initial state with principal quantum number $n_0$ and angular momentum number $l_0 = 0$. According to section 4.2.1, the interaction of the atom with a gravitational wave will transform the state of the atom such that it will have a projection in states with $\Delta l = \pm 2, \pm 4, ...$ but, because of the

magnitude of the coefficients in the decomposition, the resulting transformation can be approximated as

$$\begin{aligned} |\psi_0\rangle = |n = n_0, l_0 = 0\rangle \rightarrow |\psi\rangle & \\ &= C_{n_0,l=0}\,|n = n_0, l = 0\rangle + C_{n_0,2}\,|n = n_0, l = 2\rangle \\ &\equiv C_0\,|n_0, 0\rangle + C_2\,|n_0, 2\rangle \ , \end{aligned} \tag{5.1}$$

which presents a change in the relative phase of $C_2/C_0$ for the states $|n_0, 0\rangle$ and $|n_0, 2\rangle$. This result can be extended for the general case of $l \geq 0$ as the observations can be focused only in the transition between levels with $l = l_0$ and $l = l_0 + 2$, such that

$$|l_0\rangle \rightarrow C_0\,|l_0\rangle + C_2\,|l_0 + 2\rangle \ . \tag{5.2}$$

For convenience, we will use the notation $|n_0, l_0\rangle \equiv |0\rangle$ and $|n_0, l_0 + 2\rangle \equiv |2\rangle$ for the rest of the calculations. We have that the probability $P$ of measuring the atom in the initial state after interacting with a gravitational wave will be

$$P(S_p) = |\,\langle\psi_0|\psi\rangle\,|^2 = C_0^2(S_p) \ , \tag{5.3}$$

which depends on the the magnitude of the parameter $S_p$. Experimentally, this quantity can be estimated with a statistical error of

$$(\Delta P)^2 = \langle\psi|\psi\rangle - |\,\langle\psi_0|\psi\rangle\,|^2 = C_2^2(S_p) \ . \tag{5.4}$$

By estimating the value of the parameter $S_p$ we can acquire important information about the intrinsic properties of the gravitational fluctuation. Through error propagation theory it can be obtained that if we try to evaluate the magnitude of $S_p$ by measuring the state $|\psi\rangle$, the error in the estimation will be

$$\Delta S_p = \Delta P \Big/ \left|\frac{\partial P}{\partial S_p}\right| \ . \tag{5.5}$$

A lower uncertainty $\Delta S_p$ means a better estimation, so it is in our interest to reduce this quantity for a given measurement as much as possible. From equation 4.27 we have that the coefficient $C_0$ is

$$C_0 = 1 - S_p\kappa_0(n_0, l_0) \ , \tag{5.6}$$

where $\kappa_0$ is a constant that depends on the quantum numbers $n_0$ and $l_0$ of the initial state of the atom as

$$\kappa_0 = \frac{(n_0 + l_0 + 1)^3}{(2l_0 - 1)(2l_0 + 3)} \ . \tag{5.7}$$

This is the coefficient calculated for the transformation after a single interaction, but it can be easily extended for the case of multiple events because the coefficient $C_i$ increases linearly with the number of interactions as calculated in equation 4.35. Using equations 5.3 to 5.7, we obtain that the uncertainty in the estimation of $S_p$ will be

$$\Delta S_p = \frac{1}{2\kappa_0} \left( \frac{C_2}{C_0} \right) . \tag{5.8}$$

For the value of $C_2$ described by equation 4.27, we have that the uncertainty will depend on the principal quantum number $n_0$ of the initial state as

$$\Delta S_p \sim \frac{1}{n_0^2} \ . \tag{5.9}$$

This suggests that the measurement will be more accurate for higher excitations of the initial state, once more favouring Rydberg states.

## 5.1 Fisher information

The Fisher information is defined as the information about the state of a system that is gained after a particular measurement of said state (Savage, 1976). We seek to maximize the Fisher information so that experiments can have higher resolution with less resources (Giovannetti *et al.*, 2006; Guo-Yong & Guang-Can, 2013). Moreover, a greater amount of information per measurement will require for the experiments to be repeated fewer times, which is ideal given the rarity of particular gravitational wave events. The classical Fisher information for a particular measurement of a system can be calculated as

$$F_c = \sum_i \frac{(P_i')^2}{P_i} \ , \tag{5.10}$$

with $P_i$ the probability of finding the system in a given state $|i\rangle$ and $P_i'$ the partial derivative of the probability with respect to the estimated parameter,

$$P_i' = \frac{\partial P_i}{\partial S_p} \ . \tag{5.11}$$

Given the initial state $|\psi_0\rangle = |0\rangle$ for an atom, its interaction with a gravitational wave will leave the system in the state

$$|\psi\rangle = C_0 \, |0\rangle + C_2 \, |2\rangle \ \ , \tag{5.12}$$

so the probabilities of finding the atom in the states $|0\rangle$ and $|2\rangle$ after the transformation will be

$$P_0 = C_0^2 \ , \ P_2 = C_2^2 \ , \tag{5.13}$$

with the derivatives

$$P_0' = 2C_0C_0' \ , \ P_2' = 2C_2C_2' \ . \tag{5.14}$$

For very large values of $n_0$ and low $l_0$, which are preferable states according to the results in Chapter 4, the value of the coefficient $C_2$ can be approximated to

$$C_2^2 \approx 1 - C_0^2 \ , \tag{5.15}$$

which implies an almost unitary transformation of the system. This will be important to obtain consistent results in following calculations. Using the approximation in equation 5.15 and the value for $C_0$ in equation 5.6, we obtain the derivatives

$$C_0' = -\kappa_0 \ , \ C_2' = \kappa_0 \frac{C_0}{C_2} \ , \tag{5.16}$$

which can be substituted in equation 5.14 to get

$$P_0' = -2\kappa_0 C_0 \ , \ P_2' = 2\kappa_0 C_0 \ . \tag{5.17}$$

With these derivatives and equation 5.10 we obtain that the Fisher information for the transformed state will be

$$\begin{aligned} F_c &= \frac{(P_0')^2}{P_0} + \frac{(P_2')^2}{P_2} \\ &= \frac{(2\kappa_0 C_0)^2}{C_0^2} + \frac{(-2\kappa_0 C_0)^2}{C_2^2} = 4\kappa_0^2 \left(1 + \frac{C_0^2}{C_2^2}\right) \\ &= 4 \left(\frac{\kappa_0}{C_2}\right)^2 (C_2^2 + C_0^2) \ . \end{aligned} \tag{5.18}$$

From equation 5.15 we have that $C_0^2 + C_2^2 \approx 1$, so we get finally that the Fisher information can be calculated as

$$F_c = 4\left(\frac{\kappa_0}{C_2}\right)^2 . \tag{5.19}$$

By comparing this equation with the identity in equation 5.8, we can easily see the relation between the Fisher information and the uncertainty in the estimation of the value of $S_p$

$$F_c \sim \frac{1}{(\Delta S_p)^2} . \tag{5.20}$$

Equation 5.20 tells us that the Fisher information is inversely proportional to the square of the uncertainty of the estimated parameter, highlighting the importance of maximizing it in order to increase the resolution of measurements.

For quantum states, a more proper version of the Fisher information can be calculated. The quantum Fisher information for pure states is defined as

$$F_q = 4\left(\langle\psi'|\psi'\rangle - |\langle\psi|\psi'\rangle|^2\right) , \tag{5.21}$$

where $|\psi'\rangle$ represents the partial derivative of the vector state $|\psi\rangle$ with respect to the estimated parameter,

$$|\psi'\rangle = \frac{\partial}{\partial S_p}|\psi\rangle . \tag{5.22}$$

Given the transformed state $|\psi\rangle$ in equation 5.12, we have that the derivative vector will be

$$|\psi'\rangle = C_0'|0\rangle + C_2'|2\rangle . \tag{5.23}$$

Using the same values in equation 5.16 for the derivatives $C_i'$ gives us the value for the quantum Fisher information

$$\begin{aligned} F_q &= 4\left(\langle\psi'|\psi'\rangle - |\langle\psi|\psi'\rangle|^2\right) \\ &= 4\left(\kappa_0^2 + \kappa_0^2\frac{C_0^2}{C_2^2} - |\kappa_0 C_0 - \kappa_0\frac{C_0}{C_2}C_2|^2\right) \\ &= 4\kappa_0^2\left(\kappa_0^2 + \kappa_0^2\frac{C_0^2}{C_2^2}\right) = 4\left(\frac{\kappa_0}{C_2}\right)^2(C_2^2 + C_0^2) \\ &= 4\left(\frac{\kappa_0}{C_2}\right)^2 . \end{aligned} \tag{5.24}$$

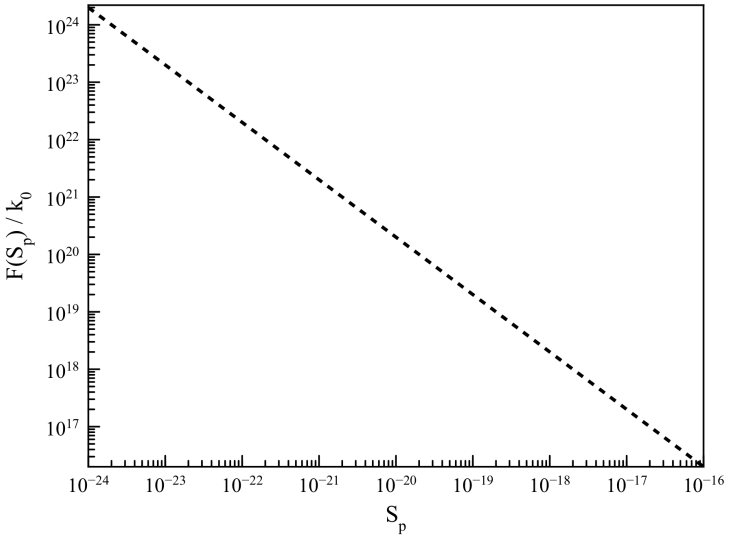


Figure 5.1: Quantum Fisher information for the state described in equation 5.12 as a function of the strain constant $S_p$. This function is normalized with the constant $\kappa_0$, which depends on the quantum number of the initial state according to equation 5.7.

This is the same value for the classical Fisher information in equation 5.19, which is a special case for $\langle\psi|\psi'\rangle = 0$. In figure 5.1 we plot the value of the calculated Fisher information as a function of the strain constant $S_p$. For small values of $S_p$, the value of the Fisher information will become asymptotically big,

$$\frac{F(S_p)}{\kappa_0} \approx \frac{2}{S_p} \ . \tag{5.25}$$

Because of the magnitude of $S_p$, this equation tells us that the information gained by measuring the atom in a state other than the initial will be very high. Although measuring a very small $S_p$ will provide an enormous amount of information about the state of the system, the probability of realizing such measurement will become extremely small because it depends directly on the value of $S_p$.

A useful quantity will be the product of the Fisher information $F$ times the probability $P_\perp$ of measuring the atom in a state $|i\rangle$ orthogonal to the initial state ($\langle i|\psi_0\rangle = 0$). By maximizing this product we can guarantee a higher success in measuring any change in the state and also a lower error in such measurement.

For the state after the interaction as described in equation 5.12, the product of the Fisher information and the probability of finding the atom in a orthogonal state will be will be

$$F(S_p)P_\perp(S_p) = 4\kappa_0^2 \ . \tag{5.26}$$

This result increases drastically with the principal quantum number of the initial state ($\kappa_0^2 \sim n_0^6$), indicating that Rydberg states will increase both the probability of measuring any change and the resolution of the experiments.

### 5.1.1 State superposition

Next we analyze the Fisher information for the state of an atom initially in a state superposition. The eigenstates $|n_0, 0\rangle$ and $|n_0, 2\rangle$ of the atom will be transformed after the interaction with the gravitational wave as

$$|n_0, 0\rangle \to C_0(n_0, 0)\,|n_0, 0\rangle + C_{+2}(n_0, 0)\,|n_0, 2\rangle \ , \tag{5.27}$$

$$|n_0, 2\rangle \to C_0(n_0, 2)\,|n_0, 2\rangle + C_{-2}(n_0, 2)\,|n_0, 0\rangle + C_{+2}(n_0, 2)\,|n_0, 4\rangle \ . \tag{5.28}$$

For large values of $n_0$ we can use the following approximations: first, from equation 4.27 we have that the value of $C_{+2}$ in the right side of equation 5.28 is much smaller than the rest of the coefficients, so we can disregard the projection of the state $|n_0, 4\rangle$. Second, by using equation 4.27 it can be calculated that the value of $C_0(n_0, 0)$ and $C_{-2}(n_0, 2)$ will be very similar, so we can treat them as the same factor ($C_{-2}(n_0, 2) \approx C_0(n_0, 0)$). This will also allow us to keep unitarity in the transformation. Using these approximations, we obtain that the eigenstates are transformed as

$$|0\rangle \to C_0\,|0\rangle + C_2\,|2\rangle \tag{5.29}$$

$$|2\rangle \to -C_2\,|0\rangle + C_0\,|2\rangle \ . \tag{5.30}$$

For an atom initially in an equal superposition of the states $|0\rangle$ and $|2\rangle$,

$$|\psi_0\rangle = \frac{1}{\sqrt{2}}[|0\rangle - |2\rangle] \ , \tag{5.31}$$

we get the transformation

$$|\psi_0\rangle \to |\psi\rangle = \frac{1}{\sqrt{2}}[(C_0 + C_2)\,|0\rangle + (-C_0 + C_2)\,|2\rangle] \;, \tag{5.32}$$

with derivative

$$|\psi'\rangle = \frac{1}{\sqrt{2}}[(C_0' + C_2')\,|0\rangle + (-C_0' + C_2')\,|2\rangle] \;. \tag{5.33}$$

The negative phase between $|0\rangle$ and $|2\rangle$ is selected here and in following calculations to maximize the change in phase as suggested in subsection 3.1.2. Using the same value for the derivative of the coefficients $C_i$ in equation 5.16, we obtain the derivative vector

$$\begin{aligned} |\psi'\rangle &= \frac{1}{\sqrt{2}}[\kappa_0(-1 + C_0/C_2)\,|0\rangle + \kappa_0(1 + C_0/C_2)\,|2\rangle] \\ &= \frac{1}{\sqrt{2}}\frac{\kappa_0}{C_2}[(C_0 - C_2)\,|0\rangle + (C_0 + C_2)\,|2\rangle] \;. \end{aligned} \tag{5.34}$$

By rewriting the vectors $|\psi\rangle$ and $|\psi'\rangle$ in terms of the coefficients $C_+ = C_0 + C_2$ and $C_- = C_0 - C_2$,

$$\begin{aligned} |\psi\rangle &= \frac{1}{\sqrt{2}}[C_+\,|0\rangle - C_-\,|2\rangle] \\ |\psi'\rangle &= \frac{1}{\sqrt{2}}\frac{\kappa_0}{C_2}[C_-\,|0\rangle + C_+\,|2\rangle] \;, \end{aligned} \tag{5.35}$$

it can be more easily observed that they are orthogonal to each other ($\langle\psi|\psi'\rangle = 0$), which from previous remarks results in the quantum and classic Fisher information having the same value. From the definition in equation 5.21, we obtain that the Fisher information for the superposition state will then be

$$\begin{aligned} F_{|0\rangle-|2\rangle} &= 4\left(\frac{\kappa_0}{C_2}\right)^2 (C_+^2 + C_-^2) \\ &= 4\left(\frac{\kappa_0}{C_2}\right)^2 \;, \end{aligned} \tag{5.36}$$

which is the same as for an initial state with no superposition in equation 5.24. This implies that no extra information can be obtained from the interaction by using atoms in an equally distributed superposition.

Although the state described in equation 5.31 may present the highest change in the relative phase after the interaction, this does not necessarily imply a better estimation from measuring the state. To calculate if the measurement of any particular initial state will provide more information about the parameter $S_p$, we analyze the general state

$$|\psi_0\rangle = A\,|0\rangle + B\,|2\rangle \ , \tag{5.37}$$

where $A$ and $B$ are arbitrary complex numbers such that $|A|^2 + |B|^2 = 1$. Using equations 5.29 and 5.30, we have that this state will be transformed into the state

$$|\psi\rangle = (AC_0 - BC_2)\,|0\rangle + (AC_2 + BC_0)\,|2\rangle \ . \tag{5.38}$$

The derivative vector will then be

$$|\psi'\rangle = -\frac{\kappa_0}{C_2}[(AC_2 + BC_0)\,|0\rangle - (AC_0 - BC_2)\,|2\rangle] \ , \tag{5.39}$$

which is evidently orthogonal to the transformed state vector ($\langle\psi|\psi'\rangle = 0$). We then have the scalar product

$$\begin{aligned}\langle\psi'|\psi'\rangle &= \frac{\kappa_0^2}{C_2^2}[AC_2 + BC_0)^2 - (AC_0 - BC_2)^2] \\ &= \frac{\kappa_0^2}{C_2^2}[(A^2 + B^2)(C_0^2 + C_2^2)] \\ &= \left(\frac{\kappa_0}{C_2}\right)^2 \ ,\end{aligned} \tag{5.40}$$

giving the Fisher information

$$F_{A,B} = 4\left(\frac{\kappa_0}{C_2}\right)^2 \ , \tag{5.41}$$

which is once again the same value as for the atom initially in a single eigenstate. Because a superposition can be seen as a rotation in the observation basis, this result tells us that no extra information from the state will be gained by changing the measurement basis.

## 5.2 Multiple atom systems

We now calculate how systems of multiple atoms are transformed by their interaction with gravitational fluctuations and estimate the Fisher information of the resulting state to examine how initial correlations between the atoms could reduce the uncertainty of the state measurements.

Let us first consider a system of two atoms. If $|\psi_0\rangle_1$ and $|\psi_0\rangle_2$ represent the initial state of the first and second atom, respectively, then the state of the whole system can be represented as

$$|\psi_0\rangle = |\psi_0\rangle_1 \otimes |\psi_0\rangle_2 \ , \tag{5.42}$$

which in this case is a separable state. If both atoms are initially in the base state $|0\rangle$, then the state of the system will be

$$|\psi_0\rangle = |0\rangle_1 \otimes |0\rangle_2 \equiv |0\rangle\,|0\rangle \ . \tag{5.43}$$

We regard the gravitational wave interacting with both atoms at the same time and in an equal way. This is based on the argument that the wavelength of the gravitational wave will be much bigger than the distance between the atoms, so its effect will be similar for both subsystems. If a gravitational wave interacts with both of them and they are statistically independent, then the state of the system will evolve as

$$\begin{aligned} |\psi\rangle &= [C_0\,|0\rangle + C_2\,|2\rangle] \otimes [C_0\,|0\rangle + C_2\,|2\rangle] \\ &= C_0^2\,|0\rangle\,|0\rangle + C_0C_2\,|0\rangle\,|2\rangle + C_0C_2\,|2\rangle\,|0\rangle + C_2^2\,|2\rangle\,|2\rangle \ . \end{aligned} \tag{5.44}$$

This transformation disregards any mutual interaction of the atoms (see section 4.3), which can be done even for Rydberg atoms if they have a large separation. The derivative of the state vector in equation 5.44 will be

$$\begin{aligned} |\psi'\rangle &= 2C_0C_0'\,|0\rangle\,|0\rangle + (C_0C_2' + C_0'C_2)(|0\rangle\,|2\rangle + |2\rangle\,|0\rangle) + 2C_2C_2'\,|2\rangle\,|2\rangle \\ &= -2\kappa_0C_0\,|0\rangle\,|0\rangle + \kappa_0(C_0^2/C_2 - C_2)(|0\rangle\,|2\rangle + |2\rangle\,|0\rangle) + 2\kappa_0C_0\,|2\rangle\,|2\rangle \\ &= -2\kappa_0C_0(|0\rangle\,|0\rangle - |2\rangle\,|2\rangle) + \frac{\kappa_0}{C_2}(C_0^2 - C_2^2)(|0\rangle\,|2\rangle + |2\rangle\,|0\rangle) \\ &= \frac{\kappa_0}{C_2}[-2C_0C_2(|0\rangle\,|0\rangle - |2\rangle\,|2\rangle) + (2C_0^2 - 1)(|0\rangle\,|2\rangle + |2\rangle\,|0\rangle)] \ . \end{aligned} \tag{5.45}$$

We use these vectors to calculate the scalar products

$$\begin{aligned}\langle\psi'|\psi'\rangle &= \frac{\kappa_0^2}{C_2^2}[8C_0^2C_2^2 + 2(2C_0^2-1)^2] \\ &= 2\frac{\kappa_0^2}{C_2^2}[8C_0^2(1-C_0^2) + 2(2C_0^2-1)(2C_0^2-1)] \\ &= 2\frac{\kappa_0^2}{C_2^2}\ ,\end{aligned} \tag{5.46}$$

$$\begin{aligned}\langle\psi|\psi'\rangle &= \frac{\kappa_0}{C_2}[-2C_0^3C_2 + 2C_0C_2(2C_0^2-1) + 2C_0C_2^3] \\ &= \frac{\kappa_0^2}{C_2^2}[2C_0^3C_2 + 2C_0C_2^3 - 2C_0C_2^3] \\ &= 2C_0C_2\frac{\kappa_0^2}{C_2^2}[C_0^2 + C_2^2 - 1] \\ &= 0\ .\end{aligned} \tag{5.47}$$

By substituting the identities in equations 5.46 and 5.47 into equation 5.21, we obtain the Fisher information

$$\begin{aligned}F_{|0\rangle|0\rangle} &= 4\left(\langle\psi'|\psi'\rangle - |\langle\psi|\psi'\rangle|^2\right) \\ &= 8\left(\frac{\kappa_0}{C_2}\right)^2\ .\end{aligned} \tag{5.48}$$

This value has double the magnitude of the information calculated for a single atom in equation 5.24. It is expected for the Fisher information to increase this way because the two independent probes will produce the same information as repeating the measurement a second time with a single probe.
If initially both atoms are in a superposition state,

$$|\psi_0\rangle_1 = |\psi_0\rangle_2 = \frac{1}{\sqrt{2}}[|0\rangle - |2\rangle]\ , \tag{5.49}$$

the initial state of the whole system can be represented as

$$\begin{aligned}|\psi_0\rangle &= \frac{1}{\sqrt{2}}[|0\rangle_1 - |2\rangle_1] \otimes \frac{1}{\sqrt{2}}[|0\rangle_2 - |2\rangle_2] \\ &\equiv \frac{1}{\sqrt{2}}[|0\rangle - |2\rangle]^{\otimes 2} \\ &= \frac{1}{2}[|0\rangle|0\rangle - |0\rangle|2\rangle - |2\rangle|0\rangle + |2\rangle|2\rangle]\ .\end{aligned} \tag{5.50}$$

This state is transformed into

$$\begin{aligned} |\psi\rangle &= \frac{1}{2}[C_- |0\rangle + C_+ |1\rangle]^{\otimes 2} \\ &= \frac{1}{2}[C_-^2 |0\rangle |0\rangle + (2C_0^2 - 1)(|0\rangle |2\rangle + |2\rangle |0\rangle) + C_+^2 |2\rangle |2\rangle] \ , \end{aligned} \tag{5.51}$$

and the derivative of the state vector will be

$$|\psi'\rangle = -\frac{\kappa_0}{C_2}(2C_0^2 - 1)[|0\rangle |0\rangle - |2\rangle |2\rangle] - 2\kappa_0 C_0[|0\rangle |2\rangle + |2\rangle |0\rangle] \ . \tag{5.52}$$

It should be noted that although the state of each atom is transformed independently ($|\psi_0\rangle_1 |\psi_0\rangle_2 \rightarrow |\psi\rangle_1 |\psi\rangle_2$), the derivative of the state vector is not calculated as the tensor product of the derivative of the individual state vectors ($|\psi'\rangle \neq |\psi'\rangle_1 |\psi'\rangle_2$). Using these vectors and following the same calculations as in the previous cases, we calculate the Fisher information to be

$$F_{(|0\rangle - |2\rangle)^2} = 8\left(\frac{\kappa_0}{C_2}\right)^2 \ . \tag{5.53}$$

Once more, this value is the same as for an initial state with no superposition in equation 5.48, further showing that no extra information can be gained by changing our measurement basis. This result also shows consistency in our calculations. In figure 5.2 we plot the Fisher information of the transformed state for different values of $n_0$. As before, it is shown that a higher principal quantum number will improve the resolution of the measurement. This same behaviour was observed for all future analyzed states.

### 5.2.1 Entangled states

Now we analyze the evolution of entangled states, which are expected to yield a lower estimation error. For two atoms initially in the maximally entangled state

$$|\psi_0\rangle = \frac{1}{\sqrt{2}}[|0\rangle |0\rangle - |2\rangle |2\rangle] \ , \tag{5.54}$$

we have the state after the interaction

$$\begin{aligned} |\psi\rangle &= \frac{1}{\sqrt{2}}([C_0 |0\rangle + C_2 |2\rangle]^{\otimes 2} - [-C_2 |0\rangle + C_0 |2\rangle]^{\otimes 2}) \\ &= \frac{1}{\sqrt{2}}[(2C_0^2 - 1)(|0\rangle |0\rangle - |2\rangle |2\rangle) + 2C_0 C_2(|0\rangle |2\rangle + |2\rangle |0\rangle)] \ , \end{aligned} \tag{5.55}$$

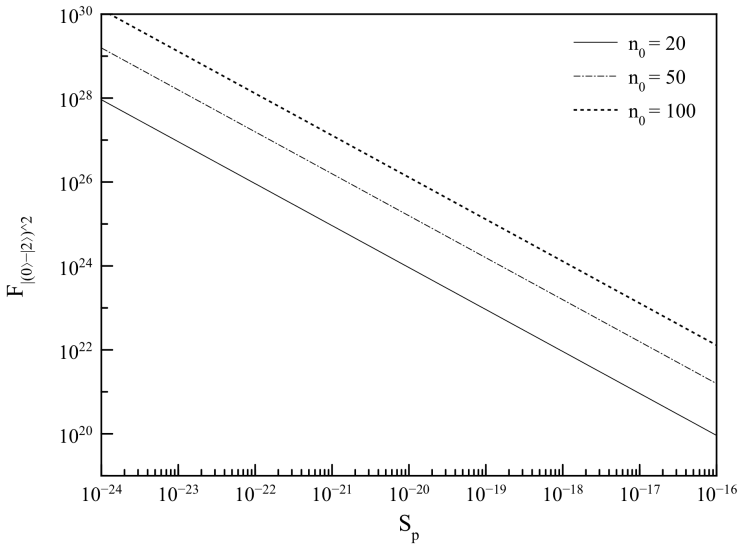


Figure 5.2: Quantum Fisher information for two initially uncorrelated atoms after their interaction with a gravitational wave for different values of $n_0$.

and its derivative vector

$$|\psi'\rangle = \frac{1}{\sqrt{2}}\frac{\kappa_0}{C_2}[-2C_0C_2(|0\rangle\,|0\rangle - |2\rangle\,|2\rangle) + (2C_0^2 - 1)(|0\rangle\,|2\rangle + |2\rangle\,|0\rangle)] \ . \quad (5.56)$$

Once more we have that the scalar product of the state vector and its derivative will be equal to zero ($\langle\psi|\psi'\rangle = 0$), with the squared modulus of the state vector equal to

$$\begin{aligned}\langle\psi'|\psi'\rangle &= 2\frac{\kappa_0^2}{C_2^2}[8C_0^2C_2^2 + 2(2C_0^2 - 1)^2] \\ &= 4\left(\frac{\kappa_0}{C_2}\right)^2 \ .\end{aligned} \quad (5.57)$$

With this we calculate the Fisher information associated with the entangled state

$$F_{|0\rangle|0\rangle-|2\rangle|2\rangle} = 16\left(\frac{\kappa_0}{C_2}\right)^2 \ . \quad (5.58)$$

The result is double the value of the one calculated for the separable state in equation 5.53. This means that entangled states can significantly reduce the uncertainty in the estimation of the parameter $S_p$ compared to statistically independent atoms.

Another kind of state that we are interested in analyzing are cat states. These are states in a quantum superposition between two macroscopically distinct vectors and have been applied in quantum metrology, significantly improving the resolution of the measurements (Facon *et al.*, 2016; Guo *et al.*, 2015). Let us consider an ensemble of 4 atoms in an initial state

$$\begin{aligned} |\psi_0\rangle &= \frac{1}{\sqrt{2}}[|0\rangle_1 |0\rangle_2 |0\rangle_3 |0\rangle_4 - |2\rangle_1 |2\rangle_2 |2\rangle_3 |2\rangle_4] \\ &\equiv \frac{|0000\rangle - |2222\rangle}{\sqrt{2}} \ . \end{aligned} \tag{5.59}$$

This is a non-separable state in which all the atoms will be found in either the state $|0\rangle$ or the state $|2\rangle$. If the atoms interact with a gravitational wave, the system will evolve into the state

$$\begin{aligned} |\psi\rangle &= \frac{1}{\sqrt{2}}([C_0 |0\rangle + C_2 |2\rangle]^{\otimes 4} + [-C_2 |0\rangle + C_0 |2\rangle]^{\otimes 4}) \\ &= \frac{1}{\sqrt{2}}[(2C_0^2 - 1)(|0000\rangle - |2222\rangle) \\ &+ (C_0^3 C_2 + C_0 C_2^3)(|0002\rangle + |0020\rangle + |0200\rangle + |2000\rangle \\ &+ |0222\rangle + |2022\rangle + |2202\rangle + |2220\rangle)] \ . \end{aligned} \tag{5.60}$$

The derivative of this vector state is

$$\begin{aligned} |\psi'\rangle = \frac{1}{\sqrt{2}} \left(\frac{\kappa_0}{C_2}\right) (2C_0^2 - 1)[ &- 4C_0 C_2 (|0000\rangle - |2222\rangle) \\ &+ |0002\rangle + |0020\rangle + |0200\rangle + |2000\rangle \\ &+ |0222\rangle + |2022\rangle + |2202\rangle + |2220\rangle] \ . \end{aligned} \tag{5.61}$$

We use these vectors to calculate the scalar products

$$\langle \psi | \psi' \rangle = 8 \frac{\kappa_0}{C_2} (2C_0^2 - 1) C_0 C_2^3 \ , \tag{5.62}$$

$$\langle \psi' | \psi' \rangle = 4 \frac{\kappa_0^2}{C_2^2} (2C_0^2 - 1)^2 (4C_0^2 C_2^2 + 1) \ , \tag{5.63}$$

which gives the Fisher information

$$F_{|0000\rangle - |2222\rangle} = 16 \left(\frac{\kappa_0}{C_2}\right)^2 (2C_0^2 - 1)^2 (1 + 4C_0^2 C_2^2 - 16 C_0^2 C_2^6) \ . \tag{5.64}$$

Given the expected value of $S_p$, the terms in the right side of equation 5.64 that are proportional to $C_2^i$ will be extremely small, so we can disregard them. With this, we get that the value of the Fisher information will be approximately

$$F_{|0000\rangle-|2222\rangle} \approx 16\left(\frac{\kappa_0}{C_2}\right)^2 . \tag{5.65}$$

This is four times the value of the information for measurements of a single atom in equation 5.41, which is equal to the expected value for an ensemble of four non-correlated atoms, meaning that the state described in equation 5.59 will not provide any improvement to the measurement's precision. This is quite an unexpected result, as the described quantum states have been calculated to significantly increase the resolution of measurements in other studies, in some cases even reaching the theoretically possible limit (Juffmann *et al.*, 2016; Martin Ciurana *et al.*, 2017). This doesn't mean that it is not possible to further decrease the uncertainty in the estimations, but simply shows that some entangled states are more useful than others in performing this task. For comparison, a system of two pairs of entangled atoms

$$|\psi_0\rangle = \frac{1}{2}[|00\rangle - |22\rangle]^{\otimes 2} , \tag{5.66}$$

will have the same number of probes as the state in equation 5.59, but entangled in a different way. Here we have that the state will be transformed into

$$|\psi\rangle = \frac{1}{2}[(2C_0^2 - 1)(|00\rangle - |22\rangle) + 2C_0C_2(|02\rangle - |20\rangle)] , \tag{5.67}$$

with derivative

$$|\psi'\rangle = 2\frac{\kappa_0}{C_2}[-2C_0C_2(|00\rangle - |22\rangle) + (2C_0^2 - 1)(|02\rangle + |20\rangle)] . \tag{5.68}$$

These vectors result in the products

$$\langle\psi|\psi'\rangle = 0 \tag{5.69}$$

$$\begin{aligned}\langle\psi'|\psi'\rangle &= 4\frac{\kappa_0^2}{C_2^2}[8C_0^2C^2 + 2(2C_0^2 - 1)^2] \\ &= 8\frac{\kappa_0^2}{C_2^2} ,\end{aligned} \tag{5.70}$$

which yield a Fisher information of

$$F_{(|00\rangle-|22\rangle)^{\otimes 2}} = 32\left(\frac{\kappa_0}{C_2}\right)^2 \ . \tag{5.71}$$

We observe the value of the Fisher information obtained with the initial state in equation 5.66 doubles that expected for the same number of atoms prepared in the entangled state described in equation 5.59, being therefore a better initial state for the estimation of the parameter $S_p$.

For the general case, the Fisher information from the measurement of an ensemble of $N$ atoms is expected to increase proportionally with the number of atoms ($F \propto N$). To prove this, we consider an ensemble of $N$ atoms initially in the state $|0\rangle$,

$$\begin{aligned} |\psi_0\rangle &= |0\rangle_1 |0\rangle_2 ... |0\rangle_N \\ &\equiv |0\rangle^{\otimes N} \ . \end{aligned} \tag{5.72}$$

The transformed state vector is calculated as

$$\begin{aligned} |\psi\rangle &= [C_0 |0\rangle + C_2 |2\rangle]^{\otimes N} \\ &= \sum_{i=0}^{N} C_0^{N-i} C_2^i |W_i\rangle \ , \end{aligned} \tag{5.73}$$

where the vectors $|W_i\rangle$ are not eigenvectors but a sum of all of the eigenvectors with $i$ number of 2s in their label *e.g.* $|W_3\rangle = |22200...0\rangle + |22020...0\rangle + |20220...0\rangle + |02220...0\rangle + \cdots$ . The derivative of this vector will be

$$|\psi'\rangle = \sum_i \frac{\kappa_0}{C_2} C_0^{N-i-1} C_2^{i-1} (i - NC_2^2) |W_i\rangle \ . \tag{5.74}$$

As in previous cases, the transformed state vector and its derivative are orthogonal, so their scalar product will be zero ($\langle\psi|\psi'\rangle = 0$). For the squared modulus of the derivative vector we have

$$\langle\psi'|\psi'\rangle = \sum_i \frac{\kappa_0^2}{C_2^2} C_0^{2N-2i-2} C_2^{2i-2} (i - NC_2^2)^2 \langle W_i|W_i\rangle \ . \tag{5.75}$$

The scalar product $\langle W_i|W_i\rangle$ will be equal to the total number of vectors that add up to form the vector $|W_i\rangle$, which can be calculated with

$$\langle W_i|W_i\rangle = \binom{N}{i} = \frac{N!}{i!(N-i)!} \ . \tag{5.76}$$

Using the proper mathematical analysis, it can be demonstrated that

$$\sum_{i=0}^{N} C_0^{2(N-i-1)} C_2^{2(i-1)} (i - NC_2^2)^2 \binom{N}{i} = N \ , \tag{5.77}$$

from which we obtain that the Fisher information will increase as

$$F_{|0\rangle^N} = 4N \left( \frac{\kappa_0}{C_2} \right)^2 \ . \tag{5.78}$$

A simple way to obtain an approximation of this result is by discarding all term in the summation in equation 5.75 with non-zero coefficient of $C_2$ ($i > 1$). This is a reasonable approximation as $C_2 \ll 1$, so these terms will be extremely small compared to the terms with $i \leq 1$. With this method of discarding the terms that are proportional to $C_2$, it can be easily obtained that an ensemble of $N$ atoms prepared in a superposition of two macroscopically distinguishable states

$$|\psi_0\rangle = \frac{|0\rangle^{\otimes N} - |2\rangle^{\otimes N}}{\sqrt{2}} \ , \tag{5.79}$$

will result in a Fisher information

$$F_{|0\rangle^N - |2\rangle^N} \approx 4N \left( \frac{\kappa_0}{C_2} \right)^2 \ , \tag{5.80}$$

even for a very large number of atoms in the ensemble, allowing us to show that this kind of entangled state will not increase the resolution of the measurement of an arbitrary number of atoms over the same number of uncorrelated atoms.

Using the relation of the Fisher information and the uncertainty in equation 5.20, we have that the error in the measurement of $N$ uncorrelated atoms will be

$$\Delta S_p \sim \frac{1}{\sqrt{N}} \ . \tag{5.81}$$

This function of the number of probes is known as the standard limit and is the maximum accuracy that can be obtained (perfect detection) using classical probes. In comparison, for $N$ atoms prepared in maximally entangled pairs ($N$ an even number),

$$|\psi_0\rangle = \frac{1}{2}[|00\rangle - |22\rangle]^{\otimes N/2} \ , \tag{5.82}$$

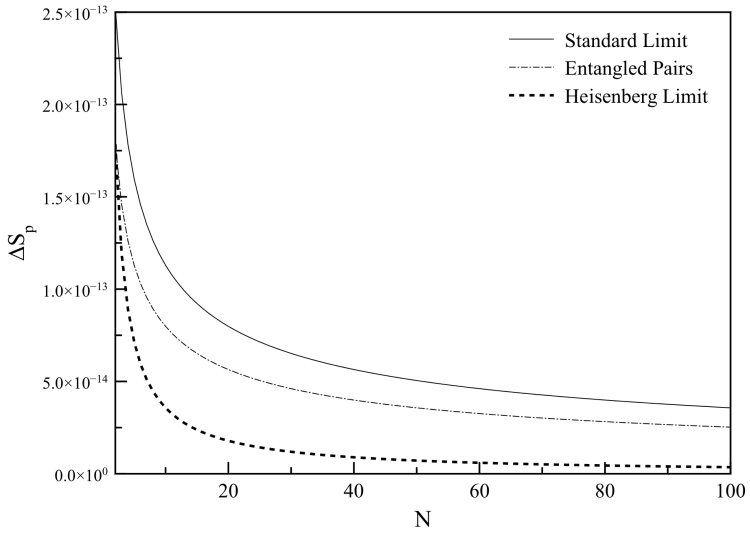


Figure 5.3: Error in the measurement for $N$ atomic probes operating between the states $|n = 50, 0\rangle$ and $|n = 50, 2\rangle$ after their interaction with a gravitational wave

using the same mathematical analysis as for entangled macroscopic state, it can be demonstrated that the value of the Fisher information will be

$$F_{((|00\rangle - |22\rangle)^{N/2}} = 8N \left(\frac{\kappa_0}{C_2}\right)^2 , \tag{5.83}$$

which is twice the value of that calculated for separable and cat states. We plot in figure 5.3 the expected uncertainty for the measurement of entangled pairs, along with the standard limit and the Heisenberg limit. The Heisenberg limit is the upper theoretical limit to the precision of any measurement and decreases as $1/N$. It can be seen that the function of the uncertainty for entangled pairs is quite far from the Heisenberg limit, so there is the possibility of finding a state that will give a lower uncertainty.

Due to the nature of the proposed interaction, and the assigned value of the coefficients $C_i$, it may not be possible to get close to the Heisenberg limit by preparing the atoms in a particular initial configuration of macroscopic state. This is because the highest contribution to the Fisher information is from terms with coefficient $C_0^{N-1}C_2$, as its derivative will not be dependent on the coefficient $C_2$, which is expected to have an extremely small magnitude. It may be possible

to approach the Heisenberg limit by estimating the state that maximizes the Fisher information according to our gathered knowledge about how the Fisher information depends on the eigenvectors from the initial state.

### 5.2.2 Optimal state

Let us consider an arbitrary eigenstate for an ensemble of $N$ atoms

$$|a_1\rangle_1 |a_2\rangle_2 \dots |a_N\rangle_N \equiv |a_1 a_2 ... a_N\rangle \ , \tag{5.84}$$

where the factors $a_i$ can be either 0 or 2, corresponding to the base and excited states such that

$$|0\rangle = |n = n_0, l = l_0\rangle \ , \ \ |2\rangle = |n = n_0, l = l_0 + 2\rangle \ . \tag{5.85}$$

Given the probability of the interaction of a gravitational wave, we can approximate the transformation in the state as

$$\begin{aligned} |a_1 a_2 ... a_N\rangle \to C_0^N |a_1 a_2 ... a_N\rangle + C_0^{N-1} C_2 [(-1)^{\frac{a_1}{2}} |(2 - a_1) a_2 ... a_N\rangle \\ + (-1)^{\frac{a_2}{2}} |a_1 (2 - a_2) ... a_N\rangle + \dots \\ \dots + (-1)^{\frac{a_N}{2}} |a_1 a_2 ... (2 - a_N)\rangle] \ , \end{aligned} \tag{5.86}$$

with derivative

$$\begin{aligned} \frac{\kappa_0}{C_2} (-N C_0^{N-1} |a_1 a_2 ... a_N\rangle + [C_0^N + (N-1) C_0^{N-2} C_2^2][(-1)^{\frac{a_1}{2}} (|(2 - a_1) a_2 ... a_N\rangle \\ + (-1)^{\frac{a_2}{2}} |a_1 (2 - a_2) ... a_N\rangle + \dots]) \ . \end{aligned} \tag{5.87}$$

Because of the magnitude of the coefficient $C_2$, this derivative can be approximated to

$$\frac{\kappa_0}{C_2} C_0^N [(-1)^{\frac{a_1}{2}} (|(2 - a_1) a_2 ... a_N\rangle + (-1)^{\frac{a_2}{2}} |a_1 (2 - a_2) ... a_N\rangle + \dots]) \ , \tag{5.88}$$

meaning that the derivative of the transformed eigenstate will be approximately a superposition of all the states that differ by the state of a single atom times a factor $C_0^N \kappa_0 / C_2$. From here also it is easy to see that the scalar product of the derivative times the transformed state will be negligible compared to the

square modulus of the derivative vector. To find the transformed state with the highest modulus of its derivative, which should maximize the Fisher information, we need to provide states such that the change in the state of a single atom by the interaction add up constructively. We consider the state for $N$ atoms

$$|Ev\rangle \equiv [|W_0\rangle - |W_2\rangle + |W_4\rangle - |W_6\rangle + ...]/\sqrt{2^{N-1}} \ , \tag{5.89}$$

where the vectors $|W_i\rangle$ are the sum of all eigenvectors with $i$ atoms in the excited state such that

$$\begin{aligned} |W_0\rangle &\equiv |000...00\rangle \\ |W_1\rangle &\equiv |200...00\rangle + |020...00\rangle + ... + |000...20\rangle + |000...02\rangle \\ |W_2\rangle &\equiv |220...00\rangle + |202...00\rangle + |022...00\rangle + ... \, |000...22\rangle \\ &\vdots \end{aligned} \tag{5.90}$$

similar to a generalized W state for $i$ excited qubits. The transformed vector for the state $|Ev\rangle$ will have a projection into $N/2$ states (each of the eigenvectors that doesn't form part of the vector $|Ev\rangle$) and they will add constructively $N$ times because of the sign of the vectors $|W_i\rangle$. From here we have that the $2^{N-1}$ vectors will be multiplied by the factor $NC_0^N\kappa_0/C_2$, which will lead to a square modulus proportional to $N^2/2^{N-1}$, which is close to the Heisenberg limit.

Using the same logic, we consider the similar state

$$|Od\rangle \equiv [|W_1\rangle - |W_3\rangle + |W_5\rangle - |W_7\rangle + ...]/\sqrt{2^{N-1}} \ , \tag{5.91}$$

which leads to the same result as the analysis for the state in equation 5.89. With both of these states, we arrive at the optimal state

$$|\psi_0\rangle_{opt} = \frac{|Ev\rangle - |Od\rangle}{\sqrt{2}} \ , \tag{5.92}$$

which is formed by an equal superposition of all eigenvectors, each of them with a very specific phase. The state $|\psi_0\rangle_{opt}$ is non-trivial, arising from an extensive analysis about the transformation of arbitrary state and the associated Fisher information. Given the derivative of the eigenvectors in equation 5.88, we obtain that the derivative vector from the optimal state will be

$$|\psi'\rangle_{opt} = \sqrt{N}C_0^N\frac{\kappa_0}{C_2}[|000...00\rangle - |000...02\rangle - |000...20\rangle - ... + |222...22\rangle] \ , \tag{5.93}$$

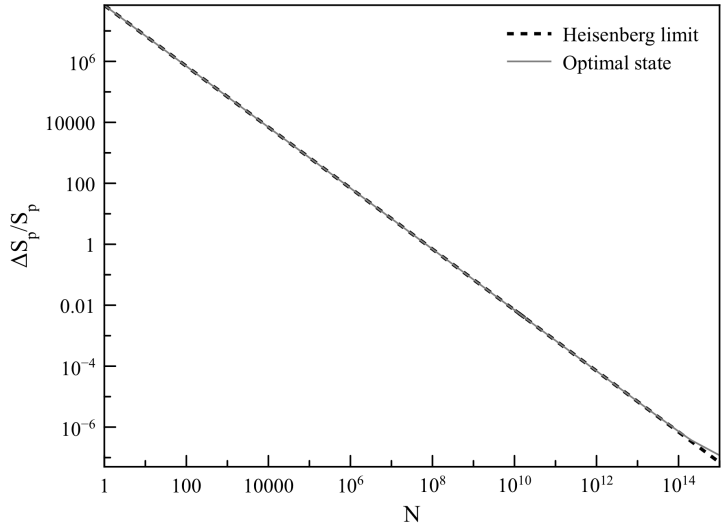


Figure 5.4: Normalized error for $N$ atomic probes with the states $|n = 50, 0\rangle$ and $|n = 50, 2\rangle$ after their interaction with a gravitational wave. The optimal state is described in equation 5.92.

which contains $N$ eigenvectors. From here we obtain that the Fisher information for the initial state in equation 5.92 will be

$$F \approx 4N^2 C_0^{2N} \left(\frac{\kappa_0}{C_2}\right)^2 , \tag{5.94}$$

which is proportional to $N^2$, almost the same as the Heisenberg limit. In figure 5.4 we compare the error associated with the measurement of the atoms initially in the state from equation 5.92 to the Heisenberg limit. The function follows closely the Heisenberg limit, deviating just a small amount for very large values of $N$. Therefore, by using an ensemble of atoms in the form described by equation 5.92 it will be guaranteed that the measurement will yield the best possible estimation of the parameter $S_p$ for given experimental resources.

As an example, for 3 atoms we have the states

$$\begin{aligned} |Ev\rangle &= [|000\rangle - |220\rangle - |202\rangle - |022\rangle]/2 \\ |Od\rangle &= [|200\rangle + |020\rangle + |002\rangle - |222\rangle]/2 \ , \end{aligned} \tag{5.95}$$

which leads to the optimal state

$$|\psi_0\rangle_{opt} = [(|000\rangle + |222\rangle) - (|200\rangle + |020\rangle + |002\rangle) - (|220\rangle + |202\rangle + |022\rangle)]/\sqrt{8} \ , \tag{5.96}$$

which can be demonstrated to be a non-separable state. This state can be expressed in terms of a Greenberger-Horne-Zeilinger state and W states as

$$|\psi_0\rangle_{opt} = \frac{1}{2}|GHZ\rangle - \sqrt{\frac{3}{8}}|W\rangle - \sqrt{\frac{3}{8}}|\overline{W}\rangle \ , \tag{5.97}$$

each of which are commonly used for quantum metrology. Individually, these states will not improve the estimation of the parameter $S_p$, according to our previous calculations.

The state described in equation 5.96 may be very hard to obtain experimentally. For 3 atomic probes a simpler state to prepare could be

$$|\psi_0\rangle = [|000\rangle - |\overline{W}\rangle]/\sqrt{2} \ , \tag{5.98}$$

which is similar to the state $|Ev\rangle$. This could lead to an uncertainty closer to the Heisenberg limit (about half the value) with fewer complications than trying to prepare the optimal state. This is just particular for a three-atom system, as in the general case an state superposition of the eigenstate $|000...000\rangle$ minus the generalized W state $|\overline{W}\rangle$ will not lead to a much better estimation of the parameter $S_p$ because there will be a bigger number of eigenstates in the projection that will not add up constructively.

From the logic used to obtain the optimal state, it can be conclude that in order that experiments should aim to generate superpositions involve as many eigenstates that differ by the state of two atoms between each other as possible. This, in combination with the amplification of the effect described in Chapter 4, could be applied for the detection of gravitational waves and other small gravitational perturbations, potentially working at different frequency and energy ranges. The technical difficulties and experiential limitations of the proposed scheme will be discussed in section 6.1.

# Chapter 6

# Conclusions

We proposed two different models of decoherence in atomic states by gravitational perturbations. In the first one, the sudden displacement of the atomic nucleus by the interaction, presented as a scattering event of a neutral particle, will partially project the wave function of the atom in a superposition of energy levels with lower energy than the initial state of the atom. The projection is done mostly over the level with closest energy to the initial state and increases with the excitation of the atom before the interaction, making the effect more prominent for Rydberg atoms. This model can be applied to the scattering of any kind of particles with neutral electric charge, namely photons and neutrons. This presents the opportunity of testing our theory by exposing atoms to different sources of cold neutrons, whose scattering should have an effect significant enough to be detected. The scattering of photons could partially explain perturbations in the signal of Rydberg atoms that is observed when they are exposed to non-resonant light. More significantly, the model can be potentially useful to the detection of theoretical particles like the ones that may compose dark matter, or at least to impose a limit to their possible mass. The detection scheme will be restricted to interactions with energy below the ionization threshold, excluding some particles with big mass like the WIMP. We gave the specific example of axions, whose interaction with the atom is calculated to be more prominent than the one expected for cosmic rays.

The calculated effect for the scattering of gravitational waves and gravitons was extremely small, making the experimental observation difficult. According to our calculations, the model can instead be more effectively applied to measure

the quantization of space. Because of the limitations of the model, we developed a second one inspired by our analysis of the potential shift and physically observable effects of gravitational waves. In the new model, a change in the local electric field of the atom by the gravitational wave is proposed. This will result in a transformation of the wave function, which was calculated to have a small projection in eigenstates with azimuthal quantum number that differ by two from the initial state, similar to the effect calculated for the case of particle scattering. We examined two possible interpretations of these results: the first one is that the atom interacts with the graviton, exchanging angular momentum. The overall effect was calculated to be higher than the one for the scattering of gravitons by the nucleus from the previous model. Secondly, the energy levels of the atom are perceived as being shifted with respect to each other, resulting in radiation previously resonant to an atomic transition becoming detuned. Here the atom will not perceive any change in its own reference frame, but rather will sense incoming photons as being energy-shifted. The frequency detuning offers the possibility of detection by looking at radiation from extra-planetary Rydberg atoms, which can be found with high energy and in large quantities. Another possibility is analyzing the coherent population-shift dynamics, in which a small deviation is expected to arise a result of the detuning.

Correlations between the atoms could increase their sensitivity to gravitational fluctuations, increasing the resolution of measurements. We analyze the evolution of different quantum states for an ensemble of multiple atoms as a result of their simultaneous interaction with a gravitational wave. With this we calculated the Fisher information for a measurement of the resulting state as a function of the strain in space. Although entangled pairs of atoms significantly increase the obtainable information of a single measurement compared to the measurement of the same number of uncorrelated atoms, calculations showed that certain superpositions of macroscopically distinguishable states will not reduce the uncertainty in the estimations as is usually the case in other studies. We were able to calculate an ideal initial quantum state for an arbitrary number of atoms, which reduce the error of measurements almost to the theoretical Heisenberg limit.

## 6.1 Discussion

Throughout this thesis we have emphasized that using Rydberg atoms will make the effect of the interaction more prominent and therefore easier to detect. This may indicate that experiments should aim to produce the highest excited state possible in order to ensure the maximum sensitivity, but several considerations should be taken into account:

The biggest limitation to the experiments is the period of measurement, especially for the detection of small continuous interactions like the effect of vacuum fluctuations or the quantization of space. The radiative lifetime of Rydberg atoms increases as $\sim n^5$, meaning higher excited states will allow for longer observation periods. For multiple trapped atoms, this time will dramatically decrease as Rydberg atoms will collide at a higher rate. The analysis of Rabi cycles described in section 4.2.3 may have an edge over the measurement of changes in state populations suggested in sections 3.3.2 and 4.2.2, as the coherence times of the dynamics surpass the mean lifetime of the state (Johnson *et al.*, 2008; Kubler *et al.*, 2010).

Some techniques can be applied to further extend the lifetime of the atoms, like physically shielding them from the radiation background, focusing on resonant frequencies. Another possibility is having the atoms inside a high-Q cavity to suppress undesired transition, which should extend considerably the lifetime of the state (Brune *et al.*, 1996; Walther *et al.*, 2006). The cavity can also be used to suppress the transition expected from the interaction *e.g.* $l_0 \rightarrow l_0 \pm 2$, which will allow the detection scheme to focus only on the observation of transition events that cannot occur by electromagnetic radiation. The Rydberg blockade can also be used for the suppression of the transition (Singer *et al.*, 2004). This will also suppress the Rabi oscillations, so it is a factor that should be taken into consideration when working with highly excited states.

Time limitations will be less problematic for the detection of a burst of gravitational waves, which last just a fraction of a second. In this case the experiment can be reset at discrete intervals and repeated until a signal is observed.

The second limitation for the accuracy of experiments is the number of atoms that can be prepared. As the energy of the atoms increases, the lower the density of the atomic ensemble will be, so experiments with highly excited atoms will

have available just a fraction of probes of those using low-energy states. This can be attributed to higher interactions between atoms, which makes them harder to contain, and to their susceptibility to externals perturbations, which will result in some loss in the trapping. Although experiments can be repeated an arbitrary number of times to compensate for lower probe numbers, this will not be possible for the detection of singular events like bursts of gravitational waves.

Observations of cosmic clouds of Rydberg atoms may be one of the best approaches for the detection of gravitational waves, as atoms can be found here in both high quantities and high energies (Gnedin *et al.*, 2009). In cases where the atoms manifest atomic blockade (Gnedin *et al.*, 2009; Wunner *et al.*, 1986), implying strong correlations among them, there is the possibility of a signal amplification as described in section 4.3.

In a more controlled experimental setting, the optimal state described in section 5.2.2 could provide the highest resolution with the lowest number of resources (number of atoms and interacting time). Nevertheless, preparing the state could be quite challenging especially for a large number of atoms. Preparing an ensemble of multiple entangled atoms or a particular simpler superpositions, dependent on the number atomic probes, could significantly reduce the error in measurements while requiring a much simpler setting.

As final remarks, the different results obtained in this study indicate that the best experiment setting in terms of maximizing the signal and reducing the error will ultimately depend on the type of gravitational fluctuation that is intended to be measured and the available experimental resources.

# References


Aasi, J. *et al.* (2015). Advanced LIGO. *Classical and Quantum Gravity*, **32**, 074001. 1

Abbott, B.P. *et al.* (2016a). GW151226: observation of gravitational waves from a 22-solar-mass binary black hole coalescence. *Phys. Rev. Lett.*, **116**, 241103. 1, 3, 45

Abbott, B.P. *et al.* (2016b). Observation of gravitational waves from a binary black hole merger. *Phys. Rev. Lett.*, **116**, 061102. 1, 3, 41, 53

Abbott, B.P. *et al.* (2017). GW170104: observation of a 50-solar-mass binary black hole coalescence at redshift 0.2. *Phys. Rev. Lett.*, **118**, 221101. 1, 3, 37, 45, 47, 53

Abend, S., Gebbe, M., Gersemann, M., Ahlers, H., Muntinga, H., Giese, E., Gaaloul, N., Schubert, C., Lammerzahl, C., Ertmer, W., Schleich, W.P. & Rasel, E.M. (2016). Atom-chip fountain gravimeter. *Phys. Rev. Lett.*, **117**, 203003. 2

Abramowitz, M. & Stegun, I.A. (1983). *Handbook of Mathematical Functions with Formulas, Graphs, and Mathematical Tables*, 785. Dover Publications. 19, 46

Afrousheh, K., Bohlouli-Zanjani, P., Petrus, J.A. & Martin, J.D.D. (2006). Determination of the $^{85}$Rb $ng$-series quantum defect by electric-field-induced resonant energy transfer between cold rydberg atoms. *Phys. Rev. A*, **74**, 062712. 49

Aguiar, O.D. *et al.* (2002). The status of the Brazilian spherical detector. *Classical and Quantum Gravity*, **19**, 1949. 2

Akamatsu, D., Inaba, H., Hosaka, K., Yasuda, M., Onae, A., Suzuyama, T., Amemiya, M. & Hong, F.L. (2014). Spectroscopy and frequency measurement of the 87 sr clock transition by laser linewidth transfer using an optical frequency comb. *Applied Physics Express*, **7**, 012401. 53

Altin, P.A., Johnsson, M.T., Negnevitsky, V., Dennis, G.R., Anderson, R.P., Debs, J.E., Szigeti, S.S., Hardman, K.S., Bennetts, S., McDonald, G.D., Turner, L.D., Close, J.D. & Robins, N.P. (2013). Precision atomic gravimeter based on Bragg diffraction. *New Journal of Physics*, **15**, 023009. 2

Amaro-Seoane, P. *et al.* (2012). Low-frequency gravitational-wave science with elisa/ngo. *Classical and Quantum Gravity*, **29**, 124016. 2

Andia, M., Jannin, R., Nez, F., Biraben, F., Guellati-Khelifa, S. & Clade, P. (2013). Compact atomic gravimeter based on a pulsed and accelerated optical lattice. *Phys. Rev. A*, **88**, 031605. 2

Andriot, D. & Gomez, G.L. (2017). Signatures of extra dimensions in gravitational waves. *Journal of Cosmology and Astroparticle Physics*, **2017**, 048. 1

Aprile, E. *et al.* (2014). First axion results from the xenon100 experiment. *Phys. Rev. D*, **90**, 062009. 37

Bateman, J., McHardy, I., Merle, A., Morris, T.R. & Ulbricht, H. (2015). On the existence of low-mass dark matter and its direct detection. *Scientific Reports*, **5**, 8058. 37, 38

Bekenstein, J.D. & Schiffer, M. (1998). The many faces of superradiance. *Phys. Rev. D*, **58**, 064014. 57

Benacquista, M.J. (2002). Gravitational radiation from black hole binaries in globular clusters. *Classical and Quantum Gravity*, **19**, 1297. 1

Bildsten, L. (1998). Gravitational radiation and rotation of accreting neutron stars. *The Astrophysical Journal Letters*, **501**, L89. 1

Bird, R., Hulstrom, R. & Lewis, L. (1983). Terrestrial solar spectral data sets. *Solar Energy*, **30**, 563 – 573. 36

Blair, A.G. (1974). Energy density of the relic radiation. *Symposium - International Astronomical Union*, **63**, 143–155. 36

Blencowe, M.P. (2013). Effective field theory approach to gravitationally induced decoherence. *Phys. Rev. Lett.*, **111**, 021302. 2

Bohr, N. (1913). The spectra of helium and hydrogen. *Nature*, **92**, 231–232. 6

Bondi, H. (1957). Plane gravitational waves in general relativity. *Nature*, **179**, 1072–1073. 2

Bonifacio, P.M., Wang, C.H.T., Mendonza, J.T. & Bingham, R. (2009). Dephasing of a non-relativistic quantum particle due to a conformally fluctuating spacetime. *Classical and Quantum Gravity*, **26**, 145013. 14

Bovy, J. & Tremaine, S. (2012). On the local dark matter density. *The Astrophysical Journal*, **756**, 89. 37

Brooks, K.J., Storey, J.W.V. & Whiteoak, J.B. (2001). H110$\alpha$ recombination-line emission and 4.8-GHz continuum emission in the Carina nebula. *Monthly Notices of the Royal Astronomical Society*, **327**, 46. 53

Browaeys, A. & Lahaye, T. (2013). Interacting cold Rydberg atoms: a toy many-body system. *Seminaire Poincare*, **17**, 125. 56

Brune, M., Schmidt-Kaler, F., Maali, A., Dreyer, J., Hagley, E., Raimond, J.M. & Haroche, S. (1996). Quantum Rabi oscillation: A direct test of field quantization in a cavity. *Phys. Rev. Lett.*, **76**, 1800–1803. 55, 83

Cadoret, M., De Mirandes, P., E.and Clade, Nez, F., Julien, L., Biraben, F. & Guellati-Khelifa, S. (2009). Atom interferometry based on light pulses: Application to the high precision measurement of the ratio h/m

and the determination of the fine structure constant. *The European Physical Journal Special Topics*, **172**, 121–136. 3

Caldirola, P. (1980). The introduction of the chronon in the electron theory and a charged-lepton mass formula. *Lettere al Nuovo Cimento (1971-1985)*, **27**, 225–228. 26

Carron, N. (2007). *An Introduction to the Passage of Energetic Particles Through Matter.*, 308. CRC Press. 27

Cooper, N. & Freegarde, T. (2013). Trapping of 85Rb atoms by optical pumping between metastable hyperfine states. *J. Phys. B At. Mol. Opt. Phys.*, **46**, 215003. 7

Copeland, E.J., Mulryne, D.J., Nunes, N.J. & Shaeri, M. (2009). Gravitational wave background from superinflation in loop quantum cosmology. *Phys. Rev. D*, **79**, 023508. 1

Damour, T. & Vilenkin, A. (2001). Gravitational wave bursts from cusps and kinks on cosmic strings. *Phys. Rev. D*, **64**, 064008. 1

de Waard, A., Gottardi, L., van Houwelingen, J., Shumack, A. & Frossati, G. (2003). Minigrail, the first spherical detector. *Classical and Quantum Gravity*, **20**, S143. 2

Deleglise, S., Dotsenko, I., Sayrin, C., Bernu, J., Brune, M., Raimond, J.M. & Haroche, S. (2008). Reconstruction of non-classical cavity field states with snapshots of their decoherence. *Nature*, **455**, 510–514. 51

Desvignes, G. *et al.* (2016). High-precision timing of 42 millisecond pulsars with the European pulsar timing array. *Monthly Notices of the Royal Astronomical Society*, **458**, 3341–3380. 2

Diaz-Torres, A. (2010). Coupled-channels density-matrix approach to low-energy nuclear collision dynamics: A technique for quantifying quantum decoherence effects on reaction observables. *Phys. Rev. C*, **82**, 054617. 27

Dickerson, S.M., Hogan, J.M., Sugarbaker, A., Johnson, D.M.S. & Kasevich, M.A. (2013). Multiaxis inertial sensing with long-time point source atom interferometry. *Phys. Rev. Lett.*, **111**, 083001. 2

Dimopoulos, S., Graham, P.W., Hogan, J.M., Kasevich, M.A. & Rajendran, S. (2009). Gravitational wave detection with atom interferometry. *Physics Letters B*, **678**, 37 – 40. 3

Dirac, P.A.M. (1927). The quantum theory of the emission and absorption of radiation. *Proceedings of the Royal Society of London A: Mathematical, Physical and Engineering Sciences*, **114**, 243–265. 22

Droz, F., Mosset, P., Wang, Q., Rochat, P., Belloni, M., Gioia, M., Resti, A. & Waller, P. (2009). Space passive hydrogen maser –performances and lifetime data –. In *2009 IEEE International Frequency Control Symposium Joint with the 22nd European Frequency and Time forum*, 393–398. 38

Dudin, Y.O., Li, L., Bariani, F. & Kuzmich, A. (2012). Observation of coherent many-body Rabi oscillations. *Nat. Phys.*, **8**, 790–794. 55, 56

Dupays, A., Beswick, A., Lepetit, B., Rizzo, C. & Bakalov, D. (2003). Proton Zemach radius from measurements of the hyperfine splitting of hydrogen and muonic hydrogen. *Phys. Rev. A*, **68**, 052503. 14

Dupont-Nivet, M., Westbrook, C.I. & Schwartz, S. (2016). Contrast and phase-shift of a trapped atom interferometer using a thermal ensemble with internal state labelling. *New Journal of Physics*, **18**, 113012. 3

Durrer, R. (2010). Gravitational waves from cosmological phase transitions. *Journal of Physics: Conference Series*, **222**, 012021. 1, 2

Dutta, S.K., Feldbaum, D., Walz-Flannigan, A., Guest, J.R. & Raithel, G. (2001). High-angular-momentum states in cold Rydberg gases. *Phys. Rev. Lett.*, **86**, 3993–3996. 49, 54

Dzuba, V.A., Flambaum, V.V. & Pospelov, M. (2010). Atomic ionization by keV-scale pseudoscalar dark-matter particles. *Phys. Rev. D*, **81**, 103520. 37

Einstein, A. (1905). Ist die Tragheit eines Korpers von seinem Energieinhalt abhangig? *Annalen der Physik*, **323**, 639–641. 14

Einstein, A. (1918). Uber Gravitationswellen. *Sitzungsber. K. Preuss. Akad. Wiss.*, **1**, 154. 2

Everitt, M.S., Jones, M.L., Varcoe, B.T.H. & Dunningham, J.A. (2011). Creating and observing N-partite entanglement with atoms. *Journal of Physics B: Atomic, Molecular and Optical Physics*, **44**, 035504. 39

Everitt, M.S., Jones, M.L. & Varcoe, B.T.H. (2013). Dephasing of entangled atoms as an improved test of quantized space time. *Journal of Physics B: Atomic, Molecular and Optical Physics*, **46**, 224003. 39

Facon, A., Dietsche, E.K., Grosso, D., Haroche, S., Raimond, J.M., Brune, M. & Gleyzes, S. (2016). A sensitive electrometer based on a Rydberg atom in a Schrodinger-cat state. *Nature*, **535**, 262–265. 3, 59, 72

Fan, H., Kumar, S., Sedlacek, J., Kubler, H., Karimkashi, S. & Shaffer, J.P. (2015). Atom based RF electric field sensing. *Journal of Physics B: Atomic, Molecular and Optical Physics*, **48**, 202001. 2

Fischer, U. (1994). Transition probabilities for a Rydberg atom in the field of a gravitational wave. *Classical Quantum Gravity*, **11**, 463. 2, 3, 6

Fixler, J.B., Foster, G.T., McGuirk, J.M. & Kasevich, M.A. (2007). Atom interferometer measurement of the Newtonian constant of gravity. *Science*, **315**, 74–77. 2

Fixsen, D.J. (2009). The temperature of the cosmic microwave background. *The Astrophysical Journal*, **707**, 916. 2

Gallagher, T.F. (2007). *Rydberg Atoms*, 10–25. Cambridge University Press. 6, 7, 17, 18, 56

Giovannetti, V., Lloyd, S. & Maccone, L. (2006). Quantum metrology. *Phys. Rev. Lett.*, **96**, 010401. 3, 61

Gnedin, Y.N., Mihajlov, A.A., Ignjatovic, L.M., Sakan, N.M., Sreckovic, V.A., Zakharov, M.Y., Bezuglov, N.N. & Klycharev, A.N. (2009). Rydberg atoms in astrophysics. *New Astronomy Reviews*, **53**, 259–265. 84

Graham, P.W., Hogan, J.M., Kasevich, M.A. & Rajendran, S. (2013). New method for gravitational wave detection with atomic sensors. *Phys. Rev. Lett.*, **110**, 171102. 2

Griffiths, D. (1995). *Introduction to Quantum Mechanics (2nd edition)*, 145,150,235–236,371–396. New Jersey: Pearson Education. 16, 17, 49

Griffiths, D. (2007). *Introduction to Electrodynamics (3rd Edition)*, 422. Pearson Education. 13

Griffiths, D.J. (1982). Hyperfine splitting in the ground state of hydrogen. *American Journal of Physics*, **50**, 698. 14

Grishchuk, L.P. (2005). Relic gravitational waves and cosmology. *Physics-Uspekhi*, **48**, 1235. 1, 2

Gross, D.J. & Jackiw, R. (1968). Low-energy theorem for graviton scattering. *Phys. Rev.*, **166**, 1287–1292. 6

Gross, M. & Haroche, S. (1982). Superradiance: An essay on the theory of collective spontaneous emission. *Physics Reports*, **93**, 301 – 396. 57

Guo, L.S., Xu, B.M., Zou, J. & Shao, B. (2015). Improved thermometry of low-temperature quantum systems by a ring-structure probe. *Phys. Rev. A*, **92**, 052112. 3, 72

Guo-Yong, X. & Guang-Can, G. (2013). Quantum metrology. *Chinese Physics B*, **22**, 110601. 3, 61

Haehnelt, M.G. (1994). Low-frequency gravitational waves from supermassive black holes. *Monthly Notices of the Royal Astronomical Society*, **2692**, 199–208. 1

Hafele, J.C. & Keating, R.E. (1972). Around-the-world atomic clocks: Predicted relativistic time gains. *Science*, **177**, 166–168. 2

Hawking, S.W. (1979). *General Relativity; an Einstein Centenary Survey*, 90. Cambridge University Press. 1

Heinrich, A.J., Gupta, J.A., Lutz, C.P. & Eigler, D.M. (2004). Single-atom spin-flip spectroscopy. *Science*, **306**, 466–469. 13

Hillas, A. (1927). *Cosmic Rays*, 26–53. Elsevier. 37

Himemoto, Y. & Taruya, A. (2017). Impact of correlated magnetic noise on the detection of stochastic gravitational waves: Estimation based on a simple analytical model. *Phys. Rev. D*, **96**, 022004. 3

Hobbs, G. *et al.* (2010). The international pulsar timing array project: using pulsars as a gravitational wave detector. *Classical and Quantum Gravity*, **27**, 084013. 2

Hogan, C.J. (1998). Cosmological gravitational wave backgrounds. *AIP Conference Proceedings*, **456**, 79–86. 1

Hogan, C.J. (2000). Gravitational waves from mesoscopic dynamics of the extra dimensions. *Phys. Rev. Lett.*, **85**, 2044–2047. 2

Hogan, J.M. *et al.* (2011). An atomic gravitational wave interferometric sensor in low earth orbit (agis-leo). *General Relativity and Gravitation*, **43**, 1953–2009. 2

Hoth, G.W., Pelle, B., Riedl, S., Kitching, J. & Donley, E.A. (2016). Point source atom interferometry with a cloud of finite size. *Appl. Phys. Lett.*, **109**, 071113. 2

Howe, D.A. & Walls, F.L. (1983). A compact hydrogen maser with exceptional long-term stability. *IEEE Transactions on Instrumentation and Measurement*, **32**, 218–223. 38

Jauncey, D.L. (1977). *Radio Astronomy and Cosmology*, 247–257. Springer. 1

Johnson, T.A., Urban, E., Henage, T., Isenhower, L., Yavuz, D.D., Walker, T.G. & Saffman, M. (2008). Rabi oscillations between ground and Rydberg states with dipole-dipole atomic interactions. *Phys. Rev. Lett.*, **100**, 113003. 53, 83

Johnson, W.R., Nilsen, J. & Cheng, K.T. (2012). Thomson scattering in the average-atom approximation. *Phys. Rev. E*, **86**, 036410. 35

Johnsson, M.T., Brennen, G.K. & Twamley, J. (2016). Macroscopic superpositions and gravimetry with quantum magnetomechanics. *Scientific Reports*, **6**, 37495. 3, 59

Juffmann, T., Klopfer, B.B., Frankort, T.L., Haslinger, P. & Kasevich, M.A. (2016). Multi-pass microscopy. *Nature Communications*, **7**, 12858. 3, 59, 73

Kimble, H.J., Levin, Y., Matsko, A.B., Thorne, K.S. & Vyatchanin, S.P. (2001). Conversion of conventional gravitational-wave interferometers into quantum nondemolition interferometers by modifying their input and/or output optics. *Phys. Rev. D*, **65**, 022002. 3

Kolb, E.W. & Turner, M.S. (1990). *The early universe.*, chap. 8. Front. Phys., Vol. 69. 26

Kolkowitz, S., Pikovski, I., Langellier, N., Lukin, M.D., Walsworth, R.L. & Ye, J. (2016). Gravitational wave detection with optical lattice atomic clocks. *Phys. Rev. D*, **94**, 124043. 3

Kostelecky, V.A. & Nieto, M.M. (1985). Evidence from alkali-metal-atom transition probabilities for a phenomenological atomic supersymmetry. *Phys. Rev. A*, **32**, 1293–1298. 18

Kubler, H., Shaffer, J.P., Baluktsian, T., Low, R. & Pfau, T. (2010). Coherent excitation of Rydberg atoms in micrometre-sized atomic vapour cells. *Nat. Photon.*, **4**, 112–116. 53, 83

Lan, S.Y., Kuan, P.C., Estey, B., Haslinger, P. & Muller, H. (2012). Influence of the coriolis force in atom interferometry. *Phys. Rev. Lett.*, **108**, 090402. 2

Lasky, P.D. *et al.* (2016). Gravitational-wave cosmology across 29 decades in frequency. *Phys. Rev. X*, **6**, 011035. 1

Lee, T.E., Haffner, H. & Cross, M.C. (2012). Collective quantum jumps of Rydberg atoms. *Phys. Rev. Lett.*, **108**, 023602. 56

Liboff, R.L. (2003). *Kinetic Theory: Classical, Quantum, and Relativistic Descriptions (third edition)*, 137–277. Springer. 26

LIGO & Virgo (2009). An upper limit on the stochastic gravitational-wave background of cosmological origin. *Nature*, **460**, 990–994. 1

Loudon, R.E. (2000). *The Quantum Theory of Light*, 16–19. OUP Oxford. 34

Low, R., Weimer, H., Nipper, J., Balewski, J.B., Butscher, B., Buchler, H.P. & Pfau, T. (2012). An experimental and theoretical guide to strongly interacting rydberg gases. *Journal of Physics B: Atomic, Molecular and Optical Physics*, **45**, 113001. 49

Lukin, M.D., Fleischhauer, M., Cote, R., Duan, L.M., Jaksch, D., Cirac, J.I. & Zoller, P. (2001). Dipole blockade and quantum information processing in mesoscopic atomic ensembles. *Phys. Rev. Lett.*, **87**, 037901. 56

Ma, Y., Miao, H., Pang, B.H., Evans, M., Zhao, C., Harms, J., Schnabel, R. & Chen, Y. (2017). Proposal for gravitational-wave detection beyond the standard quantum limit through EPR entanglement. *Nature Physics*, **13**, 776–780. 3, 59

Martin Ciurana, F., Colangelo, G., Slodicka, L., Sewell, R.J. & Mitchell, M.W. (2017). Entanglement-enhanced radio-frequency field detection and waveform sensing. *Phys. Rev. Lett.*, **119**, 043603. 3, 73

Merritt, D., Milosavljevic, M., Favata, M., Hughes, S.A. & Holz, D.E. (2004). Consequences of gravitational radiation recoil. *The Astrophysical Journal Letters*, **607**, L9. 2

Miller, M. & Olkiewicz, R. (2011). Strong decoherence in quantum systems undergoing collisions. *Physics Letters A*, **375**, 3264– 3267. 27

Nelemans, G. (2009). The galactic gravitational wave foreground. *Classical and Quantum Gravity*, **26**, 094030. 2

Oniga, T. & Wang, C.H.T. (2016). Quantum gravitational decoherence of light and matter. *Phys. Rev. D*, **93**, 044027. 2, 57

Ozeri, R., Itano, W.M., Blakestad, R.B., Britton, J., Chiaverini, J., Jost, J.D., Langer, C., Leibfried, D., Reichle, R., Seidelin, S., Wesenberg, J.H. & Wineland, D.J. (2007). Errors in trapped-ion quantum gates due to spontaneous photon scattering. *Phys. Rev. A*, **75**, 042329. 36

Parker, L. & Pimentel, L.O. (1982). Gravitational perturbation of the hydrogen spectrum. *Phys. Rev. D*, **25**, 3180–3190. 2, 3

Pedrozo-Penafiel, E., Paiva, R., Vivanco, F., Bagnato, V. & Farias, K. (2012). Two-photon cooperative absorption in colliding cold Na atoms. *Phys. Rev. Lett.*, **108**, 253004. 7

Peskin, M.E. & Schroeder, D.V. (1995). *An Introduction to Quantum Field Theory.*, 198. Westview Press. 26

Peters, A., Chung, K.Y., Young, B., Hensley, J. & Chu, S. (1997). Precision atom interferometry. *Philosophical Transactions of the Royal Society of London A: Mathematical, Physical and Engineering Sciences*, **355**, 2223–2233. 32

Pinto, F. (1995). Rydberg atoms as gravitational-wave antennas. *Gen. Relat. Gravit.*, **27**, 9. 2, 6

Poisson, E. (1993). Gravitational radiation from a particle in circular orbit around a black hole. i. Analytical results for the nonrotating case. *Phys. Rev. D*, **47**, 1497–1510. 1

Pound, R.V. & Snider, J.L. (1964). Effect of gravity on nuclear resonance. *Phys. Rev. Lett.*, **13**, 539–540. 2

Quinones, D.A., Oniga, T., Varcoe, B.T.H. & Wang, C.H.T. (2017). Quantum principle of sensing gravitational waves: From the zero-point fluctuations to the cosmological stochastic background of spacetime. *Phys. Rev. D*, **96**, 044018. 56, 57

Rothman, T. & Boughn, S. (2006). Can gravitons be detected? *Foundations of Physics*, **36**, 1801–1825. 40, 42, 51

Ryan, F.D. (1995). Gravitational waves from the inspiral of a compact object into a massive, axisymmetric body with arbitrary multipole moments. *Phys. Rev. D*, **52**, 5707–5718. 1

Ryan, F.D. (1997). Accuracy of estimating the multipole moments of a massive body from the gravitational waves of a binary inspiral. *Phys. Rev. D*, **56**, 1845–1855. 1

Sanz, A. & Borondo, F.t. (2007). A quantum trajectory description of decoherence. *Eur. Phys. J. D*, **44**, 319. 31

Savage, C., Gelmini, G., Gondolo, P. & Freese, K. (2009). Compatibility of dama/libra dark matter detection with other searches. *Journal of Cosmology and Astroparticle Physics*, **2009**, 010. 37

Savage, L.J. (1976). On rereading R. A. Fisher. *Ann. Statist.*, **4**, 441–500. 61

Schlamminger, S. (2014). Fundamental constants: A cool way to measure big g. *Nature*, **510**, 478–480. 2

Schwarzschild, K. (1916). On the gravitational field of a mass point according to Einsteins theory. *Sitzungsber. Preuss. Akad. Wiss. Berlin (Math.Phys.)*, **7**, 189–196. 41

Sesana, A. (2016). Prospects for multiband gravitational-wave astronomy after GW150914. *Phys. Rev. Lett.*, **116**, 231102. 2

Sidhu, J.S. & Kok, P. (2017). Quantum metrology of spatial deformation using arrays of classical and quantum light emitters. *Phys. Rev. A*, **95**, 063829. 3

Singer, K., Reetz-Lamour, M., Amthor, T., Marcassa, L.G. & Weidemuller, M. (2004). Suppression of excitation and spectral broadening induced by interactions in a cold gas of Rydberg atoms. *Phys. Rev. Lett.*, **93**, 163001. 53, 56, 83

Sorge, F. (2015). On the gravitational scattering of gravitational waves. *Classical and Quantum Gravity*, **32**, 035007. 6

Stancari, G., Atutov, S.N., Calabrese, R., Corradi, L., Dainelli, A., de Mauro, C., Khanbekyan, A., Mariotti, E., Minguzzi, P., Moi, L., Sanguinetti, S., Tomassetti, L. & Veronesi, S. (2007). Francium sources and traps for fundamental interaction studies. *The European Physical Journal Special Topics*, **150**, 389–392. 7

Takahashi, R., Suyama, T. & Michikoshi, S. (2005). Scattering of gravitational waves by the weak gravitational fields of lens objects. *A and A*, **438**, L5–L8. 6

Taylor, J.H. (1994). Binary pulsars and relativistic gravity. *Rev. Mod. Phys.*, **66**, 711–719. 1

Taylor, J.R. (2005). *Classical Mechanics*, 557. University Science Books. 6

Turner, M.S. (1997). Detectability of inflation-produced gravitational waves. *Phys. Rev. D*, **55**, R435–R439. 1

Uchiyama, T. *et al.* (2004). Present status of large-scale cryogenic gravitational wave telescope. *Classical and Quantum Gravity*, **21**, S1161. 2

Uys, H., Biercuk, M.J., VanDevender, A.P., Ospelkaus, C., Meiser, D., Ozeri, R. & Bollinger, J.J. (2010). Decoherence due to elastic Rayleigh scattering. *Phys. Rev. Lett.*, **105**, 200401. 36

Varcoe, B.T.H., Brattke, S., Weidinger, M. & Walther, H. (2000). Preparing pure photon number states of the radiation field. *Nature*, **403**, 743–746. 55

Vessot, R.F.C., Levine, M.W., Mattison, E.M., Blomberg, E.L., Hoffman, T.E., Nystrom, G.U., Farrel, B.F., Decher, R., Eby, P.B., Baugher, C.R., Watts, J.W., Teuber, D.L. & Wills, F.D. (1980). Test of relativistic gravitation with a space-borne hydrogen maser. *Phys. Rev. Lett.*, **45**, 2081–2084. 2

Walther, H., Varcoe, B.T.H., Englert, B.G. & Becker, T. (2006). Cavity quantum electrodynamics. *Rep. Prog. Phys.*, **69**, 1325. 55, 83

Wang, C.H.T., Bingham, R. & Mendonza, J.T. (2006). Quantum gravitational decoherence of matter waves. *Classical and Quantum Gravity*, **23**, L59. 14, 42

Wang, D.G., Zhang, Y. & Chen, J.W. (2016). Vacuum and gravitons of relic gravitational waves and the regularization of the spectrum and energy-momentum tensor. *Phys. Rev. D*, **94**, 044033. 1, 2

Weisberg, J.M., H., J. & Fowler, L.A. (1981). Gravitational waves from an orbiting pulsar. *Scientific American*, **245**, 74–82. 1, 2

Wunner, G., Kost, M. & Ruder, H. (1986). Circular states of Rydberg atoms in strong magnetic fields. *Phys. Rev. A*, **33**, 1444–1447. 84

Yamamoto, K. *et al.* (2008). Current status of the CLIO project. *Journal of Physics: Conference Series*, **122**, 012002. 2

Yang, C.N. (1947). On quantized space-time. *Phys. Rev.*, **72**, 874–874. 26

Zhao, Z.H., Liu, Y.X. & Li, X.G. (2007). Gravitational corrections to energy-levels of a hydrogen atom. *Communications in Theoretical Physics*, **47**, 4. 2, 3

Zurek, W.H. (2003). Decoherence, einselection, and the quantum origins of the classical. *Rev. Mod. Phys.*, **75**, 715–775. 29